Data Analysis to Improve Diagnostics and Biomarkers in Alzheimer's Disease: Building Bridges Between Data Science and Neuroscience

Karlsson, Linda

2026

Document Version:
Publisher's PDF, also known as Version of record

Data Analysis to Improve Diagnostics and Biomarkers in Alzheimer's Disease

Building Bridges Between Data Science and Neuroscience

LINDA KARLSSON
DEPARTMENT OF CLINICAL SCIENCES, MALMÖ | FACULTY OF MEDICINE | LUND UNIVERSITY

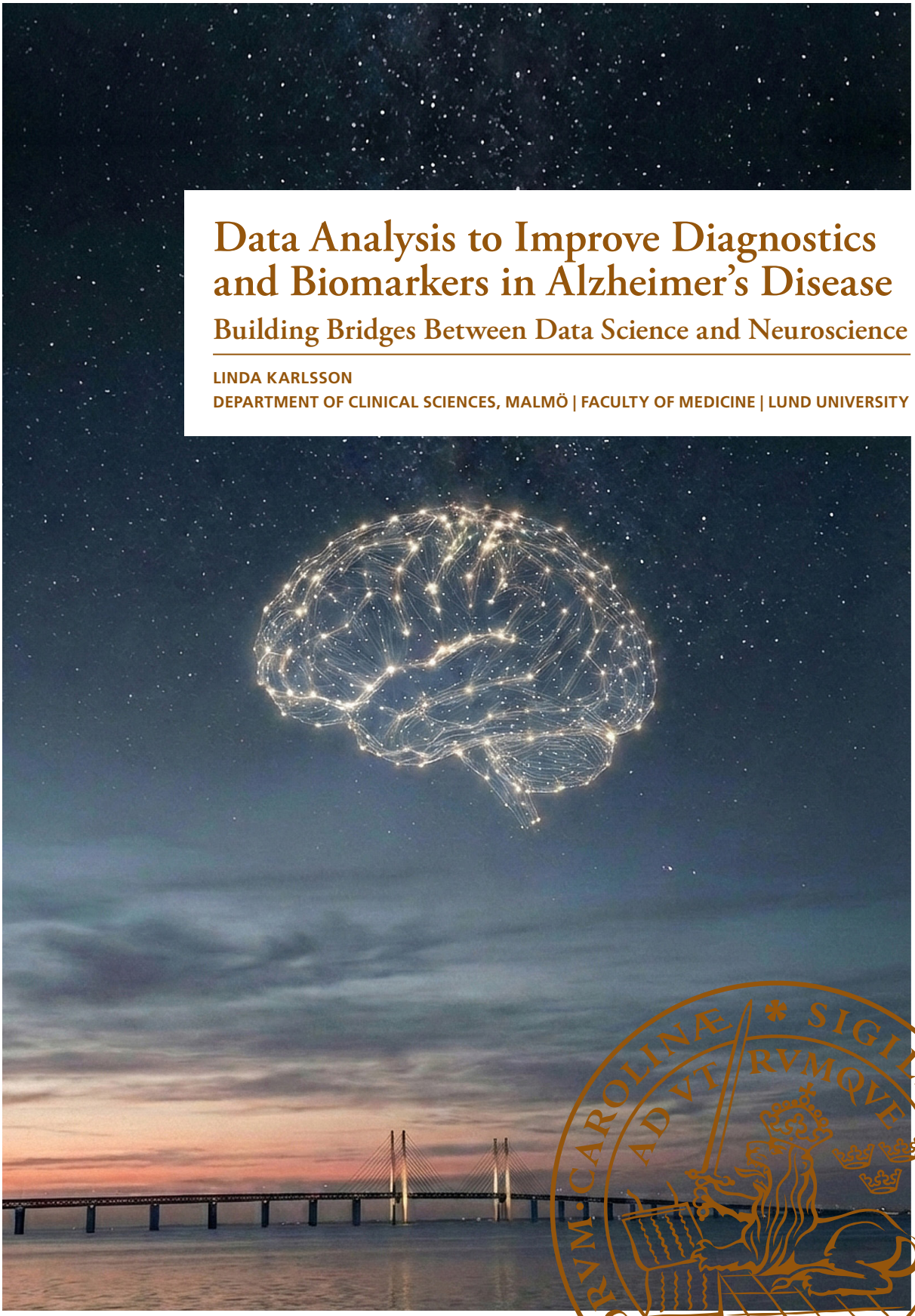

Data Analysis to Improve Diagnostics and Biomarkers in Alzheimer's Disease: Building Bridges Between Data Science and Neuroscience

Data Analysis to Improve Diagnostics and Biomarkers in Alzheimer's Disease

Building Bridges Between Data Science and Neuroscience

Linda Karlsson

LUND
UNIVERSITY

DOCTORAL DISSERTATION

Doctoral dissertation for the degree of Doctor of Philosophy (PhD)
at the Faculty of Medicine at Lund University to be publicly defended on **8th of May** at **13.30** in **Belfragesalen, BMC D15**, Lund University, Lund, Sweden.

Faculty opponent
Professor David Cash, University College London

Organization: Lund University

Document name: Doctoral dissertation **Date of issue:** 2026-05-08

Author(s): Linda Karlsson

Title and subtitle: Data Analysis to Improve Diagnostics and Biomarkers in Alzheimer's Disease: Building Bridges Between Data Science and Neuroscience

Abstract: Alzheimer's disease is a major global health challenge. Diagnosis based on clinical presentation alone is challenging since early symptoms often overlap with those of other neurodegenerative and medical conditions. In vivo biomarkers of Alzheimer's disease pathology (i.e., amyloid-β and tau) can strengthen diagnosis and guide treatment. However, different biomarkers are not always in agreement, and the best diagnostic tests are often the most burdensome in terms of cost, invasiveness, and time. Motivated by these challenges, this thesis aims to improve Alzheimer's disease diagnostics and biomarkers by enhancing accuracy, agreement, and cross-modality prediction for fluid biomarkers, cognitive assessments, and brain imaging. To this end, large, deeply phenotyped clinical datasets (including the Swedish BioFINDER cohorts and several international cohorts) were analyzed with advanced statistical and machine learning methods to identify biological patterns and develop clinically relevant prediction models.

This thesis is structured around three main aims. First, unsupervised machine learning was used to investigate co-varying properties of the cerebrospinal fluid proteome. Adjusting for such co-variations via reference protein normalization improved agreement with imaging-based measures for multiple fluid biomarkers, supporting more consistent quantification of biological Alzheimer's disease constructs (Papers I and II). Second, a self-administered, digital cognitive test battery was evaluated, which improved assessments of objective cognitive impairment in primary care. Combining the digital test with a blood biomarker resulted in high diagnostic accuracy and could be a scalable approach to improve evaluations of symptomatic Alzheimer's disease (Paper III). Third, machine learning models were developed that could estimate regional or global positron emission tomography (PET) patterns from more accessible variables. PET provides unique three-dimensional in vivo information on Alzheimer's disease pathology, but is costly and not widely available. The models offer a way to predict PET-derived information in settings where PET cannot be implemented (Papers IV, V and VI).

In conclusion, this thesis contributes to improving accuracy, agreement, and cross-modality prediction of Alzheimer's disease tests and biomarkers. It also demonstrates how a translational data science and neuroscience approach can generate clinically relevant insights and help bridge interdisciplinary collaboration and knowledge exchange.

Key words: Alzheimer's disease, biomarkers, diagnostics, neurodegeneration, machine learning, multimodal data

Classification system and/or index terms (if any) Supplementary bibliographical information

Language: English **Number of pages:** 113

ISSN and key title: 1652-8220

ISBN: 978-91-8021-865-8

Recipient's notes Price Security classification

Signature Date 2026-03-27

Data Analysis to Improve Diagnostics and Biomarkers in Alzheimer's Disease

Building Bridges Between Data Science and Neuroscience

Linda Karlsson

LUND
UNIVERSITY

Cover image by Google's AI tool Nano Banana Pro (concept by Linda Karlsson).

Published by:
Department of Clinical Sciences, Malmö
Faculty of Medicine
Lund University
Lund 2026

ISBN 978-91-8021-865-8
Series title: Lund University, Faculty of Medicine Doctoral Dissertation Series 2026:67
ISSN 1652-8220

Printed in Sweden by Media-Tryck, Lund University,
Lund, 2026

Media-Tryck is a Nordic Swan Ecolabel certified provider of printed material. Read more about our environmental work at www.mediatryck.lu.se
MADE IN SWEDEN

Table of Contents

Abstract

Alzheimer's disease is a major global health challenge. Diagnosis based on clinical presentation alone is challenging since early symptoms often overlap with those of other neurodegenerative and medical conditions. In vivo biomarkers of Alzheimer's disease pathology (i.e., amyloid-β and tau) can strengthen diagnosis and guide treatment. However, different biomarkers are not always in agreement, and the best diagnostic tests are often the most burdensome in terms of cost, invasiveness, and time. Motivated by these challenges, this thesis aims to improve Alzheimer's disease diagnostics and biomarkers by enhancing accuracy, agreement, and cross-modality prediction for fluid biomarkers, cognitive assessments, and brain imaging. To this end, large, deeply phenotyped clinical datasets (including the Swedish BioFINDER cohorts and several international cohorts) were analyzed with advanced statistical and machine learning methods to identify biological patterns and develop clinically relevant prediction models.

This thesis is structured around three main aims. First, unsupervised machine learning was used to investigate co-varying properties of the cerebrospinal fluid proteome. Adjusting for such co-variations via reference protein normalization improved agreement with imaging-based measures for multiple fluid biomarkers, supporting more consistent quantification of biological Alzheimer's disease constructs (Papers I and II).

Second, a self-administered, digital cognitive test battery was evaluated, which improved assessments of objective cognitive impairment in primary care. Combining the digital test with a blood biomarker resulted in high diagnostic accuracy and could be a scalable approach to improve evaluations of symptomatic Alzheimer's disease (Paper III).

Third, machine learning models were developed that could estimate regional or global positron emission tomography (PET) patterns from more accessible variables. PET provides unique three-dimensional in vivo information on Alzheimer's disease pathology, but is costly and not widely available. The models offer a way to predict PET-derived information in settings where PET cannot be implemented (Papers IV, V and VI).

In conclusion, this thesis contributes to improving accuracy, agreement, and cross-modality prediction of Alzheimer's disease tests and biomarkers. It also demonstrates how a translational data science and neuroscience approach can generate clinically relevant insights and help bridge interdisciplinary collaboration and knowledge exchange.

Popular scientific summary
(English)

The risk of developing dementia increases with age, and dementia is becoming a growing societal challenge as more people live longer. Alzheimer's disease is the most common form, accounting for about 60-80% of dementia cases. In Alzheimer's disease, two brain proteins (amyloid-β and tau) separately start to form clumps that the body cannot clear away. Over time, this damages brain cells and leads to typical symptoms, such as memory loss and trouble handling daily tasks. Early, accurate, and accessible diagnosis is important to make sure patients get the best available care.

Making a correct Alzheimer's diagnosis can be challenging, especially in the early disease stages. Memory naturally changes with age, and memory problems can also be caused by, for example, sleep loss, depression, or other illnesses. Clinicians therefore often use cognitive tests to establish whether memory, language, or problem solving are more impaired than expected. Furthermore, to make an accurate Alzheimer's diagnosis, it is important to examine if the two Alzheimer's proteins are actually present in the brain. This can be done with "biomarkers", which are measurements that capture changes in the body that are related to the disease. In an Alzheimer's work-up, clinicians can either use brain images that make it possible to see the clumps of amyloid-β and tau, or measure the concentration of these proteins in blood or cerebrospinal fluid (the fluid that surrounds the brain). However, these methods are not always in agreement with each other, and the best diagnostic tests are usually advanced, time-consuming, and expensive.

To address disagreement and burden of diagnostic tests, this thesis analyzes data from large clinical Alzheimer's studies where older volunteers underwent extensive evaluations: various types of cognitive tests, brain imaging, and protein measurements in body fluids. Combining many different measurements quickly creates large, complex datasets that we can learn much about the disease from. Such complex data sometimes require advanced approaches to better understand them, motivating the use of methods where computers are trained to recognize patterns and make predictions. By combining medicine and technology, the thesis addresses three specific goals related to improving fluid biomarkers, cognitive tests, and costly brain imaging.

First, we investigated why cerebrospinal fluid biomarker measures can mean different things in different people. By measuring thousands of proteins in cerebrospinal fluid, we found that individuals have different baseline protein levels, and knowing someone's baseline helps decide whether a biomarker is truly changed by disease or not. Imagine you want to compare how much coffee grounds were used to brew two cups of coffee, but you are only allowed to analyze a single drop from each cup. Here, each cup represents a person, and the coffee grounds the biomarker. If one cup is an espresso and the other is filter coffee, the drop will look very different even if the same amount of grounds was used. We identified "reference proteins" that act like a proxy for such individual differences in cerebrospinal fluid and showed in Papers I and II that they can make Alzheimer's disease biomarkers more accurate.

The second goal was to evaluate a digital cognitive test in primary care, the usual first point of contact for people with cognitive complaints. A digital format allows patients to complete the test more independently, which reduces the workload for healthcare staff. It also makes it possible to collect more detailed information than just the final test scores, for example, the time it took to complete different parts of the test. In Paper III, we found that a digital test gave better diagnostic accuracy compared with the methods commonly used today, which largely rely on paper-and-pencil tests administered by clinicians. Combining the test with a blood biomarker showed promising results and may offer a time- and cost-effective way to improve Alzheimer's disease diagnostics even when specialist resources are limited.

Finally, we trained computers to make virtual "PET images", which is an advanced brain imaging technique. PET is currently the method that most clearly shows where Alzheimer's disease proteins are located in the brain, but the technique is costly and not widely available across hospitals. In Papers IV, V, and VI, we therefore developed models that can estimate PET information from more accessible data such as fluid biomarkers and other kinds of brain imaging. These models can make some of the unique information from PET available in situations when real PET scans cannot be used.

In summary, this thesis takes several steps toward better Alzheimer's disease diagnostics, including more robust interpretation of biomarkers, more practical cognitive testing tools, and new computer-based approaches to make advanced and costly diagnostic information more accessible.

Populärvetenskaplig sammanfattning
(Svenska)

Risken att utveckla demens ökar med åldern och demens är idag ett samhällsproblem som växer i takt med att allt fler människor lever längre. Alzheimers sjukdom är den vanligaste formen av demens och står för 60–80% av fallen. Vid Alzheimers sjukdom börjar två proteiner som finns naturligt i hjärnan, amyloid-β och tau, klumpa ihop sig okontrollerat utan att kroppen lyckas städa bort dem. Detta leder så småningom till att nervceller slutar fungera, vilket kan ge typiska symtom som minnesproblem och svårigheter att klara av vardagen själv. Tidig, träffsäker och lättillgänglig Alzheimerdiagnostik är viktigt eftersom det möjliggör att varje patient kan få bästa möjliga vård.

Det kan vara svårt att ställa en korrekt Alzheimerdiagnos, framför allt tidigt i sjukdomsförloppet. Minnet försämras naturligt med åldern och minnesbesvär utöver det normala kan också bero på till exempel sömnbrist, depression eller andra sjukdomar. Vanligen används kognitiva tester för att mer objektivt mäta om exempelvis minne, språk eller problemlösning är tydligt försämrade hos en patient. Idag har det också blivit allt viktigare att bekräfta att Alzheimer-förändringar faktiskt finns i hjärnan innan en diagnos ställs. Detta kan göras med hjälp av ”biomarkörer” som mäter biologiska förändringar i kroppen. I en Alzheimerutredning kan man antingen ta bilder av hjärnan som kan visa om proteinklumpar av amyloid-β och tau finns, eller så kan man mäta koncentrationer av dessa proteiner i blod eller cerebrospinalvätska (vätskan runt hjärnan). Ibland kan man dock få olika resultat beroende på vilken metod man använt, och de mest tillförlitliga metoderna är oftast också dyrast och mest resurskrävande.

Den här avhandlingen tar itu med sådana inkonsekventa, omfattande och dyra diagnostikmetoder genom att analysera data från stora kliniska Alzheimerstudier där äldre frivilliga studiedeltagare har genomgått omfattande undersökningar, till exempel olika typer av kognitiva tester, hjärnavbildningar och mätningar av proteiner i kroppsvätskor. När många olika mätningar kombineras blir datamängden snabbt stor, och enkla metoder räcker inte alltid för att förstå mer komplexa samband. Vi använde därför mer avancerade metoder där datorer tränas för att känna igen mönster och göra förutsägelser baserat på stora datamängder. Genom att kombinera medicin och teknik undersöks tre specifika frågeställningar med slutmålet att förbättra biomarkörer i kroppsvätskor, kognitiva tester och dyra bildmetoder.

För det första studerade vi varför samma biomarkörmätning i cerebrospinalvätska kan behöva tolkas olika för olika personer. Genom att mäta tusentals proteiner såg vi att människor kan ha olika grundnivå av proteiner i cerebrospinalvätska. Om man har information om denna nivå kan man bättre tolka om en biomarkör är förändrad på grund av en sjukdom eller inte. Tänk dig att du vill jämföra mängden kaffepulver som användes för att brygga två olika koppar kaffe, men du får bara mäta på en droppe från varje kopp. Här representerar varje kopp en person, och mängden kaffepulver en biomarkör. Om den ena koppen är en espresso och den andra är en bryggkaffe kan skillnaderna se stora ut även om mängden kaffepulver från början var densamma. Vi identifierade ”referensproteiner” som kan fungera som ett slags mått för sådana individuella skillnader i cerebrospinalvätska, och visade i Artikel I och II att detta kan göra Alzheimerbiomarkörer mer träffsäkra.

Det andra målet var att utvärdera hur ett kognitivt test i digitalt format fungerade på vårdcentraler, vilket ofta är första stället patienter besöker vid en vårdutredning. Genom att göra testet digitalt kan patienten sitta självständigt vilket minskar belastningen på vårdpersonal. Man kan samtidigt lättare samla in mer detaljerad information än bara testpoäng, till exempel hur lång tid olika testmoment tar. I Artikel III såg vi att ett digitalt test gjorde diagnostiken mer träffsäker jämfört med de metoder som idag används, som är baserade på framför allt papper-och-penna-tester utförda tillsammans med sjukvårdspersonal. Att kombinera testet med ett blodprov gav lovande resultat, och kan vara ett tids- och kostnadseffektivt sätt att förbättra Alzheimer-diagnostik även utan specialistresurser.

Slutligen tränade vi datorer att skapa konstgjorda ”PET-bilder”, vilket är en avancerad metod för att ta bilder på hjärnan. PET är idag den metod som tydligast kan visa var i hjärnan Alzheimerproteiner finns, men undersökningen är dyr och svårtillgänglig. I Artikel IV, V och VI utvecklade vi modeller som kan skatta PET-information baserat på mer lättillgängliga data som till exempel biomarkörer i vätskor och andra typer av hjärnbilder. Genom sådana modeller kan delar av den unika information som PET ger bli mer tillgänglig även i situationer där riktiga PET-bilder inte kan användas.

Sammanfattningsvis bidrar avhandlingen med flera steg mot bättre Alzheimerdiagnostik: mer robust tolkning av biomarkörer, mer praktiska kognitiva testverktyg, och nya datorbaserade sätt att göra avancerade och dyra bildtekniker mer lättillgänglig.

Original papers and manuscripts included in this thesis

I. **Karlsson L**., Vogel J., Arvidsson I., Åström K., Janelidze S., Blennow K., Palmqvist S., Stomrud E., Mattsson-Carlgren N., Hansson O. Cerebrospinal fluid reference proteins increase accuracy and interpretability of biomarkers for brain diseases. *Nature Communications* 15:3676 (2024). doi: 10.1038/s41467-024-47971-5

II. **Karlsson L**., Janelidze S., Barthélemy N.R., Horie K., Therriault J., Gaetani L., Bellomo G., Schindler S.E., Vogel J., Arvidsson I., Åström K., Gordon B.A., Raji C.A., Benzinger T.L.S., Morris J.C., Nilsson J., Brinkmalm A., Palmqvist S., Stomrud E., Salvadó G., Pichet Binette A., Di Filippo M., Parnetti L., Rosa-Neto P., Blennow K., Bateman R.J., Mattsson-Carlgren N., Hansson O. Reference proteins to improve Core 1 and Core 2 Alzheimer's disease CSF and plasma biomarkers. *Brain* awaf375 (2026). doi: 10.1093/brain/awaf375

III. Tideman P.*, **Karlsson L.***, Strandberg O., Calling S., Smith R., Midlöv P., Verghese P.B., Braunstein J.B., Mattsson-Carlgren N., Stomrud E., Palmqvist S., Hansson O. Primary care detection of Alzheimer's disease using a self-administered digital cognitive test and blood biomarkers. *Nature Medicine* 31:4131-4139 (2025). doi: 10.1038/s41591-025-03965-4
Associated Research Briefing: **Karlsson L.** and Hansson O. A brief digital cognitive test improves Alzheimer's disease detection. *Nature Medicine* 31:3998-3999 (2025). doi: 10.1038/s41591-025-04024-8

IV. Mattsson-Carlgren N.*, **Karlsson L.***, Tang W., Blennow K., Zetterberg H., Bateman R.J., Schindler S.E., Barthelemy N., Palmqvist S., Stomrud E., Janelidze S., Hansson O. Prediction of continuous amyloid positron emission tomography with fluid measures of phosphorylated tau and β-amyloid. *EMBO Molecular Medicine* 18:217-231 (2026). doi: 10.1038/s44321-025-00348-7

V. **Karlsson L.**, Vogel J., Arvidsson I., Åström K., Strandberg O., Seidlitz J., Bethlehem R.A.I., Stomrud E., Ossenkoppele R., Ashton N.J., Zetterberg H., Blennow K., Palmqvist S., Smith R., Janelidze S., La Joie R., Rabinovici G.D., Pichet Binette A., Mattsson-Carlgren N., Hansson O. Machine learning prediction of tau-PET in Alzheimer's disease using plasma, MRI, and clinical data. *Alzheimer's & Dementia* 21:e14600 (2025). doi: 10.1002/alz.14600

VI. **Karlsson L**., Strandberg O., Smith R., Tang W., Arvidsson I., Åström K., Oliveira Hauer K., Janelidze S., Stomrud E., Alzheimer's Disease Neuroimaging Initiative, PREVENT-AD Research Group, Palmqvist S., Jagust W.J., Villeneuve S., La Joie R., Rabinovici G.D., Mattsson-Carlgren N., Vogel J.W., Hansson O. Generating synthetic tau-PET scans in Alzheimer's disease from MRI, blood biomarkers and demographics with deep learning. *Manuscript.*

Author's contribution to the papers

I. L.K. performed all data analyses and drafted and revised the manuscript. She contributed to study design and data interpretations together with co-authors.

II. L.K. performed all data analyses and drafted and revised the manuscript. She contributed to study design and data interpretations together with co-authors.

III. L.K. performed the statistical analyses with support from Pontus Tideman. She drafted and revised the manuscript together with Pontus Tideman. She contributed to study design and data interpretations together with co-authors. She drafted the research briefing and revised it together with Oskar Hansson.

IV. L.K. performed data analyses together with Weizhong Tang, she edited the manuscript and revised it together with Niklas Mattsson-Carlgren. She contributed to study design and data interpretations together with co-authors.

V. L.K. performed all data analyses and drafted and revised the manuscript. She contributed to study design and data interpretations together with co-authors.

VI. L.K. performed all data analyses and drafted the manuscript. She contributed to study design and data interpretations together with co-authors.

Original papers and manuscripts not included in this thesis

I. Mattsson-Carlgren N., Collij L.E., Stomrud E., Pichet Binette A., Ossenkoppele R., Smith R., **Karlsson L.**, Lantero-Rodriguez J., Snellman A., Strandberg O., Palmqvist S., Ashton N.J., Blennow K., Janelidze S., Hansson O. Plasma biomarker strategy for selecting patients with Alzheimer disease for antiamyloid immunotherapies. *JAMA Neurology* 81: 69-78 (2024). doi: 10.1001/jamaneurol.2023.4596

II. Oh H.S.H., Urey D.Y., **Karlsson L.**, Zhu Z., Shen Y., Farinas A., Timsina J., Duggan M.R., Chen J., Guldner I.H., Morshed N., Yang C., Western D., Ali M., Le Guen Y., Trelle A., Herukka S-K., Rauramaa T., Hiltunen M., Lipponen A., Luikku A.J., Poston K.L., Mormino E., Wagner A.D., Wilson E.N., Channappa D., Leinonen V., Stevens B., Ehrenberg A.J., Gottesman R.F., Coresh J., Walker K.A., Zetterberg H., Bennett D.A., Franzmeier N., Hansson O., Cruchaga C., Wyss-Coray T. A cerebrospinal fluid synaptic protein biomarker for prediction of cognitive resilience versus decline in Alzheimer's disease. *Nature Medicine* 31: 1592-1603 (2025). doi: 10.1038/s41591-025-03565-2

III. Ossenkoppele R., Salvadó G., Janelidze S., Pichet Binette A., Bali D., **Karlsson L.**, Palmqvist S., Mattsson-Carlgren N., Stomrud E., Therriault J., Rahmouni N., Rosa-Neto P., Coomans E.M., van de Giessen E., van der Flier W.M., Teunissen C.E., Jonaitis E.M., Johnson S.C., Villeneuve S., PREVENT-AD Research Group, Benzinger T.L.S., Schindler S.E., Bateman R.J., Doecke J.D., Dore V., Feizpour A., Masters C.L., Rowe C., Wiste H.J., Petersen R.C., Jack C.R. Jr., Hansson O. Plasma p-tau217 and tau-PET predict future cognitive decline among cognitively unimpaired individuals: implications for clinical trials. *Nature Aging* 5: 883-896 (2025). doi: 10.1038/s43587-025-00835-z

IV. Chaggar P., Vogel J.W., Pichet Binette A., Thompson T.B., Strandberg O., Mattsson-Carlgren N., **Karlsson L.**, Stomrud E., Jbabdi S., Magon S., Klein G., Alzheimer's Disease Neuroimaging Initiative, Hansson O., Goriely A. Personalised regional modelling predicts tau progression in the human brain. *PLOS Biology* 23: e3003241 (2025). doi: 10.1371/journal.pbio.3003241

V. Anijärv T.E., Ossenkoppele R., Smith R., Pichet Binette A., Collij L.E., Behjat H.H., Rittmo J., **Karlsson L.**, Ahmadi K., Strandberg O., van Westen D., Vogel J.W., Stomrud E., Palmqvist S., Mattsson-Carlgren N., Spotorno N., Hansson O. Hemispheric asymmetry of tau pathology is related to asymmetric amyloid deposition in Alzheimer's disease. *Nature Communications* 16: 8232 (2025). doi: 10.1038/s41467-025-63564-2

VI. Hristovska I., Pichet Binette A., Kumar A., Gaiteri C., **Karlsson L.**, Strandberg O., Janelidze S., van Westen D., Stomrud E., Palmqvist S., Ossenkoppele R., Mattsson-Carlgren N., Vogel J.W., Hansson O. Identification of distinct and shared biomarker panels in different manifestations of cerebral small-vessel disease through proteomic profiling. *Nature Aging* (2026). doi: 10.1038/s43587-026-01081-7

VII. Obara K., Janelidze S., Ito D., **Karlsson L.**, Yamamoto M., Tran S., Tsujikawa K., Nishio Y., Ogi T., Nakamura R., Atsuta N., Sobue G., Nilsson C., Katsuno M., Mattsson-Carlgren N. Complementary roles of cerebrospinal fluid amyloid and neurodegeneration biomarkers in the diagnosis and prognosis of amyotrophic lateral sclerosis. *Submitted manuscript.*

VIII. Winzell F., Arvidsson I., Overgaard N.C., Heyden A., Åström K., **Karlsson L.**, Vogel J., Hansson O., Mattsson-Carlgren N. Synthetic Alzheimer's disease dataset generation and evaluation with privacy protection. *Submitted manuscript*.

IX. Bali D., Salvadó G., **Karlsson L.**, Ashton N.J., Palmqvist S., Lantero Rodriguez J., Stomrud E., Mattsson-Carlgren N., Janelidze S., Hansson O. Tracking Alzheimer´s disease progression using longitudinal CSF and plasma biomarkers and their ratios to Aβ40. *Manuscript in prep.*

X. Rabow O., **Karlsson L.**, Cumplido Mayoral I., Janelidze S., Stomrud E., Palmqvist S., Zendehdel R., Zhao R., An L., Vogel J., Hansson O., Mattsson-Carlgren N. Multimodal Biomarkers of biological brain age: integrating brain structure and proteomics for age predictions. *Manuscript in prep.*

XI. Smith R., **Karlsson L.**, Janelidze S., Stomrud E., Palmqvist S., Hansson O., Mattsson-Carlgren N. Determining the prognostic performance of cerebrospinal fluid neurofilament light with and without reference protein adjustment. *Manuscript in prep.*

Abbreviations

Aβ	Amyloid-β
AD	Alzheimer's disease
AI	Artificial intelligence
AIC	Akaike information criterion
APOE	Apolipoprotein E
APP	Amyloid precursor protein
ARIA	Amyloid-related imaging abnormalities
AUC	Area under the curve
CI	Confidence interval
CNN	Convolutional neural network
CNS	Central nervous system
CSF	Cerebrospinal fluid
CU	Cognitively unimpaired
FDR	False discovery rate
LI	Laterality index
MAE	Mean absolute error
MAPE	Mean absolute percentage error
MAPT	Microtubule associated protein tau
MCI	Mild cognitive impairment
ML	Machine learning
MRI	Magnetic resonance imaging
MSE	Mean squared error
MTBR	Microtubule binding region
NC	Normal cognition

np-tau	Non-phosphorylated tau
NfL	Neurofilament light
NFTs	Neurofibrillary tangles
PET	Positron emission tomography
p-tau	Phosphorylated tau
RFE	Recursive feature elimination
ROI	Region of interest
SCD	Subjective cognitive decline
SUVR	Standardized uptake value ratio
SVD	Singular value decomposition
t-SNE	t-distributed stochastic neighbor embedding

Introduction

The aging brain and increasing burden of dementia

The human brain is often described as the most complex known biological structure. Beyond regulating vital functions and enabling sensory-motor control, it is also the basis of identity, memory, language, and consciousness, making it challenging to study, yet crucial to understand from a public health perspective. Throughout the human lifespan, the brain shows impressive adaption and plasticity. By early adulthood (20-40 years), most neurodevelopmental milestones in terms of size and growth rate have been reached [1]. Thereafter, brain tissue volume gradually decreases, and by late adulthood, the brain shows loss of protein homeostasis (proteostasis) [2,3] alongside a drastically increased risk of developing neurodegenerative diseases like dementia.

The lifetime risk at age 65 years of developing dementia was estimated to 22% in females and 14% in males in 2007 [4]. New estimates from 2025 reported an even higher lifetime risk of 48% in females and 35% in males at age 55 years [5]. From an individual perspective, these risk calculations highlight that many will be directly or indirectly affected by this devastating syndrome during their lifetime.

From a societal perspective, the estimates are equally severe. Given the growing world population and increased life expectancy, the number of individuals with dementia is projected to rise from 57.4 million in 2019 to 153 million in 2050 [6]. The average annual cost per person with dementia, including direct (e.g. medical, social, and residential care) and indirect (e.g., informal caregiver time) costs, has been estimated to 7,940-73,700 EUR in Europe [7], and 43,900 USD in the United States [8].

Together, these numbers reflect the growing immense human, social, and economic burden of dementia, motivating global efforts toward prevention, timely detection, and effective intervention.

Alzheimer's disease

Alzheimer's disease (AD) is the most common neurodegenerative disease, accounting for 60–80 % of all cases [9]. AD was named after the German psychiatrist Alois Alzheimer. In a case study in 1907, Alzheimer described the neuropathological changes and clinical syndrome he observed in his 51-year-old patient [10]. Although the reported symptoms were informative, we know today that this was a rather atypical AD case due to the patient's relatively young age, and since the clinical presentations can be very heterogenous. The key generalizable discovery described by Alzheimer was the neuropathological changes of AD in form of aggregated protein fibrils inside the brain. These proteins, amyloid (A)-β and tau, together with neurodegeneration and cognitive and functional decline, maintain the hallmarks defining AD today.

Neuropathological and clinical hallmarks

Amyloid-β

The production of Aβ peptides occurs during processing of the transmembrane amyloid precursor protein (APP). APP is highly expressed in neurons and has important functions related to brain development, neuronal plasticity, memory, and neuroprotection [11]. At the cell surface, APP is cleaved into biologically active fragments by secretases (specific enzymes) in two main pathways: the non-amyloidogenic (α-secretase and γ-secretase) and the amyloidogenic (β-secretase and γ-secretase) [11]. The amyloidogenic pathway produces Aβ peptides that are 37 to 49 amino acids in length (monomers), with Aβ40 (40 amino acids) being the most abundant one, but Aβ42 (42 amino acids) being more central in AD [12].

Aβ monomers can aggregate into various structures: from small, soluble oligomers, to large, insoluble fibrils and amyloid plaques [12]. Although the specific function of endogenous Aβ is not yet fully understood, multiple beneficial effects have been demonstrated related to for example nervous system repairment, protective capacity against pathogens, and regulation of synaptic activity [13]. Furthermore, preventing Aβ production to a high degree (>50%) through β-secretase inhibitors has resulted in adverse events and worsening of cognition, highlighting the peptides' essential role in brain health [14–16].

Normally, Aβ levels are regulated through multiple degradation pathways [17], but in AD, Aβ peptides accumulate in an abnormally extensive manner in the brain, resulting in extracellular deposits of Aβ plaques (Fig. 1) [12]. Aβ usually starts to aggregate in i) the neocortex, followed by ii) allocortex iii) diencephalic nuclei and striatum, iv) brainstem, and finally v) cerebellum [18]. The plaques consist mainly of Aβ42 peptides, and due to the aggregation, the cerebrospinal fluid (CSF) level of soluble Aβ42 peptides is reduced by ~50% [19,20]. The process of Aβ accumulation is slow and protracted, often initiated decades before symptom onset [21].

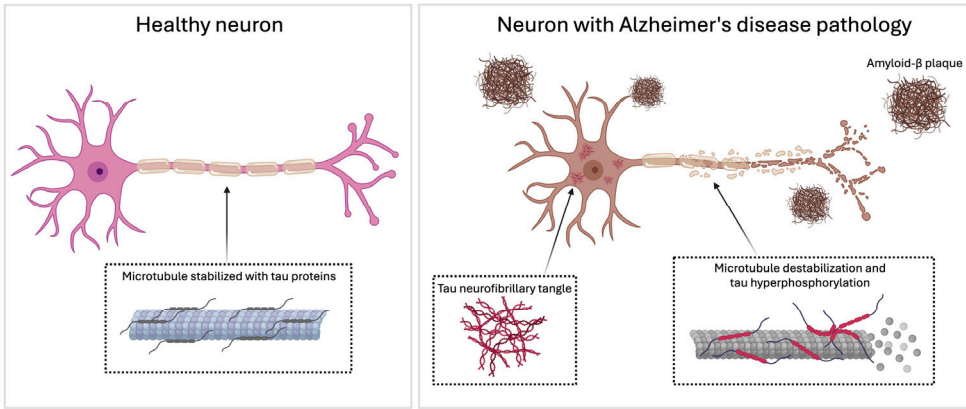

Figure 1. Neuropathological hallmarks of Alzheimer's disease. Left panel: a healthy neuron with tau proteins stabilizing the microtubule. Right panel: a degenerating neuron with extracellular Aβ-plaques and intracellular tau neurofibrillary tangles (NFTs). Tau proteins are hyperphosphorylated and can no longer stabilize the microtubule. Figure created with Biorender.

Even though abnormal Aβ pathology is a hallmark of AD and usually evident in older individuals with mild or severe cognitive impairment, its likelihood to be present in a person without cognitive symptoms is also pronouncedly increased with age. Population estimates have highlighted an increasing prevalence from approximately 20% to 40% comparing ages 60 and 80 years [22]. This suggests that in late life, even without cognitive impairment, abnormal Aβ accumulation is almost as common as its absence.

Tau

Tau proteins are produced through alternative splicing of transcripts from the microtubule-associated protein tau (MAPT) gene. In the human brain, six tau isoforms are expressed, defined by the number of N-terminal inserts (0N, 1N or 2N) and the number of C-terminal microtubule binding repeat domains (3R or 4R). In the healthy adult brain, 3R and 4R tau are expressed at approximately similar levels, and both isoforms aggregate in AD [23].

Tau is normally a soluble, microtubule-associated protein that contributes to cytoskeletal stability and supports intracellular transport. Under ordinary conditions, tau is phosphorylated at a limited number of sites, but in AD, the extent of phosphorylation increases by several-folds [24]. This hyper-phosphorylation promotes tau misfolding and insufficient stabilization of microtubules, leading to impaired neuronal functions (Fig. 1). Subsequently, tau fibrillizes into paired helical filaments and neurofibrillary tangles (NFTs). In contrast to extracellular Aβ plaques, tau deposits are primarily found intracellularly, accumulating in neuronal cell bodies and dendrites [23,25].

Pathogenic tau is suggested to have prion-like seeding and spreading properties, meaning that misfolded tau can induce other connected cells to also start having abnormal tau hyperphosphorylation. This could result in the progressive, cell-to-cell spreading of tau pathology in a chain-reaction-like manner [26].

In AD, tau pathology usually spreads in a similar spatial pattern comparing different individuals, forming the basis of a commonly used tau staging scheme called Braak staging. NFTs typically first appear in the entorhinal cortex (Stage I-II), then spread to the hippocampus and limbic regions (Stage III-IV), and finally to widespread neocortical areas (Stage V-VI) [27,28]. However, a growing body of evidence suggest that this may be an oversimplification, highlighting a substantial inter-individual variability in tau deposition patterns [29]. Accordingly, tau accumulation may be better described by subtyping or other more individualized approaches. Commonly reported tau subtypes include limbic-predominant and hippocampal-sparing variants, as well as lateralized tau deposition patterns [30–34].

Similarly to Aβ pathology, the likelihood of abnormal tau hyper-phosphorylation increases with age. Population-based estimates suggest a prevalence of <8% in individuals younger than 70 years, rising to ~65% in those aged 90+ years [35]. However, because tau hyperphosphorylation precedes tau aggregation and NFT formation, the prevalence of tau aggregation is likely substantially lower. This is discussed further in the section *Progression over time.*

Neurodegeneration

Neurodegeneration refers to the progressive loss of structure and function of neurons, ultimately leading to synaptic loss and cell death. Even in the absence of neuropathological changes, brain tissue volume shows a gradual decline with advancing age [1]. In AD, however, neurodegeneration is usually more extensive and regionally selective. Prominent neuronal loss and atrophy are typically seen first in the medial temporal lobe, most notably in the entorhinal cortex and hippocampus, as well as ventricular enlargement and atrophy in the temporoparietal cortex [36–39]. However, consistent with variations in tau deposition patterns, individual atrophy patterns can also be heterogenous and may be better described through subtyping than through a “one-fits-all” framework [40,41].

Due to the complex functional organization of the brain, neurons are largely connected through networks. These networks have been suggested as a possible reason why neurodegeneration follows certain atrophy patterns; later-affected brain regions are often anatomically connected to earlier affected sites [42].

Cognitive and functional decline

Cognition is a broad term that includes multiple domains (e.g., complex attention, executive function, learning and memory, language, perceptual-motor function, and social cognition [43]). Cognitive impairment can be assessed objectively using

neuropsychological tests tailored to the different domains [44]. In AD, memory is typically the earliest and most affected domain, but clinical presentations can be heterogenous and may involve other cognitive domains as well [45]. Moreover, clinical symptoms often overlap across neurodegenerative disorders, making it difficult to disentangle etiology based solely on symptoms [45].

In addition to cognitive decline, AD symptoms can include difficulties in performing activities in daily life, referred to as functional impairment. Functional impairment is commonly assessed through medical history taking from the patient and informants and complemented by standardized questionnaires and rating scales. Activities of daily living that typically become more demanding in mild dementia are housework and managing money. As symptoms progress, more basic activities like eating and dressing can also become challenging, eventually leading to full dependence [46].

The progression of clinical symptoms is gradual. But despite their continuous nature, to facilitate comparisons, cognitive staging is commonly performed using four categories. These categories are normal cognition (NC), subjective cognitive decline (SCD), mild cognitive impairment (MCI) and dementia (Tab. 1). Since SCD is not objectively measurable, the NC and SCD groups are sometimes combined into a cognitively unimpaired (CU) group [47].

Table 1. Syndromal staging for individuals in the Alzheimer's disease continuum, defined 2018 by the National Institute on Aging - Alzheimer's Association (NIA-AA) [47].

Clinical staging	Clinical category	Description
Stage 1	NC	Cognitive test performance within the expected range. No self- or observer report of cognitive decline.
Stage 2	SCD	Cognitive test performance within the expected range. Self-reported and/or informant/clinician documented cognitive decline. No functional impairment in daily activities.
Stage 3	MCI	Cognitive test performance below the expected range. Self-reported and/or informant/clinician-documented cognitive decline. Largely preserved daily functioning, with mild difficulties in complex activities.
Stage 4	Dementia	(Mild) Self-reported and/or informant/clinician-documented progressive cognitive impairment affecting several domains. Clear functional impairment in daily activities and no longer fully independent.
Stage 5		(Moderate) Progressive cognitive impairment and extensive functional impairment in basic activities. No longer independent.
Stage 6		(Severe) Progressive cognitive impairment and severe functional impairment in basic activities. Complete dependence.

Abbreviations: NC (Normal cognition), SCD (subjective cognitive decline), MCI (mild cognitive impairment).

Progression over time

The progression of AD hallmarks is long and protracted, and is typically conceptualized as a temporally ordered process: the first abnormal brain change being an altered metabolism of soluble Aβ, followed by Aβ plaque buildup,

increasing levels of hyperphosphorylated soluble tau, NFTs, neuro-degeneration, and finally cognitive and functional impairment (Fig. 2) [48–50]. Early Aβ pathological changes have not been proven to be causative in AD, but the amyloid cascade hypothesis [51] remains the dominant theory.

Several studies provide evidence broadly supporting this chain of events. For example, brain Aβ and tau aggregation have been linked to loss of neurons and network dysfunction, highlighting their neurotoxicity. Typically, disturbance of neuronal networks like hyperexcitability and synaptic failure appear to precede neuronal loss [52]. Furthermore, a large-scale multicenter study highlighted that aggregated tau deposition is substantially more common in individuals who already have pathological Aβ than in those without, which was observed across all cognitive stages [53]. In line with this, cognitively unimpaired individuals with Aβ and tau pathology have been shown to be at higher risk for future cognitive decline compared to those without [54]. Additionally, regional brain atrophy closely follows tau deposition patterns [55], and downstream relates to heterogenous clinical syndromes and different rates of disease progression [30,40].

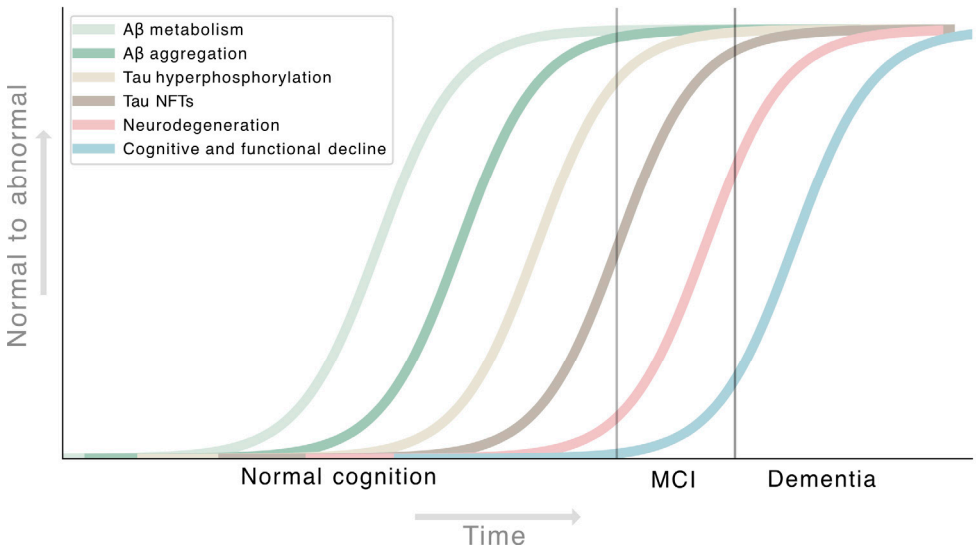

Figure 2. Schematic illustration of the typical temporal progression of the Alzheimer's disease hallmarks, modified from Jack et al. [48]. The abnormal brain changes start with an altered metabolism of soluble Aβ, followed by Aβ plaque buildup, hyperphosphorylation of soluble tau, NFTs, neurodegeneration, and finally cognitive and functional impairment. Abbreviations: Aβ (amyloid-β), NFT (neurofibrillary tangles), MCI (mild cognitive impairment).

Considering the evidence supporting pathological changes to be upstream of clinical symptoms, and since Aβ accumulation can begin decades before symptom onset [21], the window to intervene in the AD pathway is believed to be long. This has

also led to increased discussions about whether AD should be defined as a biological process independent of clinical symptoms, or a clinical-biological construct requiring clinical impairment [50,56,57]. Regardless of definition, this long preclinical phase strengthens the idea that efforts against AD may be most effective in early disease stages, and supports continued work toward timely, accurate detection and diagnosis [58,59].

Genetics

Genetic findings provide complementary evidence that mechanisms related to the Aβ pathway underlie AD dementia. The most common form of AD is sporadic, late-onset AD. Although sporadic AD is non-monogenic, its heritability is high, estimated to >50% in twin studies [60]. The strongest and most established susceptibility gene for sporadic AD is apolipoprotein E (*APOE*), which influences Aβ metabolism and aggregation [61]. *APOE* has three alleles (ε2, ε3, ε4), of which ε3 is most common, ε4 is associated with increased AD risk and earlier onset, and ε2 has a protective effect [62,63]. Still, *APOE* explains only part of the genetic risk, and large-scale genome-wide association studies have identified more than 70 loci associated with late onset-AD [64,65]. This highlights the complexity of the disease and possible involvement of multiple biological pathways.

In contrast, rare autosomal-dominant forms of AD (familial AD) are caused by highly penetrant mutations. The most common mutations are in *APP*, *PSEN1*, or *PSEN2*, which affect APP processing and typically increase production or relative abundance of aggregation-prone Aβ fragments [66]. Notably, while mutations in *MAPT* can cause familial frontotemporal dementia, comparable high-penetrance tau mutations are not a typical cause of AD [67]. Together, genetic findings implicate alterations in the Aβ pathway as a core component of AD biology.

Co-pathologies

At older ages, it is common that AD pathology co-occurs with other brain pathologies. Prevalent co-pathologies are aggregation of TAR DNA-binding protein 43 (TDP-43), aggregation of α-synuclein/Lewy bodies, and cerebrovascular disease. Co-pathologies can contribute to heterogeneity among individuals with AD, for example by influencing clinical symptoms and disease progression rates [68–70]. They can also be important to consider when investigating and diagnosing AD in vivo, and when interpreting evidence of AD pathology using biomarkers.

Biomarkers

Biomarkers, or biological markers, are measurable indicators of a biological condition, for example altered Aβ or tau metabolism or deposition. AD biomarkers can be measured in biofluids (e.g., CSF or blood) and with imaging (e.g., magnetic resonance imaging [MRI] or positron emission tomography [PET]) (Fig. 3). Before the development of AD biomarkers, it was difficult to determine if AD pathology was likely causing the clinical symptoms, and a definite diagnosis of AD could therefore only be made at autopsy [71]. In the absence of biomarkers, a clinical AD diagnosis is inaccurate in 20-30% of cases in specialized dementia clinics, and in about 40% of cases in primary care [72,73]. With the emergence of biomarkers, timely and accurate assessment of AD pathology in vivo has become possible, improving diagnosis, prognosis, trial recruitment, and clinical research [29].

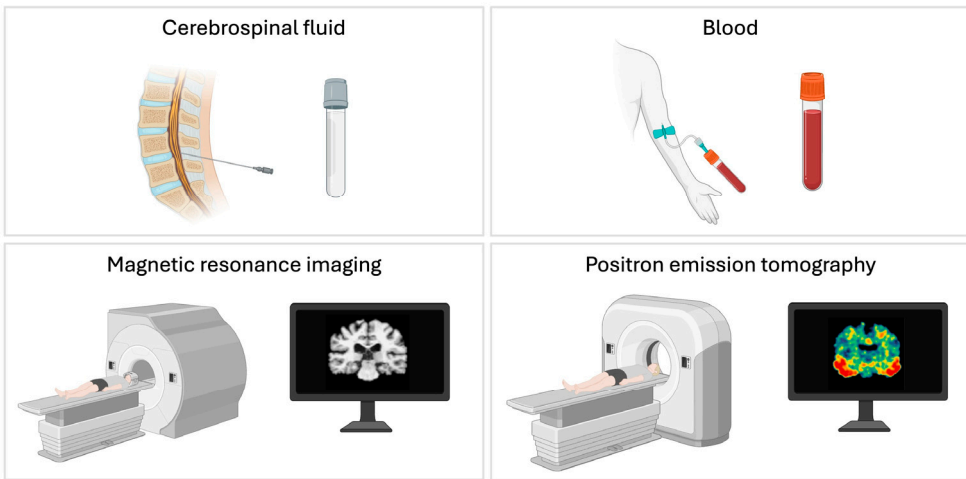

Figure 3. Alzheimer's disease biomarkers. Altered Aβ or tau metabolism is commonly measured in CSF (collected through a lumbar puncture, top left panel) or in blood (top right panel). Neurodegeneration can be seen on brain MRI (bottom left panel), while Aβ and tau deposition can be visualized using PET (bottom right panel). Figure created with Biorender.

Cerebrospinal fluid

The CSF is a colorless fluid that fills the subarachnoid space and ventricles. CSF acts like a protective "cushion" for the brain, while also transporting nutrients and removing waste from the brain and spinal cord [74]. Most of the CSF is produced in the choroid plexus and cleared into the venous system and lymphatic pathways, with a complete turnover rate of approximately four times per day. CSF moves through the subarachnoid space and ventricles via convective and pulsatile flow mechanisms [75,76]. With aging, CSF dynamics usually change. For instance, the total CSF volume typically increases and CSF production and pressure decrease [77–79].

Since CSF is in direct contact with the extracellular space of the brain, it contains many proteins that originate from the central nervous system (CNS). These proteins can therefore reflect biochemical changes occurring in the brain and be used as biomarkers for neurological diseases [74]. In addition to measuring single biomarkers, recent technological advances have made it possible to perform large-scale analyses of CSF proteins (proteomics), opening new opportunities for biomarker discovery and for improving our understanding of complex disease mechanisms [80–82].

To collect and measure CSF biomarkers or proteomics, CSF can be obtained through a lumbar puncture. During a lumbar puncture, patients are typically positioned either sitting upright or lying on their side, and a sterile spinal needle is inserted between the lumbar vertebrae to access the CSF-filled subarachnoid space. This is an invasive procedure that requires trained personnel, and it may cause mild side effects (most commonly headache), but serious complications are rare [76].

Commonly used CSF biomarkers for AD include Aβ42 and several phosphorylated-tau (p-tau) isoforms. CSF Aβ42 levels are decreased in AD, reflecting that Aβ42 fragments are deposited in oligomers and plaques, whereas CSF p-tau levels are increased as soluble tau becomes hyper-phosphorylated [29,74,83]. Together, these and other markers support the biological diagnosis of AD and offer information relevant to prognosis and disease stage [84–87].

The CSF biomarker Aβ42 has been shown to better reflect AD pathology when expressed as a ratio to CSF Aβ40, even though the levels of Aβ40 remains largely unchanged in AD [88,89]. CSF Aβ40 can therefore be viewed as a reference protein, likely accounting for inter-individual differences in soluble Aβ metabolism and/or overall CSF protein abundance. Other commonly used AD CSF biomarkers are typically not normalized to a non-disease-related reference protein [50], which raises questions of whether a similar approach could also improve the performance of these biomarkers (further investigated in Papers I and II).

Blood

Similar to CSF, the protein content of blood plasma can reflect AD pathological changes. Many of the same analytes as in CSF are measured in plasma (for example Aβ42 and p-tau isoforms), but their concentrations are several orders of magnitude lower [83]. As blood is circulated throughout the entire body, its protein content reflects many physiological phenomena beyond processes in the brain [83]. Despite this, ultrasensitive methods to quantify proteins have reliably differentiated biomarker levels between AD cases and controls [90–93]. Markers of soluble, hyperphosphorylated tau have shown particular promise [94–96]. In contrast, Aβ fragments have been more difficult to rely on in blood, likely because blood Aβ originates from both the brain and the periphery, making the signal less specific to processes in the brain [97].

A main advantage with blood biomarkers is their scalability. Blood sampling is minimally invasive and does not require advanced medical expertise, and it is relatively cheap and quick to perform [98]. These factors, together with findings suggesting that blood biomarkers can reach performance similar to CSF biomarkers in both secondary and primary care settings [73,96,99,100], underscore their potential. Blood biomarkers could revolutionize AD diagnostics, facilitating large-scale, timely and accurate in vivo assessments of AD pathology [94].

Positron emission tomography

Fluid biomarkers are informative but provide limited details regarding the spatial distribution of AD pathology. To assess where pathology is located and spreads across brain regions, in vivo imaging techniques can be used. In AD, PET enables regional assessment of Aβ plaques and tau NFTs, providing information on both extent and distribution of the pathologies.

PET is based on the injection of a radioactive tracer that has affinity and specificity for a specific molecular target (e.g., Aβ or tau aggregates). As the radionuclide (in Aβ and tau-PET most commonly fluorine-18, ^{18}F) decays, it emits a positron. After travelling a short distance, the positron annihilates with an electron, producing two 511 keV gamma photons emitted in opposite directions. These photons are detected by the PET scanner, and tomographic reconstruction from many such events yields an image of the tracer's distribution. The resolution of PET is limited by positron range, system design, reconstruction, and motion, and is typically a few millimeters in the human brain. PET is considered non-invasive but involves exposure to a small dose of radiation [101].

Both Aβ- and tau-PET exhibit high agreement with neuropathological assessments [102–105]. They have also been shown to improve differentiation of AD from other neurodegenerative disease, and to increase the confidence of clinicians [106–110]. Despite their value in clinical and research contexts, PET remains inaccessible for many patients and clinics worldwide because of its high costs, limited scanner capacity, and the need for specialized infrastructure, e.g., radiotracer production and distribution, as well as trained personnel (further addressed in Papers IV, V and VI) [29].

Magnetic resonance imaging

MRI provides high-resolution visualization of tissue and anatomical structures and can therefore be used to measure and track neurodegeneration. It is a non-invasive, highly accessible, and relatively fast diagnostic tool [111].

MRI is based on nuclear magnetic resonance, specifically the spin of hydrogen nuclei (single protons). The MRI scanner's main magnet generates a strong static magnetic field B_0 (typically 1.5 T, 3 T, or 7 T), which causes the proton spins to align with the field. This produces a net magnetization in the longitudinal direction,

while spins in the transverse plane remain out of phase so that the net transverse magnetization is approximately zero. Radiofrequency pulses B_1 then perturb the system, tipping the magnetization away from the longitudinal axis and creating coherent transverse magnetization. After the pulse, the signal decays as the spins relax back toward equilibrium, inducing a measurable radiofrequency signal in the receiver coil of the scanner. To spatially encode the signal, magnetic field gradients are applied across space so that B_0 varies in a predictable manner [111].

Measuring the relaxation time in the longitudinal direction yields a T1-weighted MRI, while the relaxation time to non-coherent transverse magnetization yields a T2-weighted MRI. These two sequences vary in terms of imaging contrast, with T1-weighted being most commonly used and the central one in this thesis. In T1 images, fat appears bright, and fluid appears dark, which is particularly useful to visualize anatomical structures and atrophy patterns. Other common MRI sequences include proton density and FLAIR (other contrasts), as well as diffusion and functional MRI (microstructural and activation measures) [111], but those are beyond the scope of this thesis.

In AD, brain MRI complements pathology-specific CSF, blood, and PET biomarkers by capturing regional atrophy and atrophy rates, as well as comorbid brain changes like vascular brain injury, microbleeds, and white matter hyperintensities. MRI is also used to help rule out other causes of cognitive symptoms, such as tumors or hydrocephalus [112,113].

Diagnosis and staging

Biological diagnosis and staging

In 2018, the National Institute on Aging and the Alzheimer's Association (NIA-AA) published a framework toward a biological definition of AD based on postmortem examination or in vivo biomarkers. Biomarkers were grouped into those of Aβ deposition (A), pathological tau (T), or neurodegeneration (N), yielding an AT(N) classification scheme [47]. In 2024, the NIA-AA published updated biomarker-based recommendations for diagnosing and staging of AD [50]. The framework now distinguished early changing Core 1 AD biomarkers from later changing Core 2 AD biomarkers, incorporating biomarkers of neurodegeneration and co-pathologies as complementary (Tab. 2). According to these recommendations, an abnormal Core 1 biomarker is sufficient to establish a biological AD diagnosis, whereas Core 2 biomarkers increase diagnostic certainty and provide prognostic and staging information. Clinical symptom staging (Tab. 1) can be integrated together with the biological framework to yield a combined biological-clinical characterization of individuals across the AD continuum.

Table 2. Categorization of Alzheimer's disease biomarkers as recommended by the NIA-AA in 2024 [50].

Biomarker category	Fluid analytes	Imaging
Core 1 Aβ-proteinopathy and hyperphosphorylated tau.	Aβ42, p-tau217, p-tau181, p-tau231	Aβ-PET
Core 2 Tau proteinopathy.	MTBR-tau243, p-tau isoforms, np-tau fragments	Tau-PET
Neurodegeneration & inflammation	NfL, GFAP	MRI, FDG-PET
Co-pathologies	αSyn-SAA	MRI, CT

Under the NIA-AA frameworks, several fluid and imaging biomarkers are intended to be used interchangeably for AT(N) or Core 1 and 2 categorization, requiring high agreement between fluid and imaging modalities (further addressed in Papers I and II). Head-to-head comparisons suggest that some analytes outperform others in terms of interchangeability with PET imaging: CSF Aβ42/Aβ40 and CSF/plasma p-tau217 generally show strong associations with Aβ-PET (Core 1), whereas CSF/plasma MTBR-tau243 and p-tau217 display particularly high concordance with tau-PET (Core 2) [99,114–117].

Clinical practice

Although the NIA-AA framework separates clinical syndrome from biological AD, the distinction is not always meaningful in clinical practice. While AD pathology can be detected before symptom onset, biomarker testing in asymptomatic individuals is generally not recommended in clinical care, as it may cause more harm than benefit due to the current absence of approved therapeutic interventions [118,119]. A clinical AD diagnosis should hence include evidence of objective cognitive impairment in at least one cognitive domain (consistent with DSM-5 [43]). Once impairment is established, biomarkers can help determine the underlaying etiology and eligibility for therapeutic interventions. Furthermore, since the pre-test probability of AD pathology is higher in individuals with symptoms than without, establishing objective cognitive impairment before biomarker testing also reduces the number of false-positive biomarker results [22,120].

Primary care is often the first point of contact for older adults who begin to experience cognitive symptoms. Usually, time and resources in primary care are limited, and practitioners are typically not specialized in neurological disorders. This can make it challenging to establish objective cognitive impairment and evaluate potential neurodegenerative causes (further addressed in Paper III). At present, AD biomarkers are not yet routinely used in primary care. Patients may therefore be referred to specialist clinics (although in practice many are not [121]), where diagnostic certainty can be increased through more comprehensive cognitive assessments and potential access to CSF, PET, and/or blood-based biomarkers.

Patients evaluated at specialist clinics are typically younger, have fewer comorbidities, higher education and socioeconomic background, and less severe cognitive impairment than patients who are not [122].

Treatment and trials

There is still no cure for AD, but major progress in treatment has been made during recent years. Historically, the main approach for treating clinical AD has involved symptomatic medication, such as cholinesterase inhibitors that increase neurotransmission. Such medication enhance communication between neuronal cells and can thereby provide modest, symptomatic improvement or stabilization of cognitive function, but do not affect the underlying pathology [123,124]. Typically, they are prescribed for mild to moderate AD symptoms, but not all individuals are responsive. The most common side effects are gastrointestinal (e.g., nausea, vomiting, diarrhea, loss of appetite). As these treatments are not specific to the underlying AD pathology, biomarker evidence is not mandatory to initiate treatment [125].

A major recent development has been the successful completion of Phase 3 trials for disease-modifying treatments of AD. Monoclonal antibody-based therapeutics like lecanemab [126] and donanemab [127] specifically target Aβ pathology. Lecanemab binds with high affinity to soluble Aβ protofibrils, while donanemab selectively binds to Aβ plaques, with both facilitating the microglia-mediated removal of aggregated Aβ-pathology from the brain. These treatments are administered via intravenous infusion either every two weeks (lecanemab) or four weeks (donanemab). Eligibility for the therapies requires biomarker evidence of AD pathology and at least mild cognitive impairment. The most frequently observed side effects are infusion related reactions and amyloid-related imaging abnormalities (ARIA), either as cerebral edema (ARIA-E) or microhemorrhages (ARIA-H). Rigorous monitoring, including clinical symptoms and MRI scans, is therefore essential during the initial treatment phase. Both lecanemab and donanemab are now available or approved for clinical use in a growing number of countries, including USA, EU, Japan, and China [125].

Despite their demonstrated ability to substantially clear Aβ from the brain, the clinical benefits observed in Phase 3 trials were modest, indicating a slower decline in function and cognition of 27% and 36% compared to the placebo groups [126,127]. The clinical benefit of donanemab was greater in patients with lower tau-PET signal [128], and it is hypothesized that these treatments may yield a greater clinical effect if initiated earlier in the disease course. Ongoing trials are investigating the efficacy of lecanemab and donanemab in populations with positive AD biomarkers but without cognitive impairment (e.g., TRAILBLAZER-ALZ3 and AHEAD 3-45). Another promising drug candidate for Aβ clearance, trontinemab, is also under investigation, which utilizes a Brainshuttle technology to more efficiently cross the blood-brain barrier [129]. This way, treatment can be

administered at lower doses, potentially reducing the risk of ARIA. Furthermore, given the complex nature of AD, targeting additional mechanisms like tau pathology and neuroinflammation might be necessary to achieve stronger clinical effects. Tau modifying treatments and anti-inflammatory therapies are also actively being developed and evaluated [130].

As disease-modifying treatments for AD enter research pipelines and clinical practice, accurate and accessible biomarkers are becoming increasingly important. They are essential to identify eligible patients and to assess therapeutic responses, both in clinical care and in trials. Continued work toward improved biomarker accuracy and accessibility can help optimize patient care and trial design in this exciting era of scientific and medical progress. This AD background forms the foundation of this thesis, and the specific aims are addressed through advanced medical data analysis.

Medical data analysis

At the heart of data analysis lies *modelling*. A *model* aims to describe a system or process without including all complex real-world details. Importantly, models are approximations created to better understand or predict reality and should not be confused with the system itself [131].

Traditional statistical modelling

Historically, medical data analysis has largely relied on statistical modelling, and statistics remains a robust and valuable toolbox for summarizing data, quantifying uncertainty, testing clinically relevant hypotheses, and guiding study design and interpretation [132]. A common distinction in statistics is between descriptive and inferential approaches.

Descriptive statistics

Descriptive statistics summarizes the study sample, for example in terms of proportions, central tendency (e.g., mean or median value) and dispersion (e.g., variance or standard deviation), often complemented by visualizations of distributions (e.g., histograms, boxplots). In medical research, such summary measures are commonly used to characterize the included study cohorts and to describe differences between groups [133].

Inferential statistics

Inferential statistics is used to draw conclusions from a study sample to a target population, typically under the assumption that the sample is representative of that population. In medical research, inference is commonly carried out within

regression modelling frameworks, where associations between covariates and outcomes are estimated while accounting for potential confounding. Confidence intervals and hypothesis testing can then quantify uncertainty, conditional on the model assumptions and the observed data [134].

Together, descriptive and inferential statistics form a foundation for evidence-based medical research, ranging from cohort characterizations to the evaluation of diagnostic tests, risk factors, and treatment effects. Many clinical questions are naturally framed in statistical terms and are still addressed using these well-established statistical modelling frameworks. Key advantages of statistical models include interpretability, transparency, and robustness to scarce data. Key limitations include their poor ability to capture complex, non-linear relationships in high-dimensional data, and their unstable behavior when underlaying assumptions are violated [135].

Artificial intelligence

Artificial intelligence (AI)-based computational methods can broaden what can be learned from complex, high-dimensional medical data. As datasets continue to expand over time, new avenues for more precise AD diagnostics and monitoring, as well as for uncovering biological insights, have opened [136].

AI is a broad term describing the ability of machines to perform tasks that typically require human intelligence, such as language understanding, pattern recognition, and decision making. Machine learning (ML) is a subset of AI and refers to algorithms whose performance improve as they are exposed to more data. Deep learning is a further subset of ML that specifically uses deep neural networks to learn from data (Fig. 4) [137].

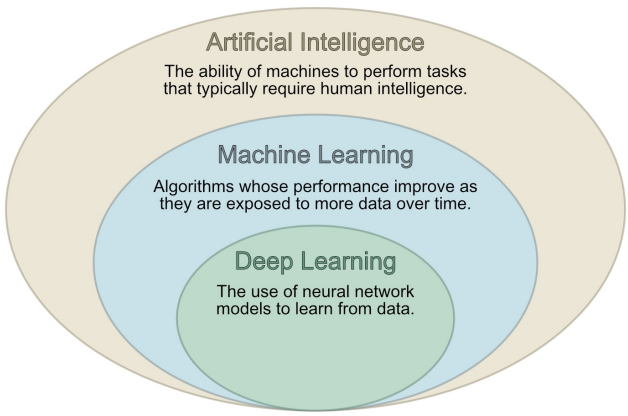

Figure 4. Machine learning is a subset of artificial intelligence, and deep learning is a subset of machine learning.

Machine learning

This thesis focuses on two main types of machine learning: supervised and unsupervised learning (Fig. 5). Unsupervised learning identifies patterns in unlabeled data. Common approaches include dimensionality reduction and clustering methods such as singular value decomposition (SVD), t-distributed stochastic neighbor embedding (t-SNE), and K-means clustering (all used in this thesis and further described in *Methods*). In contrast, supervised learning comprises algorithms that learn from labeled data, through for example classification or regression. Common methods include linear and logistic regression, support vector machines, and random forests (all used in this thesis and further described in *Methods*) [137].

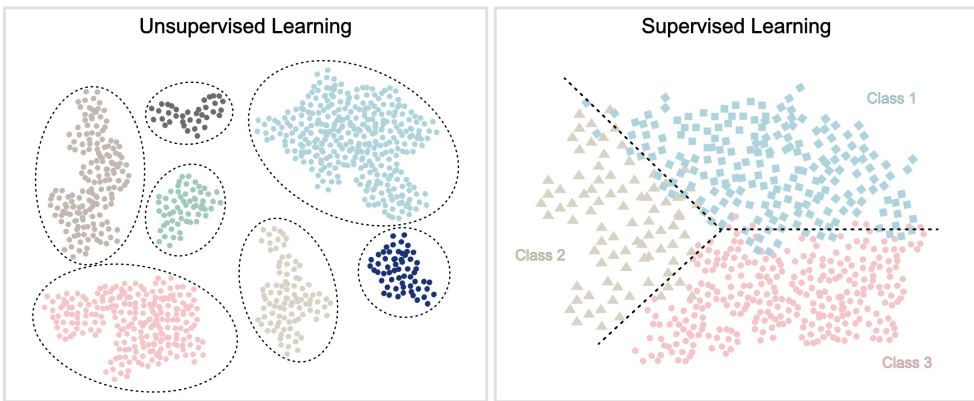

Figure 5. Examples of unsupervised machine learning using dimensionality reduction and clustering (left panel), and supervised machine learning using classification (right panel).

The same models can sometimes be used in both statistics and machine learning, for example linear and logistic regression. A key difference often lies in the objective: prediction in machine learning versus inference in statistics. In prediction, the goal is to build models that generalize well to new, unseen data, whereas inference focuses on understanding relationships in the population. How models are fitted and interpreted can therefore slightly differ depending on the purpose. For example, prediction can include a large number of input variables and performance should be evaluated on unseen data to avoid overfitting. In inference, emphasis is often placed on fewer, statistically significant variables, and evaluations are commonly performed using the same data that were used to fit the model [138].

Deep learning

Deep learning is inspired by the human brain through the construction of neural networks. Neural networks are composed of computational units that mimic neurons, commonly called artificial neurons or perceptrons [139]. A perceptron

takes a set of n input values $x_1 \ldots x_n$, learns a weight for each input value $w_1 \ldots w_n$ and a global bias b. An activation function σ is then applied to introduce non-linearity, yielding an output value y as

$$y = \sigma(\sum_{i=1}^{n} w_i x_i + b). \quad (1)$$

By arranging such units into stacked layers where each output y becomes an input to the next layer, neural networks are formed and can be trained to perform specific tasks by updating the weights based on data (Fig. 6). Neural networks rely on mathematical representations: all input data are encoded and processed as numbers within the network, stored as scalars, vectors, matrices, or higher-order tensors [137].

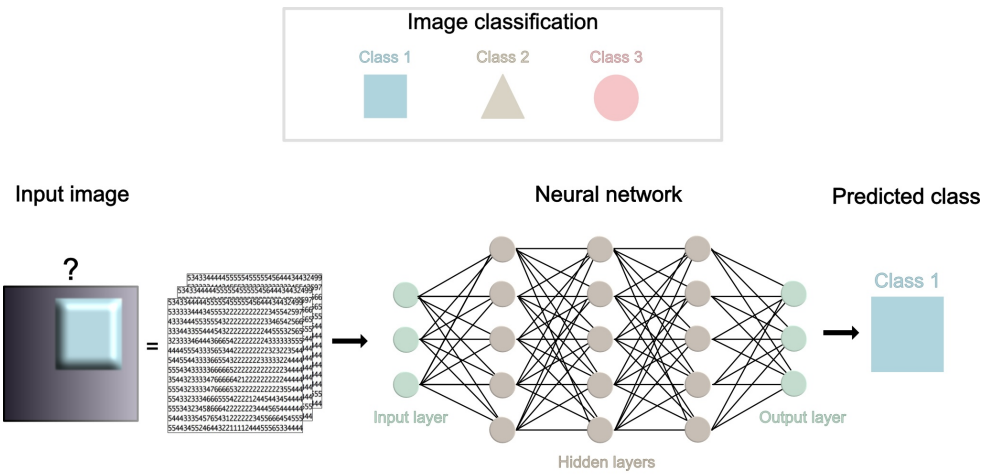

Figure 6. An example image classification pipeline using a neural network.

One class of deep learning architectures particularly well-suited for image-like data with local structures (and used in this thesis) is convolutional neural networks (CNNs). CNNs use convolutional layers as core building blocks. Convolutions are learnable filters applied to local groups of features, for example small patches of voxels in images. Each filter is a small array of trainable weights that is elementwise multiplied with voxel values in the image patch it overlaps. The products are summed to produce a single feature value for that location. The same filter is applied across the entire image as a sliding window. By stacking many convolutional layers, CNNs can build a hierarchy of representations: early layers detect simple patterns such as edges and textures, while deeper layers combine those patterns into increasingly complex, task-relevant structures. These hierarchical, spatially aware networks often perform well on medical image analysis tasks, where local context and anatomical structures are key [137].

In medical data analysis, deep learning offers several promising avenues to improve healthcare. For example, it can be applied to improve segmentation, interpretation and synthesis of medical images, advance our understanding of biomolecular structure and behavior, and accelerate the discovery of novel drugs [140–146].

Challenges

Medical data analysis poses substantial challenges compared to many other data science fields. Data collection is often slow and resource-intensive, and datasets can exhibit considerable variability due to differences between sites, equipment, protocols, and populations. Data sharing can also be difficult because of regulatory constraints and the sensitivity of human data. In addition, medical datasets can be noisy, imbalanced, and imperfectly labeled. For example, AD diagnoses that are not biomarker-confirmed may be incorrect, and variables such as cognitive test scores can fluctuate for reasons unrelated to the underlying disease process. Finally, requirements for model performance, transparency, and generalizability are often high in medicine, since errors can have vital consequences [136,147].

Rationale and aims

AD is difficult to diagnose in clinical practice. As we can expect a future higher AD prevalence and are approaching an era of disease-modifying therapies specific to AD pathology, not only accurate, but also cost-effective and scalable diagnostic tools are becoming increasingly important.

The pathological levels of Aβ and tau can be measured using multiple biomarkers, but the most accurate and informative ones are usually also expensive and/or invasive, which limits large-scale implementation. Similarly, investigating objective cognitive impairment is resource-intensive and can vary substantially across healthcare providers and countries, introducing additional heterogeneity into clinical decision making and workflows.

In parallel, AD research cohorts are becoming increasingly well-characterized with, for example, detailed demographic and cognitive assessments, multiple imaging modalities, and extensive fluid biomarker and proteomic measurements. This creates opportunities to apply more complex modelling techniques to integrate information across modalities and to better understand complementary and overlapping information in these high-dimensional data.

Consequently, this thesis aims to utilize different data modalities together with statistical and machine learning approaches to improve AD biomarkers and diagnostics, with emphasis on balancing accuracy and comprehensiveness with cost, invasiveness, and clinical feasibility (Fig. 7). Specifically, the aims are focused on:

Aim 1: Investigating co-varying properties of the CSF proteome in a data-driven manner and evaluating whether adjusting for such properties using reference protein normalization can improve AD fluid biomarkers (Paper I and II).

Aim 2: Evaluating whether a resource-efficient, self-administered digital cognitive test can support more accurate assessments of objective cognitive impairment in primary care (Paper III).

Aim 3: Developing and validating machine learning models trained to predict Aβ-PET or tau-PET burden, as well as the spatial distribution of pathology, from more accessible modalities (Paper IV, V, and VI).

Through these aims, this thesis takes steps toward improved AD biomarkers and diagnostics by leveraging previously unexplored data or data patterns in deeply phenotyped research cohorts. The translational research approach is also aimed to

build bridges between the fields of data science and neuroscience to facilitate collaboration and knowledge exchange.

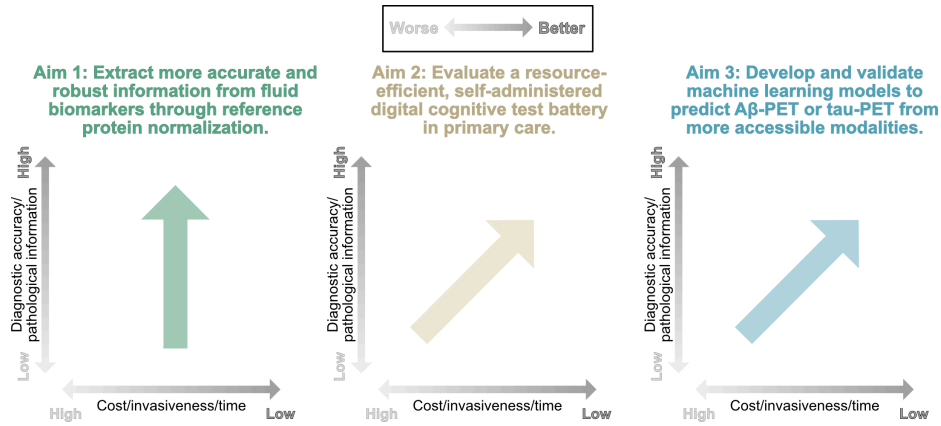

Figure 7: Specific thesis aims to improve diagnostics and biomarkers in Alzheimer's disease. Arrow directions indicate the expected benefit along two axes i) accuracy/information (diagnostic accuracy and pathological information, higher = better) and ii) burden (cost, invasiveness, and time, lower = better).

Methods

Datasets

The Swedish BioFINDER study cohorts

The prospective Swedish BioFINDER studies are deeply phenotyped longitudinal research cohorts initiated to develop diagnostic tests, identify treatment targets, and understand biological mechanisms of neurodegenerative disorders. This thesis used data from BioFINDER-1 (launched 2008; Tab. 3; NCT01208675), BioFINDER-2 (launched 2017; Tab. 4; NCT03174938) , and BioFINDER-Primary Care (launched 2020; Tab 5; NCT06120361). The studies recruit participants at Skåne University Hospital and Hospital of Ängelholm (BioFINDER-1 and BioFINDER-2) or at primary care centers in southern Sweden (BioFINDER-Primary Care). Follow-up visits are performed annually or biannually for up to 10 years.

Table 3. Population and design of the Swedish BioFINDER-1 study cohort.

Sub-cohort	Diagnosis	Inclusion criteria*	Included in paper					
			I	II	III	IV	V	VI
A n=600	**NC**	i) age ≥60 years ii) absence of cognitive symptoms iii) MMSE score 27-30 iv) do not fulfill DSM-5 criteria for MCI or dementia v) fluent in Swedish	☑	☑	⊗	☑	⊛	☑
B n=500	**SCD/MCI** MCI if less than -1.5 SD in any cognitive domain (age and education stratified test norms), otherwise SCD.	i) age 60-80 years ii) cognitive symptoms iii) MMSE score 24-30 iv) do not fulfill DSM-5 criteria for dementia v) fluent in Swedish	☑	☑	⊗	☑	⊛	⊛
C n=300	**Dementia** Includes 50 patients with familial Alzheimer's disease	i) fulfill DSM-5 criteria for dementia	⊛	⊛	⊗	⊗	⊛	⊛
D n=400	**Parkinsonian disorders**	i) fulfill criteria of Parkinson's disease, Parkinson's disease with dementia, progressive supranuclear palsy or multiple system atrophy.	⊗	⊗	⊗	⊗	⊛	⊛

☑ Included ⊗ Excluded ⊛ Included if data available (rare due to cohort design).
* Exclusion criteria for all sub-cohorts are i) significant unstable systemic illness; ii) current significant alcohol or substance misuse; iii) refusing lumbar puncture, MRI or PET.

Table 4. Population and design of the Swedish BioFINDER-2 study cohort.

Sub-cohort	Diagnosis	Inclusion criteria*	Included in paper					
			I	II	III	IV	V	VI
A n=340	**NC** Stratified to include 50% APOE ε4 carriers.	i) age 20-65 years ii) absence of cognitive symptoms iii) MMSE score 27-30 iv) do not fulfill DSM-5 criteria for MCI or dementia v) fluent in Swedish	☑	☑	⊗	☑	☑	☑
B n=300	**NC** Stratified to include 50% APOE ε4 carriers.	i) age 66-100 years ii) absence of cognitive symptoms iii) MMSE score 26-30 iv) do not fulfill DSM-5 criteria for MCI or dementia v) fluent in Swedish	☑	☑	⊗	☑	☑	☑
C n=1000	**SCD/MCI** MCI if less than -1.5 SD in any cognitive domain (age and education stratified test norms), otherwise SCD.	i) age 40-100 years ii) cognitive symptoms iii) MMSE score 24-30 iv) do not fulfill DSM-5 criteria for dementia v) fluent in Swedish	☑	☑	☑	☑	☑	☑
D n=400	**AD dementia** Biomarker confirmed in agreement with the 2018 NIA-AA criteria [47].	i) age 40-100 years ii) cognitive symptoms iii) MMSE score 12-30 iv) fulfill DSM-5 criteria for dementia due to AD v) fluent in Swedish	☑	☑	☑	⊛	☑	☑
E n=920	**Non-AD dementia or other neurodegenerative disorder**	i) age 40-100 years ii) fulfill criteria for frontotemporal dementia, PD, vascular dementia, PSP, MSA, svPPA or corticobasal syndrome. iii) fluent in Swedish.	☑	☑	☑	⊛	☑	☑

☑ Included ⊗ Excluded ⊛ Included if data available (rare due to cohort design).
* Exclusion criteria for all sub-cohorts are i) significant unstable systemic illness; ii) current significant alcohol or substance misuse; iii) refusing lumbar puncture, MRI or PET.

Table 5. Population and design of the Swedish BioFINDER-Primary Care study cohort.

Participants	Inclusion criteria*	Included in paper
Patients seeking medical care due to mild cognitive symptoms in primary care n=1200	i) age ≥40 years ii) cognitive symptoms iii) the general practitioner suspects a progressive neurodegenerative disorder iv) SCD, MCI or mild dementia	Only in Paper III.

* Exclusion criteria are i) diagnosed dementia ii) significant unstable systemic illness; iii) current significant alcohol or substance misuse; iv) refusing investigation at a Memory Clinic; v) cognitive impairment that with certainty can be explained by another condition/disease, e.g., stroke, psychotic disorder, depression, etcetera.

The studies were approved by the Regional Ethics Committee in Lund, Sweden. Furthermore, all participants gave their informed consent to participate, and the data were collected according to the Declaration of Helsinki.

To assess performance on unseen data during prediction frameworks, datasets were often split into training, validation and test sets, or evaluated using cross-validation (described in *Machine learning – Supervised learning*). Details of the specific split strategies are provided in respective paper.

External study cohorts

In Papers II, V and VI, multiple external cohorts (Tab. 6) were used for model validation, to investigate model generalizability, and/or to create a larger and more heterogenous sample for model training. This included deeply phenotyped AD cohorts, as well as cohorts focused on other dementias and neurological disorders. The cohorts were selected based on patient populations and available data modalities, with Paper II focusing on a broad range of fluid biomarkers together with Aβ-PET, tau-PET and diagnostic variables, while Paper V and VI required tau-PET and MRI. All participants gave written informed consent to participate, and the studies were approved by local institutional ethical review boards.

Biofluid measurements

Biofluid samples were collected and handled according to established preanalytical protocols. The analyses were performed by technicians blinded to all clinical and imaging data.

Immunoassays

An immunoassay measures the concentration of an analyte (e.g., a protein) by using an antibody that binds specifically and with high affinity to the analyte. A measurable signal that is proportional to the number of analyte-bound antibodies is generated, using for example radiation, fluorescence, enzymes, or other detection mechanisms. The signal is compared against a calibration curve created from solutions with known analyte concentrations, making conversion of the signal intensity into a quantitative concentration possible [158]. Building on this principle, multiple immunoassay formats and platforms for AD biomarker measurements have been developed that differ in detection mechanism, degree of automation, analytical performance, and cost [159].

Table 6. Population overview of the external study cohorts.

Cohort name	Population overview	Ref. w. details.	Included in paper		
			II	V	VI
Knight-ADRC *Charles F. and Joanne Knight-Alzheimer's Disease Research Center, Washington University,* n=376*.	Elderly participants spanning the cognitive spectrum from normal cognition to AD-dementia. Most participants were recruited from memory clinics or self-referred due to interest in dementia.	[148]	☑	⊗	⊗
TRIAD *Translational Biomarkers in Aging and Dementia, McGill University, n=190*.*	Elderly participants spanning the cognitive spectrum from normal cognition to AD-dementia. The study aims to assess dementia markers and their progression by recruiting patients from the McGill University Research Centre for Studies in Aging and from the general public.	[149]	☑	⊗	⊗
Perugia MS cohort *University of Perugia, n=56*.*	Adult individuals diagnosed with Relapsing-Remitting Multiple Sclerosis or another neurological disorder (including headache, mononeuropathy, psychiatric disorders, or dysmetabolic polyneuropathy).	[150]	☑	⊗	⊗
UCSF-ADRC *University of California San Francisco Alzheimer's Disease Research Center, n=251*.*	Elderly participants spanning the cognitive spectrum from normal cognition to different kinds of dementia as well as other neurodegenerative disorders.	[151]	⊗	☑	☑
ADNI *Alzheimer's Disease Neuroimaging Initiative, n=857*.*	Elderly participants spanning the AD continuum from normal cognition to AD-dementia. Participants were recruited across 60+ clinical sites in USA.	[152]	⊗	☑	☑
A4 *Anti-Amyloid Treatment in Asymptomatic Alzheimer's disease, n=446*.*	Aβ-positive cognitively unimpaired elderly individuals recruited for a randomized clinical trial of an amyloid-modifying therapy. Participants were recruited across 60 clinical sites in USA, Canada, and Australia. In this thesis, only baseline participant data was used (first visit before treatment).	[153]	⊗	☑	☑
OASIS-3 *Open Access Series of Imaging Studies phase 3, n=440*.*	Elderly participants spanning the cognitive spectrum from normal cognition to dementia. The dataset includes a compilation of ongoing studies in the Washington University Knight-ADRC.	[154]	⊗	☑	☑
Avid cohorts *Avid radiopharmaceuticals, n=557*.*	Participants spanning the cognitive spectrum from normal cognition to dementia. The cohorts were aimed at evaluating imaging characteristics of [^{18}F]flortaucipir. Participants were recruited across clinical sites in USA.	[155]	⊗	⊗	☑
PREVENT-AD *Presymptomatic Evaluation of Experimental or Novel Treatments for Alzheimer's Disease, McGill University, n=134*.*	Cognitively unimpaired elderly participants with a family history of sporadic AD-like dementia. Participants were recruited from the greater Montreal area.	[156]	⊗	⊗	☑
BACS *Berkeley Aging Cohort Study, n=134*.*	Cognitively unimpaired elderly participants, all community dwelling volunteers resided in the San Francisco Bay Area of California. Participants were recruited through advertisements in senior centers and in local newspapers.	[157]	⊗	⊗	☑

☑ Included ⊗ Excluded
*sample size included in this thesis.

In this thesis, immunoassays were used to measure biomarker concentrations in CSF and blood. Specifically, Papers I, II, IV, V, and VI used Roche Elecsys immunoassays run on a cobas e platform, Eli Lilly immunoassays run on a Meso Scale Discovery (MSD) platform, Simoa immunoassays developed at the University of Gothenburg, and/or Fujirebio Lumipulse immunoassays. The measured analytes included CSF and/or plasma Aβ42, Aβ40, p-tau181, p-tau217, p-tau231, total(t)-tau, N-terminal containing tau fragments (NTA), sTREM2, YKL-40, glial fibrillary acidic protein (GFAP), neurogranin, S100, α-synuclein, and neurofilament light (NfL). Details on the specific immunoassay and analytes used in each study, as well as cutoffs for when markers were binarized, are provided in the respective papers.

Mass spectrometry assays

In mass spectrometry, the analyte is converted into gas-phase ions and then accelerated through electric fields that separate ions according to their mass-to-charge ratio. This way, a spectrum characteristic of the molecule (and sometimes its fragments), is generated. The area under the spectrum peaks is proportional to the amount of analyte in the sample. Quantification is typically performed by calibrating the signal against a sample of known concentration, often a molecule of higher mass that is run together with the analyte of interest. Compared with immunoassays, mass spectrometry is generally more exact but also more expensive and technically demanding [160,161].

In this thesis, several mass spectrometry assays were used to measure biomarker concentrations in CSF and blood. Specifically, Papers II, III and IV used mass spectrometry assays developed by C2N Diagnostics, Washington University and/or University of Gothenburg. The measured analytes included CSF and/or plasma Aβ42, Aβ40, p-tau181, p-tau205, p-tau217, microtubule-binding region containing residue 243 (MTBR-tau243), np-tau181-190, np-tau195-210, np-tau212-221, and synaptosome associated protein 25 (SNAP-25). Details on the specific mass spectrometry assays and analytes used in each study, as well as cutoffs for when markers were binarized, are provided in the respective papers.

Proteomics

Proteomic analyses enable large-scale measurements of thousands of proteins in a single sample [162]. This thesis used a high throughput platform developed by Olink. The Olink technology consists of targeted antibody-based immunoassays combined with PCR-based signal amplification for detection and relative quantification of proteins (Proximity Extension Assay, PEA). The output format is Normalized Protein eXpression (NPX), which reflects $\log_2$ scaled relative protein abundances within the same measurements batch [163]. Olink proteomics was used in Papers I and II to measure proteins in CSF.

Neuroimaging

Positron emission tomography

In this thesis, Aβ-PET and tau-PET were used to quantify and regionally assess Aβ plaques and tau NFT. Aβ-PET was performed using either [^{18}F]flutemetamol, [^{18}F]florbetapir, [^{11}C]PiB, or [^{18}F]AZD4694. Standardized uptake value ratio (SUVR) images were created for the 90–110 min ([^{18}F]flutemetamol), 50-70 min ([^{18}F]florbetapir), 30-60 min ([^{11}C]PiB) and 40-70 min ([^{18}F]AZD4694) post-injection interval with whole cerebellum as reference region. Tau-PET was performed using either [^{18}F]RO948, [^{18}F]flortaucipir or [^{18}F]MK6240. SUVR images were created for the 70-90 min ([^{18}F]RO948), 75-105 min or 80-100 min ([^{18}F]flortaucipir), and 90-110 min ([^{18}F]MK6240) post-injection interval using inferior cerebellar cortex as reference region. All studies used at least one PET biomarker, with details on the specific tracers provided in the respective papers.

T1-weighted MRI

Isometric 1 mm^3 T1-weighted 3.0 T MRI images were acquired across the cohorts included in this thesis. Images were skull-stripped and segmented using FreeSurfer v.6.0 (https://surfer.nmr.mgh.harvard.edu/), resulting in native space parcellations of the participant's brain using the Desikan-Killiany (FreeSurfer) atlas (Fig. 8).

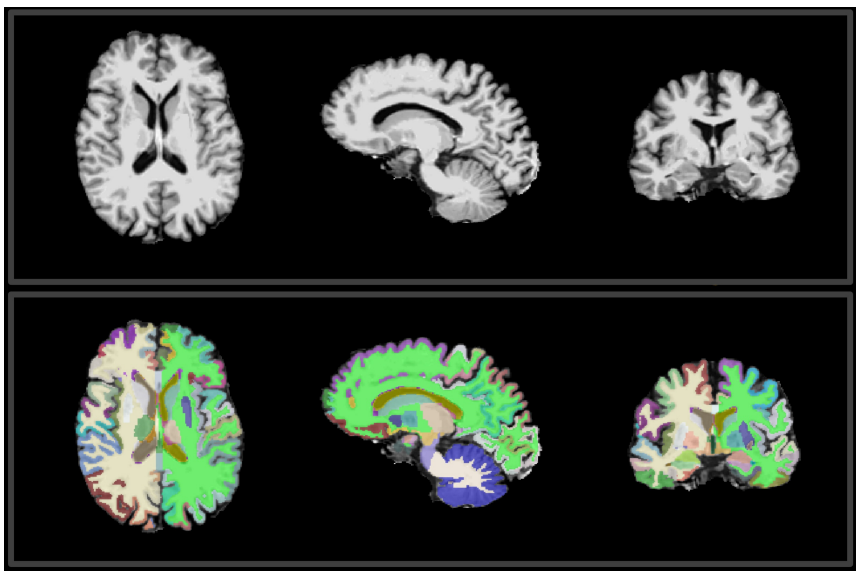

Figure 8. T1-weigthed brain MRI and FreeSurfer segmentation. Example of a T1-weigthed brain MRI (top) and the corresponding FreeSurfer parcellation/segmentation overlay according to the Desikan-Killiany atlas (bottom).

Image processing

FreeSurfer-derived segmentations and parcellations were combined to define MRI regions of interest (ROIs). Furthermore, PET images were rigidly co-registered to a corresponding T1-weighted MRI from the same participant. The FreeSurfer-derived masks were applied to extract mean SUVR values within ROIs in the PET images. Cutoffs for when ROIs were binarized are provided in each paper. All studies used MRI and PET ROIs only, except for Paper VI, where the full 3D scans were used. Image preprocessing in Paper VI was therefore more extensive (described in detail in the paper).

In Papers V and VI, a tau-PET laterality index (LI) was used to compare the relative accumulation of tau NFTs in the left versus right brain hemispheres, calculated as

$$LI = \frac{x_{i,Left} - x_{i,Right}}{(x_{i,Left} + x_{i,Right})/2}, \quad (2)$$

where x_i is the SUVR of brain region *i*.

Cognitive testing

Established cognitive measures

In this thesis, several well-established cognitive measures were used to objectively assess cognitive impairment, including the Mini Mental State Examination (MMSE), Alzheimer's Disease Assessment Scale - Cognitive Subscale (ADAS-Cog), Trail Making Test (TMT), verbal fluency tests, and Symbol Digit Modalities Test (SDMT), Montreal Cognitive Assessment (MoCA), Cambridge Neurophysiological Test Automated Battery – Paired associates learning (CANTAB PAL), Preclinical Alzheimer's Cognitive Composite (PACC), Clinical Dementia Rating (CDR), Repeatable Battery for the Assessment of Neuropsychological Status (RBANS), Tab. 7. The measures vary in extensiveness, difficulty, and targeted cognitive domains, often making them complementary and appropriate at different stages of cognitive impairment and for different research questions. All measures were used in Paper III where cognitive assessments were central. Only commonly available measures were used in Papers IV and V.

Table 7. Summary of the well-established cognitive measures used in this thesis.

Name	Description	Ref. for details	Included in paper		
			III	IV	V
MMSE	Consists of 11 parts covering five areas of cognition: orientation, registration, attention, recall and language. Target population: moderate to severe impairment. Scoring: 0-30 (higher = better).	[164]	☑	☑	☑
MoCA	Consists of a one-page form that similarly to MMSE assesses multiple cognitive domains but aimed to be more sensitive in earlier stages. Target population: mild impairment. Scoring: 0-30 (higher = better).	[165]	☑	⊗	⊗
ADAS-Cog Word Recall	Consists of a 10-word list that the test-taker memorizes. Recall is then assessed in multiple trials, both immediate and delayed. Target population: mild to moderate impairment. Scoring: 0-10 for each trial.	[166]	☑	☑	☑
TMT A & B	Tests visual attention and task switching. The test-taker should connect items with lines in a certain sequence as quickly as possible. Target population: mild to moderate impairment. Scoring: time to completion (seconds, lower = better).	[167]	☑	☑	⊗
Verbal fluency (animals)	Generate as many words as possible within a semantic category (e.g., animals) for one minute. Target population: mild impairment. Scoring: number of correct (higher = better).	[168]	☑	☑	⊗
SDMT	Match specific symbols to numbers using a reference key for 90 seconds. Tests processing speed, attention, and visual-spatial memory. Target population: mild impairment. Scoring: number of correct (higher = better).	[169]	☑	☑	⊗
Mini-Cog	Short screening test that consists of a three-word delayed recall task and clock drawing. Target population: moderate impairment. Scoring: 0-5 (higher = better).	[170]	☑	⊗	⊗
RBANS	Extensive test battery, consisting of 12 subtests that test five domains: immediate memory, delayed memory, visuospatial, language, and attention. Target population: mild to moderate impairment. Scoring: age and population normed index scores.	[171]	☑	⊗	⊗
CDR	Assesses dementia severity through a semi-structured interview with a patient and informant. Categories: memory, orientation, judgment/problem-solving, community affairs, home/hobbies, and personal care. Target population: very mild to severe impairment. Scoring: 0 to 3 in each category (lower=better).	[172]	☑	⊗	⊗
CANTAB PAL	A digital test that assesses visual associative memory on a touchscreen. Target population: mild impairment. Scoring: total errors adjusted (lower=better).	[173]	☑	⊗	⊗

☑ Included ⊗ Excluded

BioCog

All cognitive tests described above, except CANTAB PAL, were administered by healthcare personnel using paper and pencil. In Paper III, a new self-administered, digital cognitive test battery, BioCog, was evaluated. BioCog comprises a word list test with immediate and delayed recall/recognition, a processing speed task, and questions about orientation to the weekday, date, month and year (Fig. 9). Its subtests were inspired by ADAS-Cog, SDMT, and MMSE, and it is provided on a tablet.

Regarding psychometric properties, higher BioCog performance was observed in younger individuals, and performance was slightly better among those with higher education. The BioCog subtests showed high correlation with the paper-and-pencil measures they were designed to resemble, and limited overlap with tests targeting other cognitive domains. The average completion time was 11 minutes, and test instructions were self-reported as comprehensible or neutral by 98% of participants. Additional details and psychometric properties of BioCog are provided in Paper III.

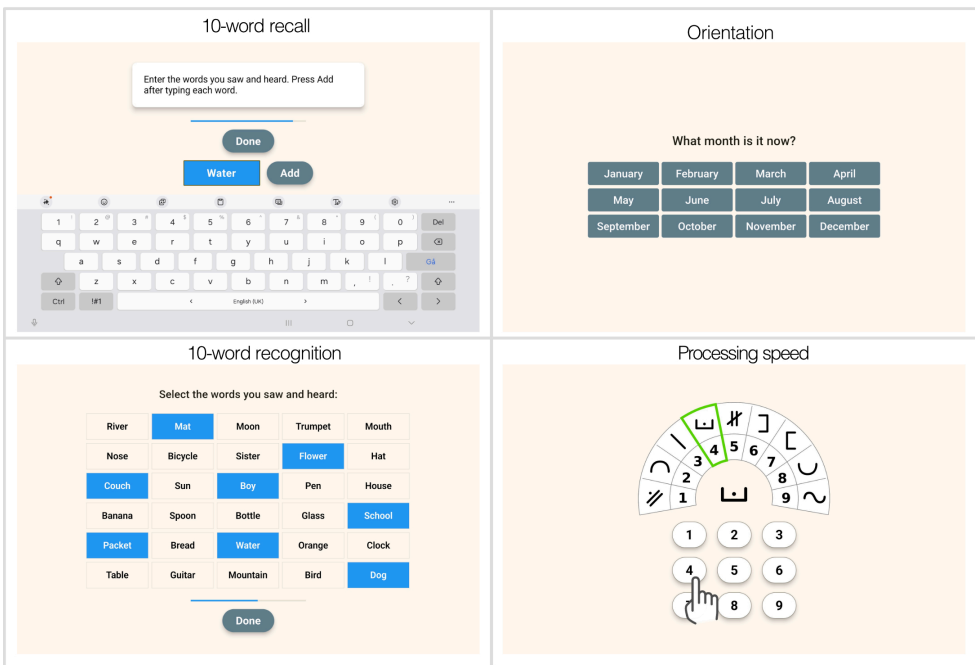

Figure 9. Graphical interface of the self-administered, digital cognitive test battery BioCog. Figure reprinted from [174] (CC BY).

Statistical analyses

Associations

Standardization

Since many variables in the datasets were measured on different scales (e.g., cognitive tests with different score ranges and fluid biomarkers with different dynamical ranges), their magnitudes and estimated effects in models were not directly comparable. To address this, variables were standardized (z-scored) to a common standard scale in all studies. For a variable x with mean $\bar{x}$ and standard deviation σ, the standardized value z is

$$z = \frac{x - \bar{x}}{\sigma}. \quad (3)$$

After standardization, a one-unit change corresponds to a one standard deviation change in the original variable, facilitating comparison of coefficients in regression models and often improving numerical stability during model fitting [131].

Correlation

Correlation coefficients were used to quantify the strength and direction of association between two quantitative variables. The relationships were assessed as strictly linear (e.g., Pearson's correlation) or more generally monotonic (e.g., Spearman's rank correlation). Pearson's correlation r is a parametric measure, defined as the covariance of two variables divided by the product of their standard deviations. It ranges from -1 to 1 (interpretations in Tab. 8). Spearman's rank correlation coefficient ρ is a non-parametric, rank-based measure of monotonic correlation that does not require normally distributed variables. It also ranges from -1 to 1 and is interpreted in a similar manner as Pearsons's correlation (Tab. 8) [175].

Table 8. Common interpretation of Pearson and Spearman correlation coefficients [175].

Absolute correlation coefficient	Interpretation
0.00-0.10	Negligible correlation
0.10-0.40	Weak correlation
0.40-0.70	Moderate correlation
0.70-0.90	Strong correlation
0.90-1.00	Very strong correlation

Regression analysis

Regression models were used to estimate the relationship between a dependent variable (outcome, response variable) y and M independent variables (predictors, covariates) x_m. This is done by fitting a model to N observations (in this thesis typically the number of participants).

Linear Regression

In linear regression, a continuous dependent variable y_n is modelled as

$$y_n = \beta_0 + \sum_{m=1}^{M} \beta_m x_{nm} + \varepsilon_n \quad (4)$$

for observation n, where β_0 is the intercept, β_m represents the expected change in y per unit increase in x_m, and ε_n the residual. The parameters are commonly estimated using ordinary least squares, which minimizes the sum of squared residuals. In addition to a linear relationship, assumptions include normally distributed residuals and no strong collinearity between covariates [131]. Linear regression was a main method in Papers I and II.

Logistic Regression

In logistic regression, the probability p_n of a binary dependent variable is modelled as

$$p_n = \frac{1}{1+\exp\left(-\left(\beta_0 + \sum_{m=1}^{M} \beta_m x_{nm}\right)\right)} \quad (5)$$

for observation n, where β_0 is the intercept, and β_m represents the expected change in log-odds of y per unit increase in x_m. The parameters are commonly calculated using maximum likelihood estimation. Assumptions include independent observations, a linear relationship between the covariates and the log-odds, and no strong collinearity between covariates [176]. During fitting, a common rule of thumb for a robust logistic regression inference model is to use a minimum of 10 events per independent variable (EPV) to avoid biased regression coefficients [177]. Logistic regression was a main method in Papers I, II, and III.

Evaluation

Continuous outcome variables

Continuous outcomes were visualized in scatter plots of observed versus predicted values. Evaluation metrics included Pearson's correlation r, the coefficient of determination R^2 (i.e. proportion of shared variance), and error-based measures such as the mean absolute error (MAE), mean squared error (MSE) or mean absolute percentage error (MAPE).

Binary outcome variables

Binary outcomes were summarized using a confusion matrix, which displays the number of true positives (TP), false positives (FP), false negatives (FN), and true negatives (TN) (Fig. 10). Based on this, a straightforward overall performance measure is accuracy. Other common metrics derived from the same quantities are sensitivity, specificity, positive predictive value (PPV), and negative predictive value (NPV) (Fig. 10).

	Positive prediction	Negative prediction	
Positive observation	**TP**	**FN**	Sensitivity TP/(TP+FN)
Negative observation	**FP**	**TN**	Specificity TN/(FP+TN)
	PPV TP/(TP+FP)	NPV TN/(FN+TN)	Accuracy (TP+TN)/(TP+FP+FN+TN)

Figure 10. Confusion matrix and corresponding evaluation metrics for assessment of models using a binary outcome variable.

Because many binary models output class probability (e.g., logistic regression), classification requires choosing a decision threshold. The optimal threshold depends on the aim. For example, screening for a disease typically prioritizes high sensitivity (lower cutoff), whereas selecting individuals for treatment prioritizes high specificity (higher cutoff). A threshold can be chosen to target a desired sensitivity or specificity, or by maximizing Youden's index, defined as sensitivity + specificity – 1 (used in Paper III) [178]. Another approach to improve both sensitivity and specificity is a two-cutoff method that defines an intermediate zone for uncertain cases that could be further assessed [94,179,180]. This way, only more certain cases are classified, but at the cost of required follow-up for a number of cases (used in Paper III).

Performance across all possible thresholds was visualized using a receiver operating characteristics (ROC) curve, which plots sensitivity against 1 – specificity. The area under the ROC curve (AUC) summarizes the model's discrimination, with an AUC = 0.5 indicating chance-level and AUC = 1 perfect performance. Since ROC AUC evaluates discrimination across all thresholds, it is usually less sensitive to class imbalance compared to accuracy.

All the studies in this thesis reported at least one of the metrics described above and/or summarized performance in a confusion matrix.

Standardized regression coefficients

In linear regression with standardized input data, the effect sizes of individual predictors were assessed by directly comparing their β-coefficients. In logistic regression, standardization enabled a similar comparison of predictors but on the log-odds scale. During inference analysis, confounding variables (i.e. variables related to both the predictor and outcome) were included as covariates in the models to reduce bias in the estimated associations [181]. This included for example adjustment for age and sex to estimate effects independent of these characteristics and to assess whether they themselves influenced the outcome.

In addition to confounding, a suppressor variable can strengthen the association of another predictor by accounting for variance in that predictor that is irrelevant to the outcome. Typically, a suppressor is not itself associated with the outcome, but shares this irrelevant variance with the predictor, thereby "purifying" the main predictor [182]. Adjustment for a suppressor variable can lead to a larger absolute standardized β-coefficient for the main predictor, and a β-coefficient in opposite direction for the suppressor, an important concept for reference protein normalization in Papers I and II.

Significance testing

P-value

Significance testing was used to formally assess the evidence for a difference or effect. This was done by comparing the results to a null hypothesis H_0 (typically assuming no effect) and calculating the probability that results at least as extreme as those observed would have occurred if H_0 were true, known as a p-value. By setting a pre-defined threshold for rejecting H_0 (commonly 0.05 or 0.01), a p-value below this level was considered statistically significant.

Confidence interval

Confidence intervals provided a complementary way to quantify uncertainty by estimating a likely range of values for the parameter. For example, 95%-confidence intervals were constructed such that, under repeated sampling, they would contain the true parameter in 95% of repeated samples.

Bootstrapping

Many methods exist to estimate p-values and confidence intervals. In this thesis, a standard non-parametric bootstrap procedure was most frequently used [183]. From N true observations, an equal number of observations were sampled randomly with replacement to obtain a bootstrap dataset. The relevant metric was then calculated for the bootstrap dataset, and this was repeated many times (between 1,000 and 10,000 iterations across the studies) to obtain a bootstrap distribution of the metric.

To compute p-values, comparisons were usually made between two variables (for example two biomarkers in Papers I and II, or two cognitive tests in Paper III). The difference between the two variables was bootstrapped and the p-value was calculated as the proportion of replicates in which the difference was < 0 (one-sided) or twice this proportion (two-sided). Similarly, a confidence interval for such a comparison was obtained from the quantiles of a bootstrap distribution, for example using the 0.05 quantile for a one-sided 95%-confidence interval or the 0.025 and 0.975 quantiles for a two-sided one.

Multiple testing correction

When performing multiple statistical tests, the probability of finding a false positive result increases. In this thesis, the false discovery rate was controlled for using the Benjamini-Hochberg method [184]. Given m tests, the p-values were sorted in ascending order $p_{(1)} \leq \cdots \leq p_{(m)}$ and adjusted as

$$p_{(i)}^{adjusted} = \min_{j \geq i} \frac{m}{j} p_{(j)}, \tag{6}$$

where $\min(j \geq i)$ is the cumulative minimum ensuring the sequence increases monotonically.

Machine learning

Unsupervised learning

Unsupervised learning techniques were used in Paper I to investigate patterns in high-dimensional proteomics data.

Singular value decomposition

A singular value decomposition (SVD) was used to create a mutual component from multiple reference proteins. An SVD is a factorization of a matrix $\boldsymbol{A}$ of size $m \times n$ and rank r as

$$\boldsymbol{A} = \mathbf{U}\boldsymbol{\Sigma}\boldsymbol{V}^T, \tag{7}$$

where $\boldsymbol{U}$ and $\boldsymbol{V}$ are orthogonal matrices of sizes $m \times m$ and $n \times n$, and $\boldsymbol{\Sigma}$ is a matrix of size $m \times n$ with r non-zero diagonal elements Σ_{ii} that are the singular values of $\boldsymbol{A}$. If sorting Σ_{ii} in descending order and keeping only the first $k < r$ components, the matrix can be reduced to an optimal low-rank approximation which often is sufficient to describe most of the original variability [185]. In Paper I, SVD was used by constructing $\boldsymbol{A}$ from three reference protein candidates and letting the first SVD component represent a mutual CSF reference component.

T-distributed stochastic neighbor embedding

t-SNE was used to visualize high-dimensional data in a two-dimensional map while preserving similarity of pairwise points. Accordingly, proteins of short distance in the t-SNE map could be interpreted as similarly expressed. t-SNE is a non-linear method that mainly preserves local neighborhood structure while global distances are less certain [186]. The embedding is obtained by minimizing the Kullback-Leibler divergence between pairwise similarity distributions in the high and low-dimensional spaces

$$\min_{\{y_i\}} \sum_{i \neq j} p_{ij} \log \frac{p_{ij}}{q_{ij}}. \quad (8)$$

Here, y_i is the two-dimensional coordinate of protein i, p_{ij} the similarity between proteins i and j in the original high-dimensional space, and q_{ij} the corresponding similarity between y_i and y_j in the two-dimensional space. The optimization was performed using gradient descent.

K-means clustering

K-means clustering was used to group proteins based on their coordinates in the t-SNE map by minimizing squared distances to their assigned cluster centers [187]. The algorithm requires a pre-selected number of clusters K which centres are randomly initialized. The optimization is then carried out by iterating the following steps:

Assignment step: Each protein is assigned to the nearest cluster based on the Euclidean distance to the cluster centres.

Update step: The cluster centres are updated as the average of all proteins assigned to that cluster.

These two steps are repeated until convergence, defined as no further change in assignments or centre positions below a selected tolerance. In Paper I, K was chosen based on visual inspection in the t-SNE map and the clustering is therefore referred to as semi-supervised.

Supervised learning

Supervised learning techniques were used for different prediction tasks in Papers I, III, IV, V, and VI.

Machine learning estimators

Different classification and regression tasks may benefit from different ways of separating classes or fitting continuous outcomes during prediction [188]. ML estimators can therefore be both linear and non-linear, and their suitability depends

on the input features, the outcome, and underlaying data structure. In Papers I and III, linear models were used for prediction. In Papers IV and V, a broader set of ML estimators was evaluated before selecting the model most appropriate for each task. All used estimators are summarized in Tab. 9 and described in the corresponding papers.

Table 9. Summary of machine learning estimators used in this thesis.

Class	Description	Estimators
Linear models	The used linear models were based on linear or logistic regression (see *Statistical Analyses*). To prevent overfitting and manage multicollinearity, L1 and/or L2 regularization hyperparameters were sometimes included, either with only L2 penalty (Ridge) or both L1 and L2 (ElasticNet) [188].	Linear/logistic, Ridge, ElasticNet
Support vector machines	Support vector machines find an optimal hyperplane that either separates the classes (classification) or that fits to the data points (regression). Before finding the hyperplane, data can be mapped to a higher-dimensional space using a kernel function, making a non-linear separation/fit possible [189].	Support vector machines
Nearest Neighbors	A k-nearest neighbors model stores the training data and predicts the label of a new data point based on its similarity/distance to the training points. For classification, the prediction is typically determined by a majority vote among the k nearest neighbours, where k is a hyperparameter specifying the number of votes [190].	k-nearest neighbors
Decision trees	A decision tree infers predictive rules from input features in a hierarchical tree structure. It consists of a root node and internal nodes that split the data into subsets based on feature thresholds, and leaf nodes that output a final class (classification) or predicted value (regression). Starting at the root, each sample follows a sequence of decisions (branch) until reaching a leaf. Splits are typically chosen to minimize impurity or error, and hyperparameters like depth control the tree's complexity [191].	Decision trees
Ensembles	Ensemble methods combine multiple individual classifiers/regressors, often decision trees, to improve predictive performance and robustness. The individual models can be trained in parallel and their prediction averaged (e.g., Random forests), or trained sequentially to correct the errors of the previous ones (Boosting models). Common hyperparameters include the number of estimators, max depth of each tree, and learning rate [192].	Random forest, ExtraTrees, XGBoost, CatBoost, AdaBoost, GradientBoost

Feature selection

Before training a prediction model, a set of relevant input features must be selected. This involves balancing the need to retain as much informative signal as possible against the risk that redundant or irrelevant features add noise and can increase overfitting. Some estimators incorporate implicit feature selection during training (e.g., tree-based methods), while others do not. In Papers III, IV and V, an initial inclusive feature set was defined in line with the study aims, after which smaller subsets were derived using different selection methods. In Paper III, recursive

feature elimination (RFE, eliminating the weakest feature until highest performance is reached) was performed based on standardized logistic regression coefficients. In Paper IV, feature selection was made using SHAP values (see *Feature contribution* below). In Paper V, features were selected based on F-statistics (linear association with the outcome), mutual information (non-linear information shared with the outcome), RFE using random forest feature importance, or by retaining the top 95% of features ranked by cumulative random forest feature importance.

Model optimization

Because the goal of prediction modelling is high performance on new, unseen data, model selection should prioritize generalization rather than maximal fit to the training set. In this thesis, different approaches were used to achieve this.

In Paper III, the best model was selected using the Akaike Information Criterion (AIC), which balances goodness of fit and model complexity as

$$\mathrm{AIC} = 2k - 2\ln(\hat{L}), \tag{9}$$

where k is the number of estimated parameters and $\hat{L}$ is the maximum likelihood [193].

In Papers I, IV and V, the best model was selected based on performance in k-fold cross-validation on the training set. In k-fold cross-validation, the data are split into k folds, the model is trained on $k-1$ folds and evaluated on the remaining fold. This is repeated k times so that each fold serves as the validation set once, allowing all observations to contribute to both training and validation while evaluating performance on held-out data [194].

Apart from evaluating model fit using AIC or cross-validation, model optimization can include tuning hyperparameters. In Papers IV and V, hyperparameter tuning was performed using cross-validation combined with Bayesian optimization. Bayesian optimization searches the hyperparameter space by using information from previous evaluations to efficiently balance exploration of new regions with exploitation of known promising configurations [195,196].

Model evaluation

Supervised machine learning models in Papers I, III, IV, V and VI were evaluated using the same methods as the statistical models (see *Statistical analyses - Evaluation*). A key difference, however, was that machine learning models were consistently assessed on unseen data, using cross-validation, a held-out test set, and/or external cohorts.

Feature contribution

In Papers IV and V, Shapley Additive exPlanations (SHAP) was used to quantify each feature x's contribution to the prediction $f(x)$. SHAP computes Shapley values by averaging a feature's contribution over all possible combinations of the other input features, thereby accounting for interactions. A local linear model $g(x')$ that converges to the original model $f(x)$ when $x' \approx x$ is created as

$$g(x') = \phi_0 + \sum_{i=1}^{M} \phi_i x_i', \tag{10}$$

where x' is the binary inclusion/exclusion of a feature, M is the number of features, ϕ_0 is the model output without any input features, and ϕ_i are the Shapley values [197].

Machine learning pipelines

In Paper IV and V, rigorous feature selection, estimator selection and hyperparameter tuning was performed using cross-validation with Bayesian optimization on a training set. An overview of the optimization pipelines is shown in Fig. 11. Both pipelines were implemented in Python and are publicly available on GitHub.

Paper IV: https://github.com/DeMONLab-BioFINDER/continuous-abpet-prediction
Paper V: https://github.com/DeMONLab-BioFINDER/karlsson-predict-taupet

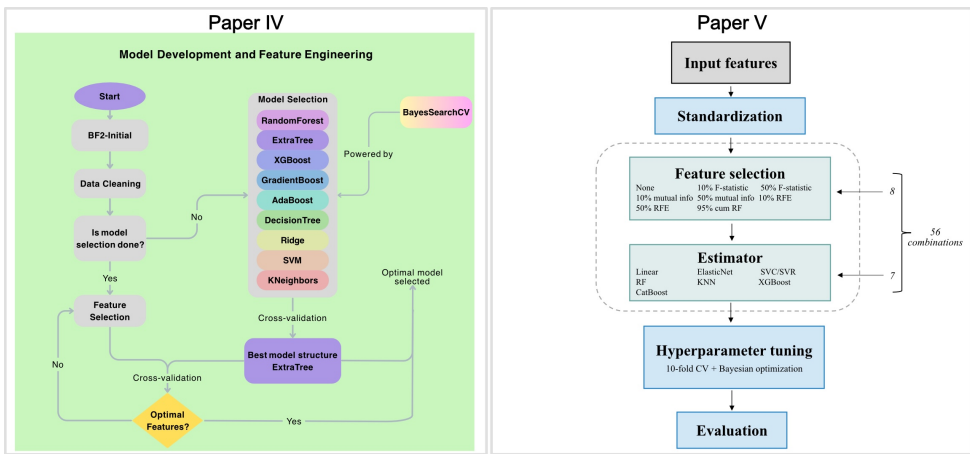

Figure 11. Machine learning pipelines implemented in Papers IV and V. Modified figures reprinted from [198,199] (CC-BY and CC-BY-NC).

Deep learning U-Net model

In Paper VI, a deep learning 3D U-Net model was optimized and trained to generate synthetic tau-PET scans. A U-Net consists of an encoder that downsamples the input to learn hierarchical features and a decoder that upsamples these features to reconstruct the output. The encoder and decoder are connected via a bottleneck that reflects the most compact latent representation. Furthermore, skip connections link corresponding encoder and decoder levels to preserve high-resolution spatial information [200].

The model was trained with an L1-based loss combining a global reconstruction term and a term restricted to the cortical mask as

$$\mathcal{L}(x, \hat{x}) = \frac{1}{N_v} \left|\left|x - \hat{x}\right|\right|_1 + \frac{\alpha}{N_v} \left|\left|m \odot (x - \hat{x})\right|\right|_1, \quad (11)$$

where $\odot$ denotes elementwise multiplication, $x, \hat{x} \in \mathbb{R}^{H \times W \times D}$ are the true and predicted images, N_v is the number of voxels, and $m \in \{0,1\}^{H \times W \times D}$ is a FreeSurfer-derived cortical mask with $\alpha = \frac{1}{2}$. Training was performed using the Adaptive Moment Estimation (Adam) optimizer [201].

When building the U-Net, different U-Net architectural designs, input features and hyperparameters were systematically evaluated. Performance improved with increased network depth and the inclusion of residual and attention units [202,203]. Adding tabular variables as separate channels in the bottleneck further improved performance compared to as separate initial channels. The final model was a 3D U-Net with residual units in the encoder and decoder, an attention unit in the bottleneck, and ~110M trainable parameters (Fig. 12). For further details see Paper VI.

Computational resources

Computationally demanding model training and optimization was performed on the Bianca Cluster, which is a part the National Academic Infrastructure for Supercomputing in Sweden (NAISS). Bianca is dedicated to analyses of sensitive data, providing 4480 cores in the form of 204 dual CPU (Intel Xeon E5-2630 v3) Huawei XH620 V3 nodes with 128 GB memory, and ten nodes with two NVIDIA A100 40GB GPUs each.

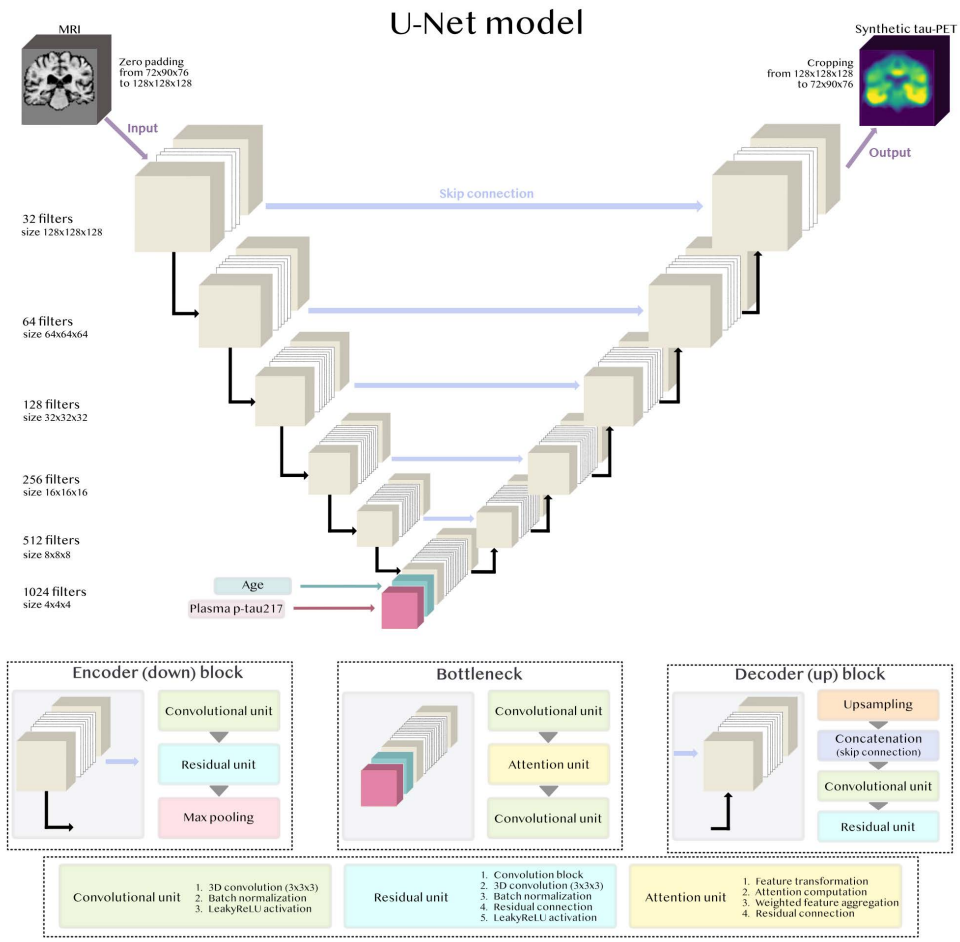

Figure 12. Deep learning model optimized to generate synthetic tau-PET in Paper VI.

Main results

Paper I

When using CSF biomarkers to diagnose AD, a biomarker concentration is usually compared to a population-based cutoff value. Although uncomplicated, this approach sometimes results in discordance between CSF biomarkers and other AD biomarkers (e.g., PET) [204,205]. One striking example of how a more individualized method can increase the concordance between biomarker modalities is CSF Aβ42, which shows higher agreement with Aβ-PET when normalized to CSF Aβ40 [83,88,206]. Since CSF Aβ40 does not change with AD pathology, it can simply be regarded as a reference protein, representative of the concentration the disease-related marker would have had if no pathology would have been present. Inspired by this, in Paper I [207] we investigated co-varying properties of the CSF proteome and showed that several CSF biomarkers can benefit from reference protein normalization.

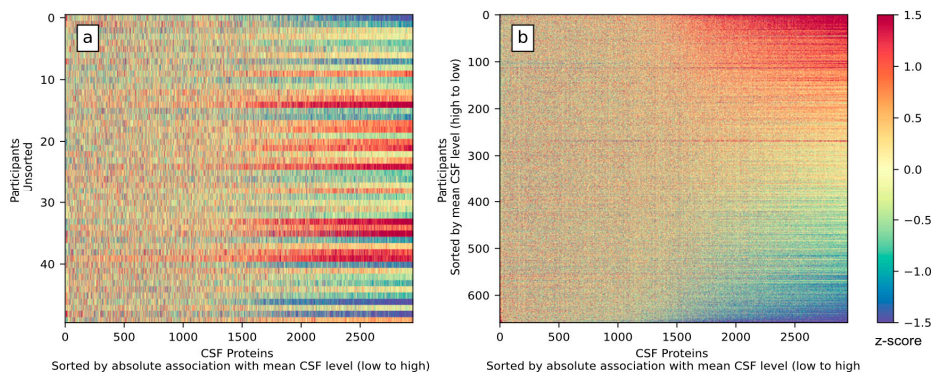

Figure 13. Many CSF proteins vary in concordance with an individual protein level. Each participant (row) shows the standardized concentration of 2944 CSF proteins (column), sorted by increasing association with the mean standardized CSF protein level. **a)** a subset of 50 randomly selected participants. **b)** all 658 participants sorted by mean standardized CSF level. Figure reprinted from [207] (CC BY).

In a BioFINDER-2 training set (80%, n=658), we observed from proteomic measurements (2944 proteins) that many CSF proteins co-vary (Fig. 13). By averaging the z-scored proteins (columns), each participant (row) was assigned a

value indicating how many standard deviations their protein level deviated from the population mean. The AD biomarkers CSF Aβ42 and CSF p-tau181 were associated with this mean level (β = 0.24, P < 1e-10 and β = 0.34, P < 1e-20, respectively). CSF Aβ40 (β = 0.44, P < 1e-37) was associated even more strongly, as expected given its lack of a disease-related signal.

By performing unsupervised t-SNE dimensionality reduction and semi-supervised K-means clustering on the proteomic data, we identified a protein cluster with favorable reference protein characteristics (Fig. 14; cluster 11; 219 proteins including Aβ40). These proteins showed higher brain expression and greater enrichment at cell surfaces and membranes than the other CSF proteins.

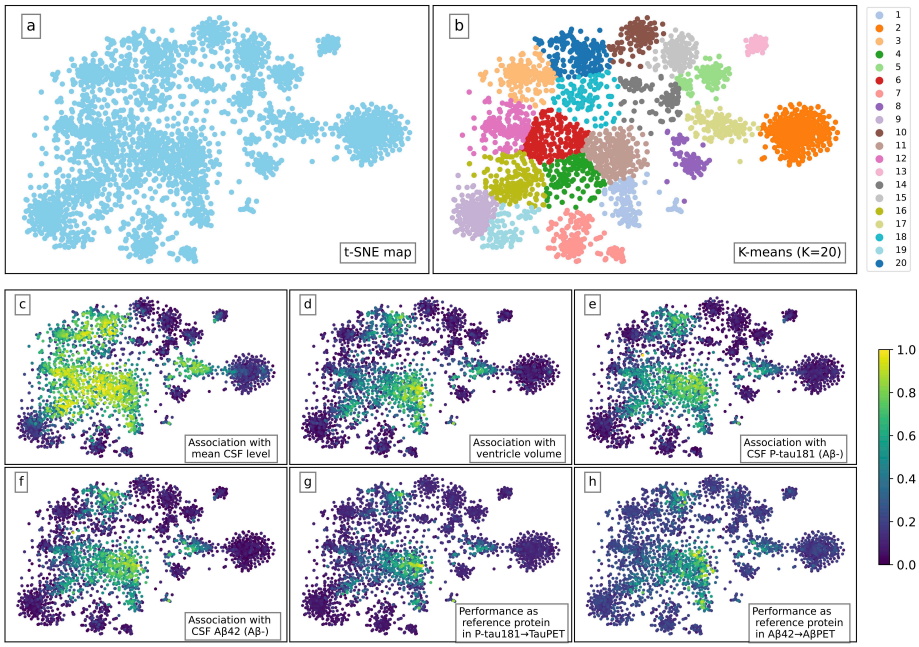

Figure 14. Dimensionality reduction reveals a cluster of CSF proteins with desired reference protein characteristics. Each scatter point illustrates one of the 2944 CSF proteins in the two-dimensional t-SNE space created from BioFINDER-2 training set (n=658). **a)** raw t-SNE map. **b)** semi-supervised K-means clustering (K = 20). **c)-h)** desired reference protein characteristics, min-max scaled (higher values = more suitable as a reference protein). **c)** association with mean standardized CSF protein level.* **d)** association with ventricular volume.* **e)** association with CSF p-tau181 in Aβ-negative controls.* **f)** association with CSF Aβ42 in Aβ-negative controls.* **g)** AUC when used as reference protein to improve concordance between CSF p-tau181 and tau-PET. **h)** AUC when used as reference protein to improve concordance between CSF Aβ42 and Aβ-PET. *adjusted for age and sex. Figure reprinted from [207] (CC BY).

Next, six candidates from cluster 11 were selected and evaluated together with the mean standardized CSF level and Aβ40 as potential reference proteins for CSF Aβ42 and p-tau181. Aβ-PET, tau-PET, and progression to dementia were used as

outcome variables in logistic regression models, and evaluations were performed on the left-out BioFINDER-2 test set (20%, n=172) or external cohort BioFINDER-1 (n=904). All normalization markers improved performance compared to no reference (Fig. 15). CSF Aβ42→Aβ-PET showed highest performance with Aβ40 as reference protein, and CSF p-tau181→tau-PET with CBLN4 or NTRK3.

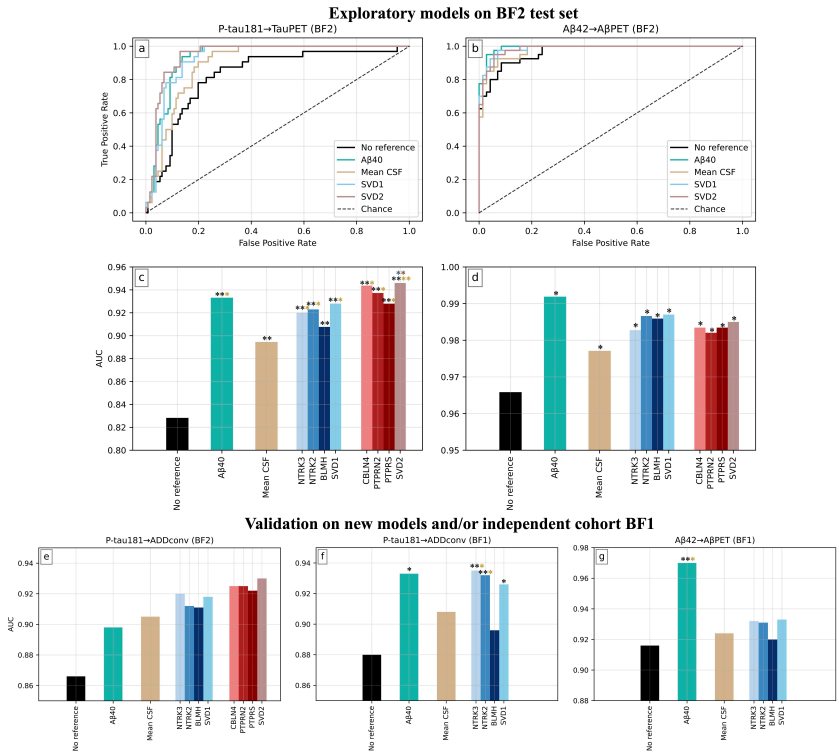

Figure 15. Performance evaluation of Aβ42 and p-tau181 with and without reference protein normalization. Logistic regression models fitted using the BioFINDER-2 training set and evaluated using the BioFINDER-2 test set. ROC curves and AUCs when predicting **a)**, **c)** tau-PET status with CSF p-tau181, **b)**, **d)** Aβ-PET status with CSF Aβ42, and **e)** progression to dementia with CSF p-tau181. Logistic regression models fitted and evaluated using the external BioFINDER-1 cohort. AUCs when predicting **f)** progression to dementia with CSF p-tau181, and **g)** Aβ-PET status with CSF Aβ42. SVD correspond to the first component of a singular value decomposition created from the three reference protein candidates of same color. AUCs were compared with bootstrapping (n_{iter} = 2000). All models were adjusted for age and sex. *P < 0.05, **P < 0.01 (FDR corrected) compared to the bar of same color as asterisk. Figure reprinted from [207] (CC BY).

We further investigated how AT(N) grouping was affected by reference protein normalization. We were particularly interested in the A-T+ group, for which several studies have reported findings [208–210], even though this group is difficult to explain pathophysiologically (A-positivity is expected before T-positivity in AD, see Fig. 2 [47]). When adjusting CSF p-tau181 for the reference protein CBLN4,

overall T grouping concordance increased from 76% to 89%, and the number of discordant A-T+ cases (PET negative and CSF positive) decreased from n=36 to n=9 (Tab. 10).

Table 10. Adjusting for a reference protein (here CBLN4) results in higher T grouping concordance between CSF p-tau181 and tau-PET. Concordance matrices for participants from the BioFINDER-2 training set. A-grouping was performed with CSF Aβ42/Aβ40 (cutoff 0.08 [211]). T-grouping was performed (left) p-tau181 > 21.8 pg/ml [208] or (right) p-tau181 > 39.0 + 10.1c_{CBLN4} (logistic regression model).

Without reference *Tau cutoff: CSF p-tau181 > 21.8*				
PET CSF	A-T-	A-T+	A+T-	A+T+
A-T-	285	6		
A-T+	36	1		
A+T-			63	26
A+T+			86	137
Accuracy = 486/640 (76%)				

With reference *Tau cutoff: CSF p-tau181 > 39.0 + 10.1c_{CBLN4}*				
PET CSF	A-T-	A-T+	A+T-	A+T+
A-T-	312	6		
A-T+	9	1		
A+T-			105	10
A+T+			44	153
Accuracy = 571/640 (89%)				

Based on these results, it is likely that the CSF-based A-T+ profile largely represents individuals with high average CSF proteomic levels. Such individuals consequently also show increased levels of other CSF biomarkers (Fig. 15).

In conclusion, adjusting for individual mean CSF protein levels, by for example using a reference protein, improves the accuracy of CSF biomarkers, and reduces the risk of false positive research findings.

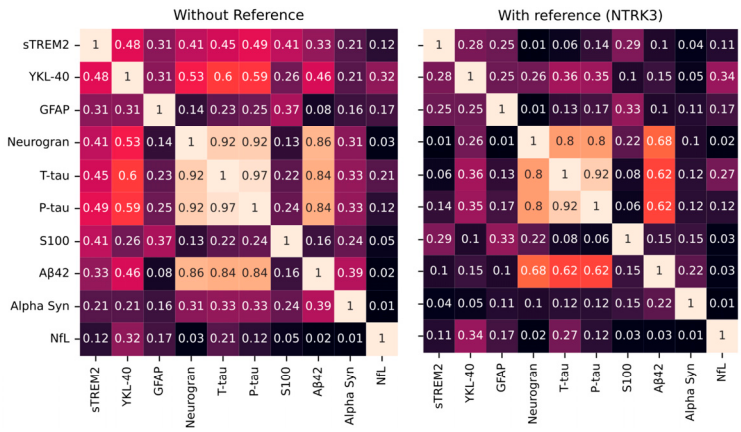

Figure 15. Correlations between CSF proteins decrease when adjusting for a reference protein. Partial correlation matrices for ten biomarkers in BioFINDER-2 cognitively unimpaired Aβ-negative participants, adjusted for age, sex, (left panel) and a reference protein (right panel, here NTRK3).

Paper II

Based on the findings in study I, Paper II [212] further investigated fluid biomarker normalization using the reference protein Aβ40, and np-tau, another commonly used normalization marker. The study was particularly targeted toward when biomarkers of different modalities are used interchangeably, as was recommended in the revised criteria for diagnosis and staging of AD in 2024 [50]. Apart from evaluating additional AD biomarkers, we here moved beyond binary regression models and examined continuous relationships. Furthermore, we aimed to assess if reference protein normalization also could improve blood-based biomarkers.

Reference protein normalization was performed by calculating the ratio between the fluid biomarker and reference protein. CSF Aβ40 normalization resulted in significantly increased associations between CSF biomarkers and early and late-stage tau-PET load (Fig. 16a-b).

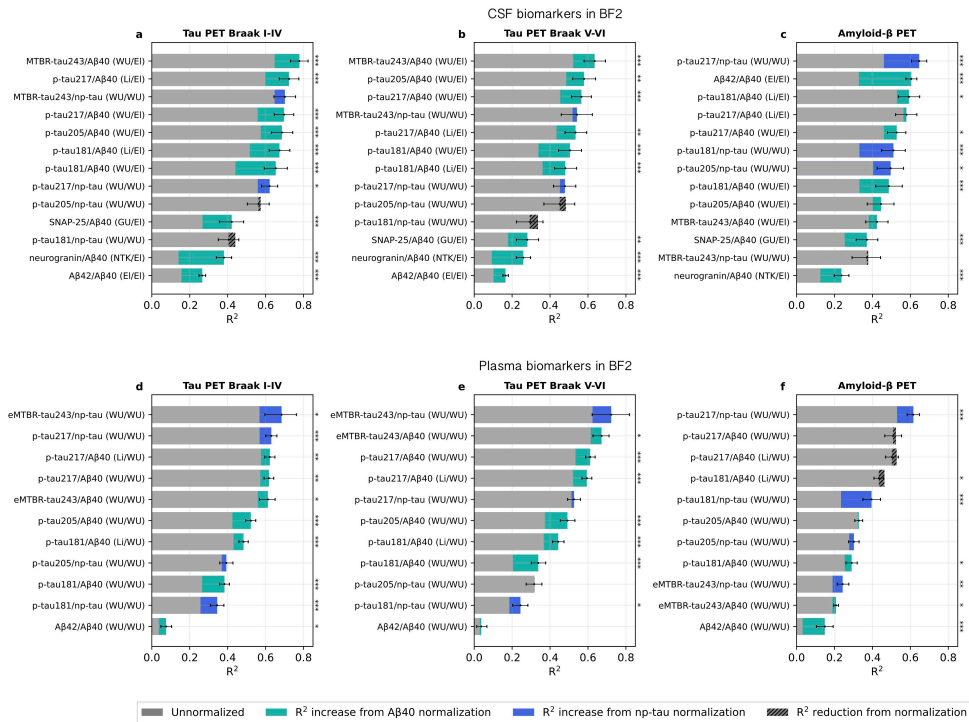

Figure 16. Reference protein normalized CSF and plasma biomarkers show stronger associations with tau and Aβ-PET. a)-c) CSF biomarkers; **d)-f)** plasma biomarkers. Error bars represent 95% confidence intervals for the bootstrapped R^2 difference between the normalized and unnormalized biomarker. *P < 0.05, **P < 0.01, ***P <0.001 (FDR corrected). Figure reprinted from [212] (CC BY).

Similarly, CSF Aβ40 normalization increased associations between CSF biomarkers and Aβ-PET load, but np-tau normalization yielded even higher improvement for p-tau markers (Fig. 16c). Plasma biomarkers also showed stronger associations with tau-PET and Aβ-PET when normalized to plasma Aβ40 or plasma np-tau compared to unnormalized (Fig. 16d-f). In Fig 17, scatter plots of the fluid biomarkers with highest tau-PET correlation with and without normalization are exemplified.

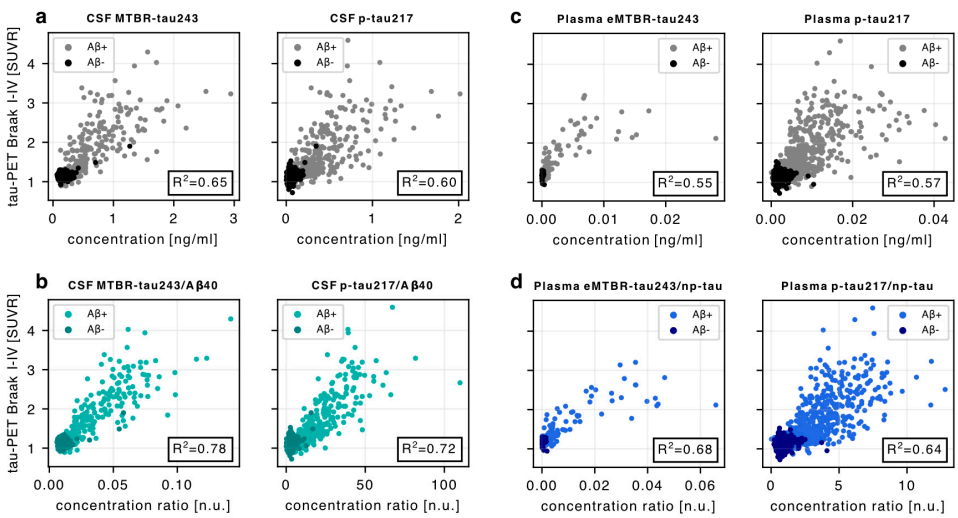

Figure 17. Scatter plots showing associations with temporal meta-ROI tau-PET load for unnormalized and normalized CSF and plasma biomarkers. a) CSF unnormalized; **b)** CSF Aβ40-normalized; **c)** plasma unnormalized; d) plasma np-tau normalized. Figure reprinted from [212] (CC BY).

Improved concordances between fluid biomarkers and PET through reference protein normalization were seen for multiple AD biomarkers, and for both mass spectrometry and immunoassays. The findings were also robust when i) applying the reference protein as covariate instead of ratio, ii) for Aβ-positive individuals only, and iii) for AT-classification (binary PET outcome) instead of regression. Furthermore, the main results were successfully replicated in the external cohorts Knight-ADRC and TRIAD, even though they had slightly different cohort compositions (e.g., more early disease-stage participants) and used other PET tracers.

In conclusion, reference protein normalization with Aβ40 and np-tau can enhance the precision and utility of AD fluid biomarkers, and it shows high robustness and generalizability across cohorts and assays.

Paper III

It can be challenging to determine if a person has objective cognitive impairment, especially in primary care where time and resources are limited. Doing this accurately and efficiently has become increasingly important as such impairment is necessary for eligibility for the recently approved anti-amyloid therapies [126,127]. Furthermore, current recommendations for the newly developed blood tests for AD are that they should be used exclusively in patient populations with objective symptoms [118,213]. Not only does this requirement remove unnecessary burden for patients (that otherwise potentially learn that they have preclinical AD at a stage where no treatment can be provided), but it also increases the likelihood that a positive biomarker truly reflects AD pathology (higher pre-test probability [120]).

To facilitate cognitive evaluations, in Paper III [174] we developed a brief, self-administrated digital cognitive test battery: BioCog. Based on the scores and time variables from this digital test, we created a predictive logistic regression model in the BioFINDER-2 secondary care cohort (n=223) and evaluated it in the independent BioFINDER-Primary Care cohort (n=403).

BioCog identified objective cognitive impairment (RBANS as reference standard) with 85% accuracy in the primary care cohort (Fig. 18), outperforming both primary care physicians (Fig. 18; 73% accuracy) and commonly used paper-and-pencil tests (Table 11; 67–75% accuracy).

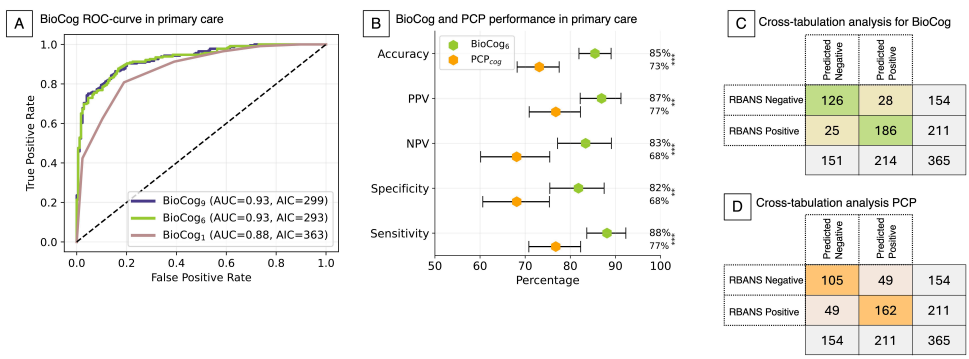

Figure 18. BioCog performance for predicting objective cognitive impairment in the primary care cohort. a) ROC curves for three BioCog models using one ($BioCog_1$), six ($BioCog_6$) or nine ($BioCog_9$) input variables, selected with RFE. **b)** $BioCog_6$ compared to a primary care physician's diagnosis of SCD versus MCI/dementia. Error bars indicate 95% CI, center point mean value. CI and two-sided p-values were computed using bootstrapping and adjusted for multiple comparisons. ** = P < 0.01, *** = P < 0.001. **c)** Cross-tabulation analysis for $BioCog_6$. **d)** Cross-tabulation analysis for primary care physician. Figure reprinted from [174] (CC BY).

Table 11. Head-to-head comparison between $BioCog_6$ and other cognitive tests when predicting objective cognitive impairment in the primary care cohort. Performance was calculated using the $BioCog_6$ model (established in the secondary care cohort) or using prespecified cutoffs from literature [165,214–216]. Confidence intervals and two-sided p-values were computed using bootstrapping and adjusted for multiple comparisons.

	Cutoff(s) for positivity	**Accuracy** (95% CI, P_{FDR} compared against $BioCog_6$)	**PPV** (95% CI, P_{FDR} compared against $BioCog_6$)	**NPV** (95% CI, P_{FDR} compared against $BioCog_6$)	**Specificity** (95% CI, P_{FDR} compared against $BioCog_6$)	**Sensitivity** (95% CI, P_{FDR} compared against $BioCog_6$)
$BioCog_6$	>0.575	84% (81%-88%)	84% (79%-89%)	84% (79%-90%)	79% (73%-85%)	88% (84%-92%)
MMSE	<27	71% (67%-76%, 0.0007)	81% (75%-87%, 0.30)	64% (58%-70%, 0.0007)	80% (75%-86%, 0.70)	64% (58%-71%, 0.0007)
MoCA	<26	67% (62%-71%, 0.0007)	63% (58%-68%, 0.0007)	93% (86%-100%, 0.06)	27% (20%-34%, 0.0007)	98% (96%-100%, 0.0007)
Mini-Cog	<4	75% (71%-79%, 0.0007)	78% (72%-83%, 0.02)	71% (64%-78%, 0.0007)	72% (65%-79%, 0.08)	77% (71%-83%, 0.0007)
CANTAB	>41	76% (71%-80%, 0.0007)	78% (73%-83%, 0.03)	73% (66%-79%, 0.001)	72% (65%-79%, 0.08)	78% (73%-84%, 0.001)

We next evaluated how the digital cognitive test combined with blood biomarkers would affect diagnostic performance of clinical AD (objective cognitive impairment + AD pathology) in the primary care cohort. When a physician would suspect that a neurodegenerative disease is a reasonably possible cause of the patient's symptomatology, we suggest a two-step approach: 1) establishing objective cognitive impairment using $BioCog_6$, and 2) blood biomarker testing in those classified as impaired in 1) (Fig. 19a). Accordingly, we evaluated an outcome of cognitive impairment according to RBANS and a clinical AD consensus diagnosis done by dementia experts (including CSF analysis or Aβ-PET assessments). The BioCog and blood test combination resulted in an accuracy of 90% for this outcome, significantly higher than today's standard of care (70% accuracy; based on primary care clinical evaluation including physician assessment, brief cognitive testing and CT brain imaging), and higher than using the blood test alone (80% accuracy); Fig 19b-e.

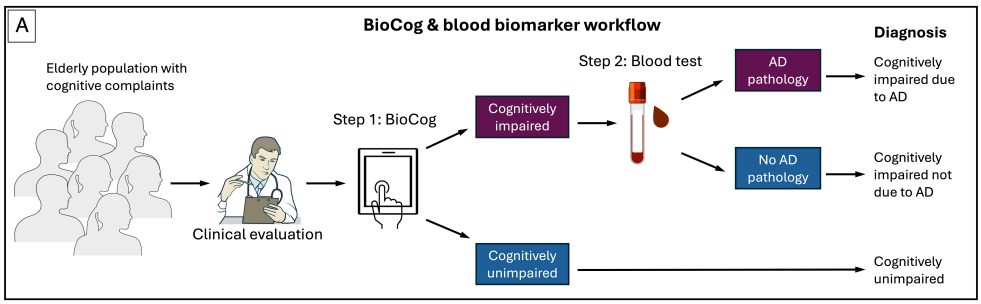

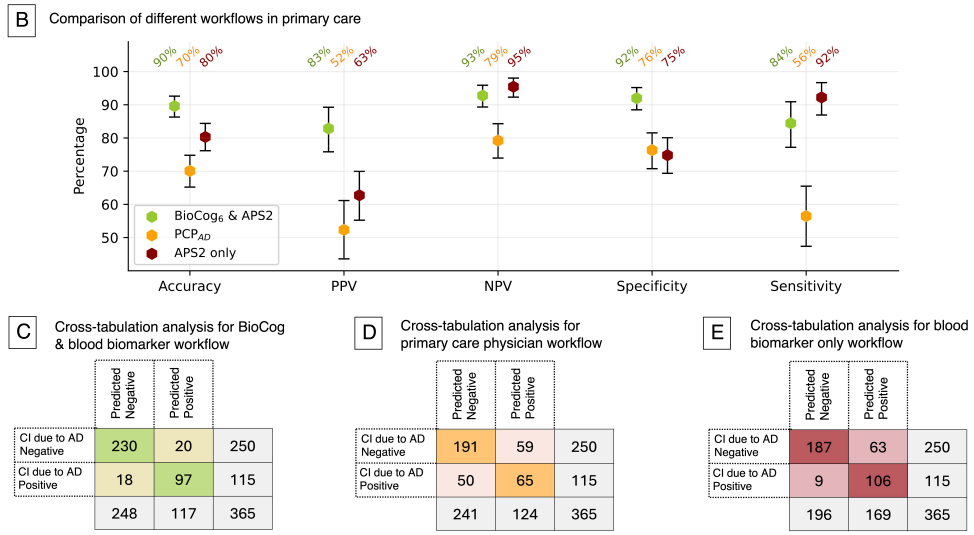

C Cross-tabulation analysis for BioCog & blood biomarker workflow

	Predicted Negative	Predicted Positive	
CI due to AD Negative	230	20	250
CI due to AD Positive	18	97	115
	248	117	365

D Cross-tabulation analysis for primary care physician workflow

	Predicted Negative	Predicted Positive	
CI due to AD Negative	191	59	250
CI due to AD Positive	50	65	115
	241	124	365

E Cross-tabulation analysis for blood biomarker only workflow

	Predicted Negative	Predicted Positive	
CI due to AD Negative	187	63	250
CI due to AD Positive	9	106	115
	196	169	365

Figure 19. Comparing a digital testing and blood biomarker-based diagnostic workflow to the current standard clinical evaluation in the primary care cohort. a) Our proposed primary care diagnostic workflow for AD, consisting of a physician's assessment and digital cognitive testing, followed by blood biomarker testing only in the individuals with cognitive impairment. **B)-E)** Evaluation of the proposed workflow with $BioCog_6$ and Amyloid Probability Score-2 (based on blood biomarkers) compared against a standard clinical evaluation by primary care physicians (PCP_{AD}), and against using only APS2 without any cognitive assessment. Error bars indicate 95% confidence intervals, central point mean value. Illustrations in a) adapted from NIAID NIH BIOART (https://bioart.niaid.nih.gov). Figure reprinted from [174] (CC BY).

In conclusion, this proof-of-concept study demonstrated that a self-administered digital cognitive test could reliably detect cognitive impairment, and when combined with a blood biomarker test, it could accurately identify clinical AD in primary care patients evaluated for a neurodegenerative disease. Digital cognitive tools offer a promising approach to improve AD detection, supporting physicians in making earlier, more accurate diagnoses in a resource efficient manner.

Paper IV

Aβ-PET can be used to accurately measure the extent of Aβ plaque accumulation in AD, but the method is costly and not widely accessible. Fluid biomarkers are more scalable, but it is unclear how well they can predict the actual Aβ burden measured by PET, and what fluid biomarkers are most informative during such prediction. To address this, in Paper IV [198] we investigated prediction of continuous Aβ-PET load with machine learning using fluid biomarkers and clinical variables. We used the BioFINDER-2 cohort (n=1140) for main analyses, split into training (80%) and test (20%) sets, and evaluated generalizability by applying the models in BioFINDER-1 (n=238).

During model optimization, Extra Tree Regressor models showed highest cross-validation performance. CSF Aβ42/Aβ40 and plasma p-tau217 assays were the most influential features (Fig. 20a) but with complementary signals: CSF Aβ42/40 was most important to identify Aβ plaque presence, while plasma p-tau217 best tracked increasing amyloid plaque burden once positivity was established (Fig. 20b).

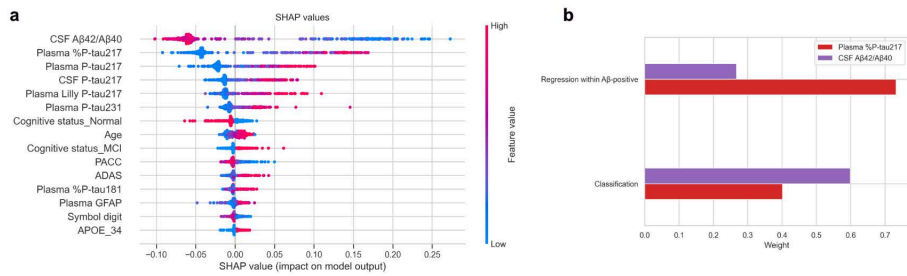

Figure 20. Analysis of feature importance. a) SHAP values for the top 15 features with highest impact. **b)** The Extra Tree regressor/classifier weighted feature importance of plasma %P-tau217 and CSF Aβ42/Aβ40 (scaled so in total 100%). Figure reprinted from [198] (CC BY).

Based on this feature analysis, we trained a final Extra Tree Regressor with CSF Aβ42/Aβ40, plasma p-tau217 and age. In the left-out test set, R^2 was 0.79 and mean absolute percentage error 7% (Fig 21a). Errors increased with higher Aβ-PET load (Fig. 21b) and were on average 5% in Aβ-negative individuals and 11% in Aβ-positives (Fig. 21c).

The models exhibited comparable but slightly lower performance in the independent cohort BioFINDER-1 compared to BioFINDER-2 (Fig. 22; $R^2 = 0.67$ and MAPE = 10%). Performance remained high for a more clinically relevant plasma-only workflow (avoiding cost and invasiveness of CSF sampling), with R^2 of 0.73 and MAPE of 8% in the BioFINDER-2 test set.

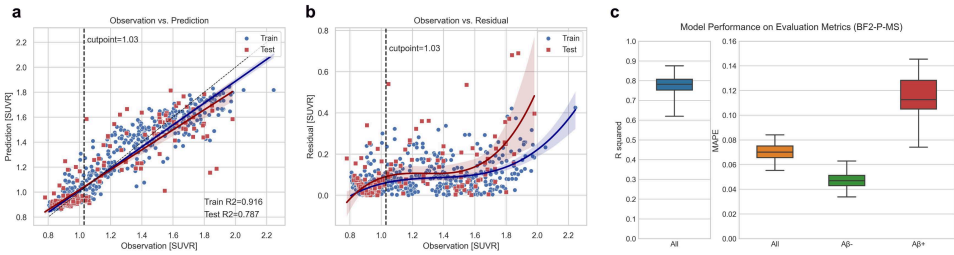

Figure 21. Performance of the best machine learning model (Extra Trees Regressor) when predicting continuous Aβ-PET burden in BioFINDER-2. Input features were plasma %p-tau217, CSF Aβ42/Aβ40 and age. **a)** Observations versus predictions. **b)** Observations versus residuals. **c)** Test set performance stratified by Aβ-PET status. Uncertainty estimates generated using bootstrapping, with box plots showing quartiles (IQR = Q3–Q1) with median as center line and whiskers extending to minimum and maximum points. Figure reprinted from [198] (CC BY).

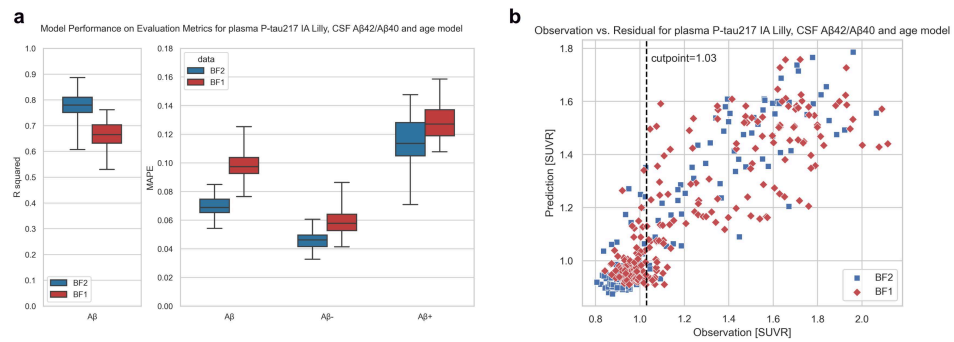

Figure 22. Model performance in the external cohort BioFINDER-1. Input features were plasma p-tau217, CSF Aβ42/Aβ40 and age. **a)** Performance stratified by Aβ-PET status. Uncertainty estimates generated using bootstrapping, with box plots showing quartiles (IQR = Q3–Q1) with median as center line and whiskers extending to minimum and maximum points. **b)** Observations versus predictions. Figure reprinted from [198] (CC BY).

In conclusion, fluid biomarker-based machine learning models can explain a high proportion of variance in overall Aβ-PET SUVR, suggesting that fluid biomarkers could substitute Aβ-PET in some applications (e.g., first stage triaging or enrichment in clinical trials). Furthermore, the study highlights distinct biomarker dynamics across stages of AD pathology, where soluble Aβ changes are closely linked to the presence of amyloid plaques, while plasma p-tau217 continues to increase as plaque burden builds up.

Paper V

Tau-PET can be used to accurately measure the extent and distribution of tau aggregates in AD, but like Aβ-PET, the method is costly and not widely accessible. Not only the burden of tau pathology, but also its spatial distribution, is closely linked to AD stage, heterogeneity, and prognosis [27,30,54]. Strategies are needed that reduce reliance on tau-PET, without compromising the ability to capture both the load and spatial pattern of the pathology.

To address this, in study V [199] we investigated the ability of various machine learning models to predict tau-PET composites from low-cost and non-invasive features. We focused on three scalable input feature categories: clinical variables, blood biomarkers, and structural MRI segmentations, comparing them separately and in combination. We included n=1195 participants from BioFINDER-2 with all data available, split into 80% train and 20% test sets. The best hyperparameter tuned machine learning models, selected based on cross-validated BioFINDER-2 training data, were evaluated in the BioFINDER-2 sets, external cohorts ADNI and UCSF-ADRC, and for models without blood biomarkers, also in external cohorts OASIS-3 and A4.

When predicting tau-PET load in the temporal meta-ROI, tree-based ML models and blood biomarkers consistently produced highest performance (Tab. 12, Fig. 23a-d). The best estimator was a CatBoost model with clinical variables, blood biomarkers, and structural MRI as input, yielding R^2=0.66-0.72 and MAE=0.15-0.17 SUVR across cohorts. Errors increased with higher tau load and cognitive stage, and plasma biomarkers had largest impact on performance in the non-AD dementia group (Fig. 23e).

Table 12. The best models for predicting temporal tau load. Best model for each input feature combination. Abbreviations: RFE (recursive feature elimination), lr (learning rate), n_{est} (number of estimators). Colors: **BioFINDER-2 train CV**, **BioFINDER-2 test**, **BioFINDER-1**, **other external**.

Input feat.	Feat. sel. + estimator	Estimator params	R^2	R^2	R^2	R^2
Cli	None + CatBoost	depth = 3; lr = 0.0215; n_{est} = 291	0.361	0.375	0.378	0.297
Pla	95% RF + CatBoost	depth = 10; lr = 0.0105; n_{est} = 471	0.632	0.590	0.586	0.594
MRI	50% F-statistic + SVR	kernel = rbf; C = 1.59	0.524	0.466	0.460	0.531
Cli + Pla	None + CatBoost	depth = 5; lr = 0.0296; n_{est} = 299	0.697	0.630	0.652	0.610
Cli + MRI	None + CatBoost	depth = 4; lr = 0.0412; n_{est} = 500	0.554	0.536	0.478	0.488
Pla + MRI	10% RFE + CatBoost	depth = 7; lr = 0.0429; n_{est} = 443	0.696	0.650	0.644	0.678
Cli + Pla + MRI	95% RF + CatBoost	depth = 5; lr = 0.0419; n_{est} = 500	0.717	0.684	0.662	0.687

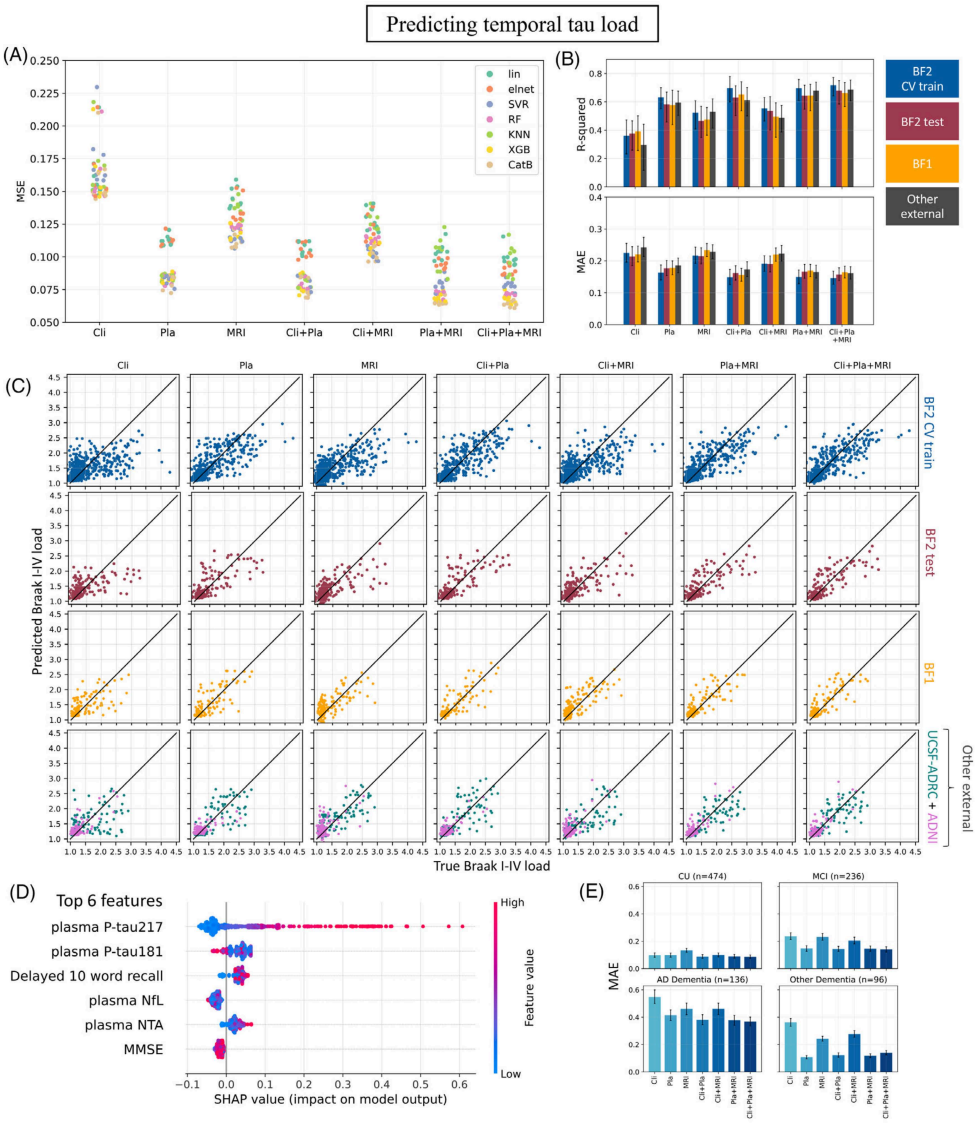

Figure 23. Performance evaluation when predicting tau load in the temporal meta-ROI. **a)** MSE in the cross-validated BioFINDER-2 training set for different feature selection + ML estimator combinations. **b)** R^2 and MAE of the best ML pipelines in a). **c)** Scatter plots of true versus predicted temporal tau load for the best pipelines in a). **d)** Top SHAP feature contributions in the model including all input features, evaluated on the cross-validated BioFINDER-2 training set. **e)** MAE of the best ML pipelines in a) stratified by cognitive status in the cross-validated BioFINDER-2 training set. Abbreviations: Cli (clinical variables), Pla (plasma biomarkers), CU (cognitively unimpaired). Figure reprinted from [199] (CC BY-NC).

For tau-positive individuals, we next predicted if the tau-load was distributed symmetrically or asymmetrically between the two hemispheres for that same ROI (temporal meta). Here, SVR ML models with MRI variables consistently produced highest performance (Tab. 13, Fig. 24a-c). The best model was an SVR model with clinical variables, blood biomarkers, and structural MRI as input, showing R^2=0.30-0.44 and MAE=6.8-9.6 across cohorts. A model solely based on MRI had almost identical performance (R^2=0.28-0.41 and MAE=7.1-9.6 across cohorts), while models without MRI showed poor or very poor predictions ($|R^2|$=0.0014-0.28 and MAE=8.8-13 across cohorts). The MRI features contributing most were temporal lobe MRI gray matter volumes and cortical thicknesses (Fig. 24d-e).

Table 13. The best models for predicting temporal tau asymmetry (laterality index). Best model for each input feature combination. Blood biomarkers were not available in all external cohorts. Abbreviations: RFE (recursive feature elimination), MI (mutual information). Colors: **BioFINDER-2 train CV**, **BioFINDER-2 test**, **BioFINDER-1**, **other external**.

Input feat.	Feat. sel. + estimator	Estimator params	R^2	R^2	R^2	R^2
Cli	None + SVR	kernel = rbf; C = 0.9495	0.00681	-0.0093	-0.0307	-0.0234
Pla	50% MI + SVR	kernel = poly; C = 0.5510	-0.0029	-0.139	-0.275	-
MRI	50% RFE + SVR	kernel = rbf; C = 29.43	0.406	0.280	0.374	0.380
Cli + Pla	None + SVR	kernel = rbf; C = 1.177	0.00140	-0.0293	-0.0366	-
Cli + MRI	50% RFE + SVR	kernel = rbf; C = 1000	0.410	0.320	0.397	0.361
Pla + MRI	50% F-statistic + SVR	kernel = rbf; C = 30.51	0.429	0.296	0.423	-
Cli + Pla + MRI	50% F-statistic + SVR	kernel = rbf; C = 1000	0.436	0.297	0.410	-

In conclusion, tau-PET composites could be predicted with moderate to high performance using accessible input features in ML models. Models showed high generalizability to left-out test data and external cohorts. The different input modalities provided complementary predictive information, where plasma biomarkers (particularly plasma p-tau217) resulted in best prediction of tau load, while MRI variables best predicted the spatial distribution of tau.

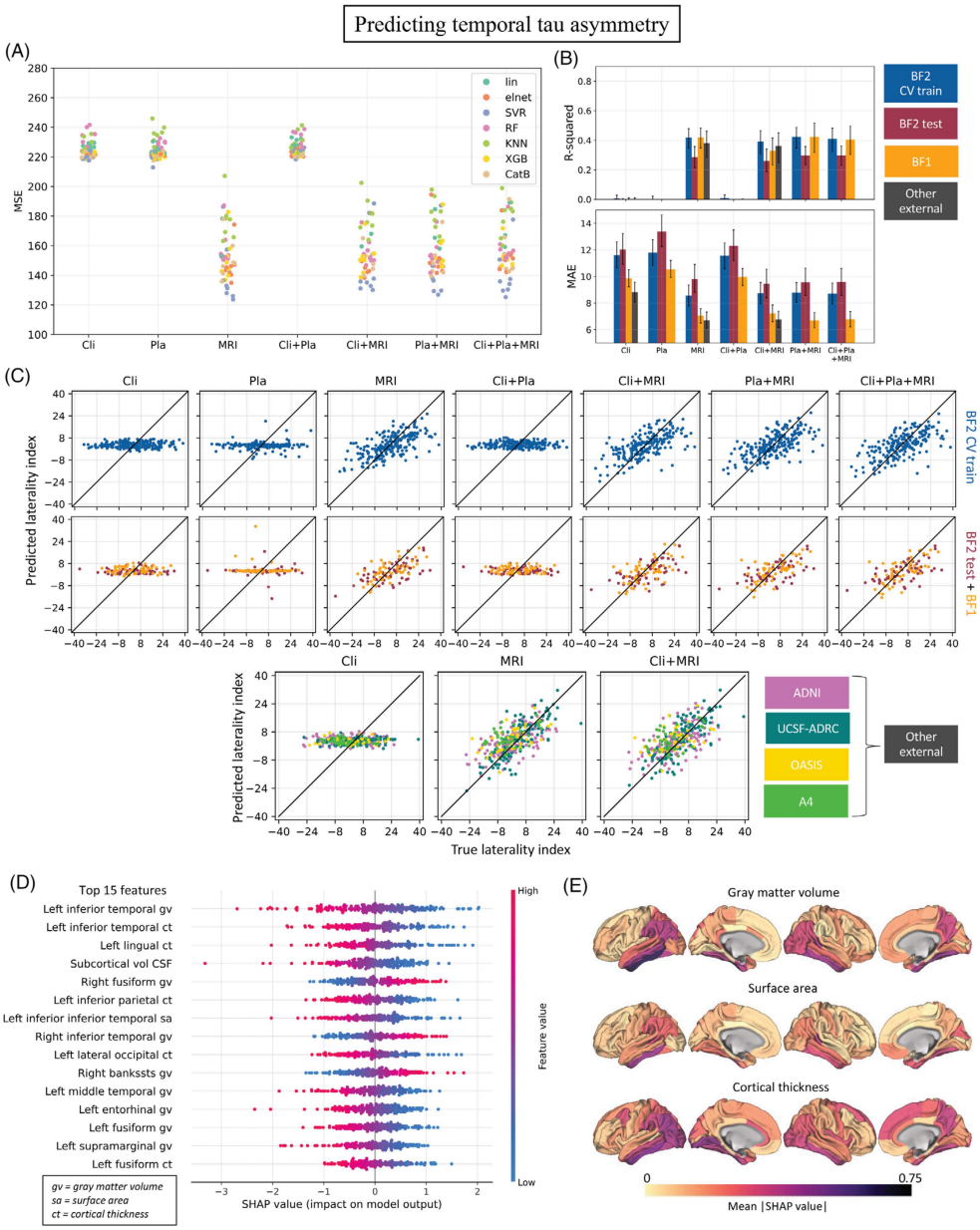

Figure 24. Performance evaluation when predicting tau asymmetry (laterality index) in the temporal meta-ROI. **a)** MSE in the cross-validated BioFINDER-2 training set for different feature selection + ML estimator combinations. **b)** R^2 and MAE of the best ML pipelines in a). **c)** Scatter plots of true versus predicted temporal tau load for the best pipelines in a). **d)** Top SHAP feature contributions in the model including all input features, evaluated on the cross-validated BioFINDER-2 training set. **e)** visualization of the SHAP feature contribution analysis for MRI FreeSurfer variables. Abbreviations: Cli (clinical variables), Pla (plasma biomarkers), CU (cognitively unimpaired). Figure reprinted from [199] (CC BY-NC).

Paper VI

In Paper VI, the aim was to further advance tau-PET prediction by moving beyond regional composites and now generate full synthetic tau-PET scans from accessible variables. Based on the findings in Paper V, we combined MRI, blood biomarkers, and clinical variables and implemented deep learning models for the task. We gathered data from 13 AD cohorts (n = 5,191), split into train (n = 3,815), validation (n = 698), and test (n = 678) sets. Participants represented a broad spectrum of clinical diagnoses, including cases with normal cognition (47.4%), subjective cognitive decline (7.53%), mild cognitive impairment (19.0%), AD dementia (15.2%), non-AD dementia (4.71%) and other neurological disorders (6.18%). Different deep learning model architectures and input features were systematically compared, yielding a final 3D U-Net model with MRI, age and plasma p-tau217 as input (Fig. 12).

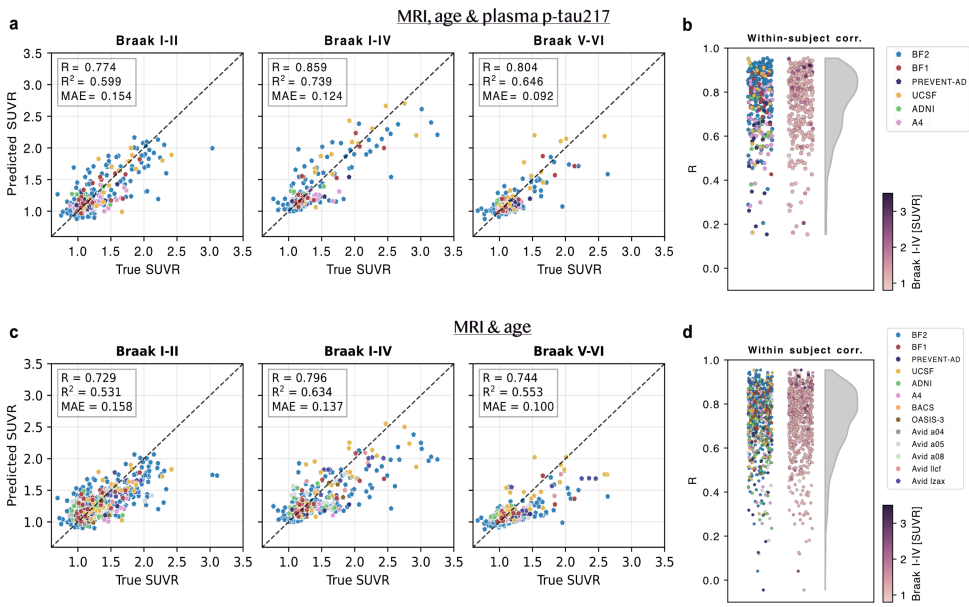

Figure 25. Evaluation of tau load and spatial similarity in synthetic versus true tau-PET in the test set. Tau load evaluation using **a)** MRI, age and plasma p-tau217 and **c)** MRI and age as input to the U-Net model. Within-subject regional correlation between true and synthetic tau-PET using **b)** MRI, age and plasma p-tau217 and **d)** MRI and age as input to the U-Net model.

Performance was evaluated on the held-out test set for i) an optimal input feature configuration (MRI, age and plasma p-tau217) and ii) more constrained one (MRI and age) (Fig. 25). Comparing the true and synthetic tau-PET regarding tau load in

Braak regions, correlations were strong (Fig. 25a, 25c). Furthermore, spatial tau deposition patterns, assessed using within-subject correlations across FreeSurfer regions, were on average strong but had relatively high variability across subjects (Fig. 25b, 25d).

To complement the quantitative evaluations, ten representative cases with varying Braak I-IV burden from multiple cohorts are visualized in Fig. 26. The synthetic images generally appeared smoother than true scans. Including plasma p-tau217 resulted in more accurate estimation of tau load compared to without but had only minor impact on spatial distribution patterns.

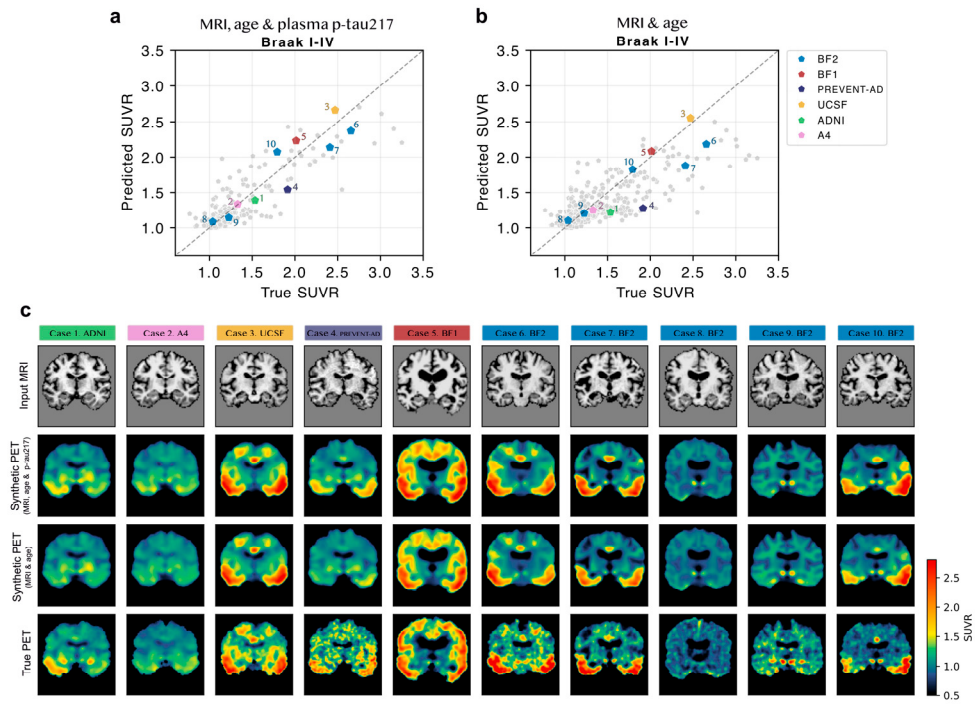

Figure 26. Ten representative example cases from the test set. Corresponding Braak I-IV prediction is marked out in **a)** and **b)**. In **c)** the input MRI (first row), synthetic tau-PET based on MRI, age and plasma p-tau217 (second row), synthetic tau-PET based on MRI and age (third row), and true tau-PET (fourth row).

In an independent cohort without true tau-PET (BioFINDER-1), we assessed if synthetic tau-PET could predict progression to dementia in cognitively unimpaired individuals (n=358) using Cox regression models. The synthetic scans captured prognostic information for cognitively unimpaired individuals comparable to true tau-PET [54]. This included distinction between early and late stages of tau accumulation: 12-fold higher risk for synthetic tau-PET positivity in early AD

regions, and 45-fold higher risk for synthetic tau-PET positivity in late AD regions, compared to synthetic tau-PET negativity (Fig. 27a). This distinction was not seen directly from the input features when using the same stratification approach, suggesting that synthetic tau-PET added information beyond what was easily extractable from the input data (Fig. 27b).

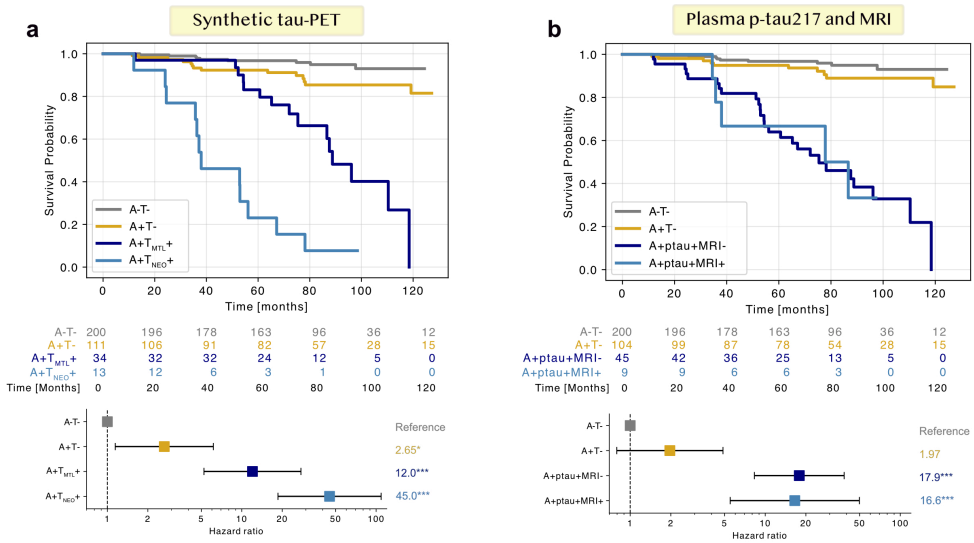

Figure 27. Clinical utility of synthetic tau-PET for assessing progression to dementia. Kaplan-Meier and Cox regression analyses showing the risk of progression to dementia for cognitively unimpaired individuals in the independent BioFINDER-1 cohort (subjects with no true tau-PET). T-status was derived by **a)** synthetic tau-PET ROIs or **b)** plasma p-tau217 and an MRI AD signature ROI. This analysis imitated the study design in Ossenkoppele, Pichet Binette et al. (2022) [54].

In conclusion, from structural MRI, age and plasma p-tau217 (clinically accessible and non-invasive features), synthetic tau-PET scans could be generated with deep learning, showing promising resemblance to true tau-PET. Performance was highest for scans generated with plasma p-tau217 but remained strong using only MRI and age, demonstrating flexibility to settings with limited data. This study represents a step toward scalable, non-invasive, yet spatially information-rich in vivo assessments of tau pathology, and provides insights into complementary characteristics of the input features.

Discussion and future perspectives

The work of this thesis has taken steps toward improved diagnostics and biomarkers in AD by either increasing the diagnostic accuracy/pathological information obtained from existing tools, or through new approaches that reduce test burden in terms of cost, invasiveness, and/or time. This was achieved by applying statistical and machine learning methods across multiple data modalities in deeply phenotyped AD cohorts. Specifically, **Papers I and II** investigated co-varying properties of the CSF proteome, resulting in a reference protein normalization method that improved biomarker performance across analytes, assays, and AD cohorts. **Paper III** showed that a resource-efficient, self-administered digital cognitive test improved assessments of objective cognitive impairment and, when combined with blood biomarkers, can help diagnose AD in primary care. Finally, **Papers IV, V and VI** developed and evaluated machine learning models to predict Aβ-PET or tau-PET from more accessible modalities. The approach showed promising performance, with potential to reduce reliance on costly PET imaging while increasing access to the unique information PET provides.

Implications from main findings

Individual proteomic CSF levels

In Paper I, we observed a signal of inter-individual variability in overall CSF protein levels, and adjustment for this signal improved the precision of CSF biomarkers. What remains unclear is what this variability represents biologically. In Paper I, we speculate that one explanation could be differences in CSF production and clearance rates, since the signal was associated with age and sex, and CSF turnover has also been reported to vary with age and sex [77,78,217,218]. We also suggested ventricular volume as a potential contributor. Since CSF fills the ventricles, differences in ventricular volume are related to CSF volume [219] which could influence CSF protein dilution, consistent with observations from a study on the genetic regulation of CSF protein expression [220]. Notably, a similar pattern of inter-individual variability in global CSF protein levels was reported in an independent study published shortly after Paper I [221]. More recently, this variability has been suggested to potentially reflect a combination of CSF turnover rate and blood-brain barrier integrity [222].

These aspects support that individualized CSF protein levels represent a biological signal that potentially arises from a combination of mechanisms. Future work is needed to clarify the exact factors driving this variability and how to best adjust for it in different applications.

Fluid biomarker ratios

In Paper II, we found that reference protein normalization using Aβ40 and np-tau increased associations with Aβ- and tau-PET for a broad range of CSF and blood biomarkers. Interestingly, for CSF biomarkers, associations with AD pathology (measured by PET) were consistently stronger with Aβ40 normalization than with Aβ42 normalization. This is a notable finding given that the hybrid ratios that have been suggested for clinical use and are part of the Core 1 and Core 2 classification framework combine p-tau and Aβ42 [50,223,224]. Plasma biomarkers are also increasingly being explored in the context of p-tau and Aβ42 ratios [225–227]. It is possible that plasma biomarkers might benefit from a broader exploration of optimal plasma reference proteins, potentially through a similar proteomic search as in Paper I but for plasma instead of CSF. In general, biomarker ratios have been more frequently proposed than single markers also in other contexts, for example using synaptic CSF proteins to represent cognitive impairment [228–230]. Although fluid biomarker ratios can improve diagnostic performance in several contexts, combining two measures introduces two sources of measurement noise rather than one, which can limit robustness.

We also observed in Paper II that reference protein ratio normalization had a smaller impact on longitudinal biomarker measurements than on cross-sectional associations. This suggests that factors driving overall CSF proteome differences are relatively stable within an individual over time. Reference protein normalization may therefore primarily refine between-person comparisons, while offering more limited benefit for within-person longitudinal monitoring. Longitudinal tracking is increasingly relevant in the era of approved and developing disease-modifying treatments for AD. Fluid biomarkers can detect group-level differences between treated and placebo participants, but their performance for individualized monitoring of change and during treatment remains less certain [231,232]. Improving fluid biomarkers in a longitudinal context remains an important area for future work.

Digital cognitive tests in primary care

In Paper III, we showed that digital cognitive testing has the potential to enhance the clinical work-up for AD in primary care, particularly when combined with blood biomarkers. Beyond increasing diagnostic accuracy, the broader value of digital cognitive tests lies in their potential to increase efficiency, standardization and

scalability of cognitive assessments [233,234]. Importantly, these tools are not intended to replace the evaluation of physicians, but to help create a more comprehensive basis for decision-making.

Our work provides a first proof-of-concept highlighting that a digital cognitive test can add diagnostic value in primary care. Future studies are needed to assess whether physicians find such a test useful in practice, and the effects on clinical workflows. Furthermore, future work should also investigate the test's generalizability to other populations and explore digital tools for longitudinal monitoring.

Machine learning-based PET prediction

Aβ-PET and tau-PET are two of the most informative tools in AD, but their high cost and specialized infrastructure requirements contributes to inequities in AD diagnostics and substantially increases costs and logistical demands in clinical trials.

Aβ-PET

As discussed in Paper IV, accurate machine learning-based predictions of global Aβ-PET burden from fluid biomarkers may substitute Aβ-PET in some applications (e.g., first stage triaging or enrichment in clinical trials), but not all. True Aβ-PET scans are likely difficult to replace with such models in applications where high certainty is required (e.g., treatment initiation and tracking) [235].

A core methodological challenge for Aβ-PET prediction is that Aβ pathology accumulates early in the disease course, when more accessible imaging modalities like structural MRI remain largely unchanged. Consequently, the spatial distribution of Aβ pathology is hard to infer. Other MRI modalities may capture Aβ-related changes better, but they are less routinely acquired, potentially constraining scalability and model training. However, the added value of full synthetic Aβ-PET images may be limited in many clinical contexts, since global burden rather than spatial detail often is more relevant for clinical decision making [236].

Tau-PET

Since tau NFTs are more closely related to neurodegeneration and clinical phenotypes (see *Introduction*), tau-PET is more relevant than Aβ-PET to synthesize in full 3D using structural MRI. Consistent with this, we showed in Papers V and VI that both tau burden and spatial information can largely be captured from more accessible modalities, e.g., MRI, blood biomarkers, and clinical variables. Plasma p-tau217 was the most efficient marker for tau load in these two studies, but more tau-specific fluid biomarkers (e.g., MTBR-tau243 [116,117]) may further improve tau-PET prediction in future models.

Beyond MRI-based approaches, other studies suggest that tau-PET can be synthesized using alternative imaging modalities, such as FDG-PET or ultra-low-dose tau-PET [237,238]. This may offer practical options to reduce the need for full-dose tau-PET but would still require PET infrastructure.

Although the quantitative and qualitative results on tau-PET synthesis in Paper VI are promising, the clinical impact of synthetic tau-PET on decision-making, prognosis, and trial outcomes remains unclear and should be evaluated in prospective studies. A specific limited application may be related to treatment monitoring, since both fluid biomarkers and imaging can change in non-standard ways during Aβ-removal. For example, structural MRI has shown reductions in brain volume that would typically be interpreted as atrophy but may instead reflect treatment-associated effects [239]. Robust generalization of synthetic tau-PET to treatment-monitor settings will likely require model training and validation using data from individuals that have received such therapy.

Clinical perspectives

Biomarker interchangeability

Aging is the leading risk factor for neurodegenerative diseases, but precise boundaries between healthy and pathological brain aging are not well defined [240]. As biomarker-based detection moves earlier in the disease course, this creates both potential benefits (e.g., earlier explanation of symptoms, adapted care, and the possibility to plan) and risks (e.g., psychological stress, possible overdiagnosis, and added burden on the healthcare system). With this in mind, a key clinical goal is for diagnostic tests to be actionable and consistent across settings. Biomarker frameworks that allow multiple biomarker modalities to be used to assess the same biological construct (e.g., AT(N) grouping or Core 1 and 2 classification [47,50]) are therefore appealing. Many of the research questions presented in this thesis were aligned with the aim of using biomarker modalities interchangeably, for example reference protein normalization (Papers I and II) and cross-modality machine learning models (Papers IV, V and VI), improving agreement and prediction between modalities.

At the same time, biomarkers are not fully interchangeable in a biological sense: they reflect partially distinct processes and may change at different points along the disease continuum. Even fluid biomarkers that can be used to assess the same constructs (e.g., different p-tau isoforms for Core 2 categorization) have been shown to have different temporal dynamics [241,242]. Biomarker discordance should therefore not only be treated as a limitation, but can also be informative for understanding disease mechanisms, particularly when different markers provide complementary signals across the AD continuum.

Precision medicine in AD

Precision medicine aims to customize medical care to each patient's unique profile, in contrast to a "one-size-fits-all" approach. Given the biological and clinical complexity of AD, individualized, biomarker-guided diagnostic and treatment pathways may be required to optimize care [243]. Several of the findings in this thesis can be framed in the context of precision medicine and targeting individual heterogeneity.

Normalization

One obvious example is the reference protein normalization method in Papers I and II. Historically, the use of fluid biomarkers has largely relied on population-based cutoffs. Our underlaying idea was that individuals may have different physiological levels of fluid biomarkers, which we were able to observe in proteomics data. Comparing disease-related changes in biomarkers to an estimate of this individual baseline (e.g., a reference protein) improved their precision, advancing more individualized fluid biomarker use.

Reference protein normalization can adjust for confounding when quantifying associations between fluid biomarkers, or act like a suppressor variable when fluid biomarkers are used as predictors of other modalities. Yet, the benefit from normalization depends on the relationship between the outcome, main predictor, and reference. First, there needs to be a reasonably strong association between the main predictor and outcome, or there is too little signal for normalization to enhance. Second, if the association is already close to perfect, normalization may not be necessary and could potentially introduce more noise due to measuring two markers instead of one. Third, the reference protein and the main predictor must share the irrelevant signal that the normalization is intended to remove. This may not hold if, for example, the main predictor and reference protein originate from different cell types or reflect distinct biological processes.

Normalization is widely used in medicine. For example, urinary biomarkers are routinely normalized to account for dilution differences [244,245]. Similarly, PET images are usually quantified using SUVR, where tracer uptake is normalized to a reference brain region that is not expected to show specific binding [29,235]. Atrophy on MRI is also commonly adjusted for intracranial volume to account for differences in brain size [246].

It is likely that normalization will play a role in improving other parts of AD diagnostics as well, particularly cognition. Measuring cognition is difficult since it can fluctuate for many reasons (e.g., sleep, mood, concentration, stress, depression, dementia). Furthermore, individuals often have different base level abilities, so population-based cutoffs for cognitive impairment (even though typically age and education adjusted [247–249]) can likely lead to both false negatives and false positives. Normalization to an individualized cognitive measure could be a potential

way to address this, and digital tools hold promise for actively or passively collecting longitudinal data to enable person-specific reference levels. Paper III is an early step in this direction, illustrating a use-case where a self-administered digital tool can make cognitive evaluations more rigorous without increasing healthcare resource burden.

Pathological subtypes

Another key source of heterogeneity in AD is variation in tau accumulation (and downstream atrophy) patterns (see *Introduction*). Tau-PET provides valuable spatial information but is unlikely to be widely used to investigate tau patterns clinically due to its high cost and limited accessibility. In Papers V and VI, we predicted both load and spatial aspects of tau accumulation using machine learning, highlighting a potential avenue toward assessing individual tau-PET like accumulation patterns and thereby aligning with precision medicine goals. More research is needed to determine how information on individual tau patterns through synthetic PET might affect clinical decision-making, as well as its utility for trial recruitment and for evaluating treatment effects.

Medical data analysis and modelling

General limitations of data and models

As described in the *Introduction*, there are several fundamental challenges in analyzing medical data. One issue is the sensitive nature of the data, which limits open data sharing. This is particularly problematic for machine learning models, since exposure to larger and more diverse training cohorts often is key for robust performance. Several potential avenues to mitigate this exist, all of which could be relevant to further improve the prediction models in this thesis.

One possibility is through federated learning. Federated learning is a technique that decentralizes the training process of a model. The model, or its current parameters, is sent to different locations where data is stored locally. The model is then trained further at each location, and only the resulting updates are shared and aggregated to obtain an improved global model. In this way, the sensitive raw data can remain local. Potential negative aspects are that dataset heterogeneity related to location can slow model convergence, and the training process becomes less transparent [250,251].

Another promising method is to generate synthetic datasets that resemble the original cohorts in terms of distributions and statistical structure but differ at the individual level. This way, data can be shared without original participants being identifiable. Although synthetic data could enable broader data sharing, it is not always clear where the boundary lies between preserving clinically relevant signal and ensuring strong privacy [252,253].

Lastly, hospitals are increasingly building large data lakes and data pools, which are centralized, secure repositories that can support standardized storage, access procedures, and anonymization pipelines at scale. If implemented well, these infrastructures could substantially improve data access and enable more consistent and cost-efficient multi-site analyses. However, establishing and maintaining such structures can be challenging in terms of cost, governance, and security, and population biases as well as data noise (such as inconsistent diagnoses or diagnostic criteria that evolve over time) may limit the practical usefulness [254,255].

In addition to data sensitivity, it is important to keep in mind that medical data itself may have many limitations. Prediction models will usually perform best on individuals who resemble the training population, while generalization to other settings, sites, or patient groups can be less certain. Rare cases are particularly challenging as they often are underrepresented or entirely absent from training cohorts, making both learning and evaluation unstable. Beyond sample size, additional risks include biases in cohort composition, site- and protocol-specific effects, and missingness that is not random, all of which can reduce real-world robustness [256].

AI in medicine

Healthcare systems face growing challenges related to supply and demand, and AI has the potential to help address this gap, for example through decision support, automation, planning, and multimodal data integration [257]. This thesis highlights one such use case for AD healthcare: predicting informative PET composites (Paper IV and V) or synthesizing full tau-PET scans (Paper VI) from more accessible variables.

An important first step in developing AI for medicine is to identify problems where an AI solution is clinically relevant and implementable. This requires more than just technical and practical feasibility. The target outcome should also be clinically meaningful, and performance should reflect healthcare priorities (e.g., low-cost access to 3D pathological tau information not otherwise available). To achieve this, multidisciplinary collaboration is typically required, for example combining expertise in machine learning with medical domain knowledge (as was an objective of this thesis). A second consideration is that a substantial part of building effective AI models in medicine relates to the underlying data. In practice, data collection and pre-processing are often the most time-consuming stages of the work, and inherent biases and noise can affect translation to real-world settings.

With these and other requirements in mind, AI holds promise in many medical applications beyond the examples in this thesis. In addition to task-specific models, a class with high potential is AI models that can learn more general representations of data and then be fine-tuned for more specific clinical purposes, e.g., foundation

models [258–260]. A closely related direction is multimodal modelling, where multiple data modalities can be combined to better reflect AD heterogeneity and to make use of whatever data are available for a given patient [261]. Additionally, natural language processing (NLP) has recently showed substantial methodological progress and may be useful in cognitive evaluations, where the clinical interview and narrative descriptions of symptoms often contain rich diagnostic information [262,263].

Despite these methodological advances, relatively few AI tools have been translated to medical practice. Common barriers include limited external validation, uncertainty about generalization across sites and patient groups, potential risk of hallucinations, regulatory and liability constraints, integration with clinical workflows, and the need for ongoing monitoring after deployment as populations and practices change.

Future AD data initiatives

There are many exciting ongoing data initiatives and advances in AD research aimed at further increasing diagnostic accuracy, reducing burden of tests, and improving our mechanistic understanding of the disease. Collaborative efforts are made to collect and share large amounts of research data, for example across Alzheimer's disease research centers (ADRCs) in the US [264,265], or the long-term prospective UK Biobank study including half a million individuals [266]. Furthermore, initiatives in China are aimed to accelerate AD research and provide cognitive screening to up to 80% of its older adults [267,268]. In parallel, technological development is expanding what can be measured outside specialized centers, including for example portable MRI techniques [269], and minimally invasive self-sampling blood biomarker tests [270].

Other promising data analysis areas include multi-omics, which generate thousands of data points per individual and can be paired with advanced machine learning methods to improve understanding of disease mechanisms [82,271–273]. Finally, biomarkers of co-pathologies are becoming increasingly important for determining whether AD pathology is the main driver of symptoms and for characterizing disease heterogeneity (see *Introduction*). Recent progress has for example enabled measurements of α-synuclein in vivo using seed amplification assays [274]. Continued efforts to measure additional pathologies in vivo, such as TDP-43 [275], can hopefully further improve diagnostic precision and our understanding of neurodegenerative diseases.

Concluding remarks

This thesis advances more accurate and less burdensome AD diagnostics and biomarkers by applying statistical and machine learning methods to multimodal data. The work addressed clinically relevant questions and contributed to building bridges between the fields of data science and neuroscience, promoting collaboration and knowledge exchange across disciplines.

The main findings from this thesis are the following:

1. The observation that there are inter-individual differences in CSF protein abundance. Adjusting for these differences with reference proteins improves biomarker precision and reduces the risk of false positive findings (Paper I).
2. The finding that CSF Aβ40 and np-tau are promising reference proteins. Normalization to them strengthened biomarker associations with PET and supported better interchangeability between fluid and imaging markers for AD diagnosis and staging (Paper II).
3. The finding that a brief self-administered digital cognitive test battery could identify cognitive impairment in primary care with higher accuracy than standard paper-and-pencil testing and assessment of primary care physicians. Combined with blood biomarkers, this approach could be a time- and cost-effective way to improve clinical AD diagnosis when specialist resources are limited (Paper III).
4. The development of machine learning models that could largely predict amyloid-PET and tau-PET load and/or spatial distribution from fluid biomarkers, MRI, and clinical variables, with plasma p-tau217 and MRI showing particular promise (Papers IV and V).
5. The development of deep learning models that can synthesize tau-PET images well from structural MRI, blood biomarkers, and clinical data. These models have potential to provide tau-PET approximations in settings with no access to costly PET scans (Paper VI).

Artificial intelligence declaration

Generative artificial intelligence language models (including GPT-5.2 and Gemini 3 Pro) were used solely for language editing, including grammar checks, sentence rephrasing, and synonym suggestion. The author takes full responsibility for the content of this thesis.

Acknowledgements

Many people contributed to my journey toward a PhD, and I am deeply grateful to everyone, including those not mentioned by name.

First and foremost, I would like to thank **all the study participants** in the Swedish BioFINDER cohorts and the other research cohorts included in this thesis. Your selfless contributions and time dedicated to research have made it possible to achieve scientific discoveries that will hopefully benefit many future generations. Thank you for your part in working toward a future where fewer people suffer from neurodegenerative diseases.

To my main supervisor **Oskar Hansson**, being part of the fantastic team that you have built and pursuing research in line with your vision has been a true honor. Thank you for believing in me, for trusting me with increasingly important tasks, and for your guidance and strong support throughout my PhD. I also find it very inspiring that, although you have already achieved more than most people do in their lifetimes, you never get comfortable, but remain very ambitious and keep challenging yourself in new ways. Unfortunately, despite my best efforts, I have not proven much of a challenge in our weekly squash matches, which you usually win. Nevertheless, I feel very lucky to have been able to share my passion for sports with you in addition to the science, resulting in a lot of laughter, focus(!), and fun times.

To my co-supervisor **Niklas Mattsson-Carlgren**, if it had not been for your openness and warm welcome when I first reached out as a curious MSc student, completely new to the field of medicine, I would probably never have joined the group. I am forever grateful to you for believing in me, continuously sharing your expertise, giving me thoughtful feedback, and supporting me throughout my PhD journey.

To my co-supervisor **Jacob Vogel**, I am so glad that your move to Sweden aligned so perfectly with the start of my PhD. Your involvement in all my projects has not only increased their quality tremendously, but also led to many fun and rewarding discussions. Thank you for teaching me what high quality science looks like, for highlighting the importance of celebrating success, and for caring about your trainees beyond science.

To my co-supervisor **Ida Arvidsson**, it has been invaluable to share my journey from engineering toward medicine with someone who shares the same engineering

background and passion for medical applications. Throughout my PhD, you have been someone I could constantly rely on, and I am so glad that you continued supervising me even after your transition to industry. Thank you for always taking the time to listen and discuss, for your thoughtful feedback, and for your kindness.

To my co-supervisor **Kalle Åström**, you are an inspiration and a role model to me, particularly in the way you pursue high level research while maintaining your curiosity, humor, and down-to-earth energy. You always take the time to care for and see people beyond their research, and I always look forward to our meetings to learn more about mathematics, data science, ski trips, and swimming classes.

Thank you to my colleagues **Pontus Tideman** and **Weizhong Tang**, with whom I worked closely during some of my PhD projects. **Pontus**, it was a joy to team up with you. Thank you for always answering my basic clinical questions and for bringing humor and kindness every time we talk. **Weizhong**, thank you for all our very niche machine learning discussions, your constant generosity, and your wise advice. I look forward to a new badminton match the next time we meet.

Thank you to the many brilliant minds and hard workers behind the Swedish BioFINDER studies, especially **Erik Stomrud, Sebastian Palmqvist, Shorena Janelidze, Danielle van Westen, Rik Ossenkoppele,** and **Olof Strandberg**. A particular thank you goes to **Ruben Smith**, it has been a pleasure to work with such a kind and caring expert, and to **Nicola Spotorno**, for sharing your extensive knowledge, always taking the time to listen, and giving insightful advice. Thank you also to **Camilla Orbjörn, Pilar Lorenzo,** and **Sinh Tran** for your precision in the lab and for always contributing to a friendly work environment outside of it. In addition, I am very grateful to everyone at the **Memory Clinic** for their fantastic contributions to data collection and their deep care for each and every study participant.

I want to thank the postdocs who have been such a great inspiration to me, both for the high-quality science they produce and for their care and support for others. You are all amazing role models. **Alexa Pichet Binette,** you have a brilliant mind and always bring warmth, support, and positivity wherever you go. **Gemma Salvadó,** I will always look up to your intelligence and your ambitious drive, and remain a little jealous of all the Spanish sports accomplishments in football and tennis where Sweden unfortunately falls far behind. **Ines Hristovska,** although you are often freezing, you are also like a sun, always spreading warmth and positive energy around you. **Harry Behjat,** I have truly appreciated having someone who shares my passion for mathematics and gets me even when I go deeper into the technicalities of my work. **Irene Cumplido Mayoral**, thank you for being so warm, generous and caring, always making people feel seen and appreciated. **Nina Schultz**, thank you for your "allt ordnar sig" mentality that always makes problems feel less difficult and for being such a fun, genuine, and inspiring person to be around.

Thank you to all my fellow PhD students who became my friends along the way. **Anika (Lindblom-)Wuestefeld**, you have been my person in the group from day

one. I am so thankful for your constant support, understanding, and care, and for our close friendship, which I hope will remain just as permanent as our PhD degrees. **Divya Bali**, no matter how bad my day has been or how stressed you are, it is impossible not to smile around you. Thank you for always spreading joy, showing support, letting me taste your delicious lunches, and being someone I can trust. **Anna Orduña Dolado**, you are such a kind and generous person. Thank you for your constant support, for being someone I can always trust and talk to, and for sharing your travel-guide and dancing talents. **Amanda Annettesdotter**, thank you for your constant kindness, support, and ability to see and care for everyone. **Toomas Erik Anijärv**, thanks for all the research and non-research discussions, and the fun table tennis matches! **Noëlle Warmenhoven**, thank you for your constant kindness and for always empowering others. **Sophie Mastenbroek**, thank you for always being helpful and for your amazing stroopwafel cakes.

Thank you to everyone in the **DeMON lab**, it has been a pleasure to share research environments and build strong connections with all of you. In particular, I want to thank **Xiao Yu**, **Lijun An**, **Léa Chauveau**, **Jonathan Rittmo,** and **Gabriele Vilkaite**. I would also like to thank the **Computer Vision and Machine Learning** group at LTH for their welcoming atmosphere and technical input on my research.

During my PhD, I have had the great pleasure of supervising several talented and ambitious students. Thank you to **Alma Lennartsson**, **Ruoyi Zhao**, **Vassilis Georgelis**, **Gustav Laurell**, **Ossian Rabow**, and **Richard Smith**.

I am also very grateful to **MultiPark**, **Kungliga Fysiografiska Sällskapet**, and the **Faculty of Medicine** for supporting and funding my research, and for making it possible to present it at international scientific conferences. I would also like to thank our collaborators at **Gates Ventures** for their research support and for their initiatives to make workflows and data available through the Global Research and Imaging (GRIP) platform.

Thank you to all the collaborators at **Washington University**, **the University of California San Francisco, the University of California Berkeley, the University of Perugia,** and **McGill University**, for making it possible to carry out more rigorous, collaborative, and generalizable research.

Att bli forskare kräver mer än fyra års doktorandutbildning, det är så mycket annat som har byggt min väg hit och hjälpt mig hitta balans i vardagen.

Jag vill därför tacka min familj **Ingrid Aggeryd, Karl-Göran Karlsson** och **Maria Karlsson** för ert stöd. **Mamma**, du är den starkaste person jag känner och en stor förebild för mig. Du har alltid kämpat för att jag ska få utmanas och utvecklas trots att jag hade lätt för skolan, vilket har motiverat mig mycket. Jag är också så tacksam för att du klokt nog alltid påmint mig om att också prioritera skolan även när mina fotbollsambitioner varit som störst, vilket har öppnat så många möjligheter för mig i livet. **Pappa**, du är min trygga person som följt sina drömmar och jobbar med sin

stora passion. Det har varit mycket inspirerande att se, och en stor anledning till att jag vågat följa min magkänsla både i fotbolls- och karriärval. Tack för att du alltid stöttat mig, som när du live-streamat mina fotbollsmatcher i USA mitt i natten, och för allt kul vi gör tillsammans, till exempel vandringsresor, padelmatcher och Båstadtennis. **Maria**, jag har alltid sett upp till dig och är så stolt över att ha dig som storasyster. Vi har varit igenom så mycket tillsammans och du är en av få personer som jag alltid känner att jag kan vara mitt avslappnade jag runt. Tack för att du alltid varit så snäll trots att din jobbiga lillasyster så ofta ville tävla! Ditt stöd och din villkorslösa kärlek betyder så mycket för mig.

Tack också till alla personer som blivit en del av min familj. **Gunilla Härefelt**, det är alltid roligt att umgås med dig! Stort tack för ditt stora stöd och intresse för min forskning. **Mattias Fridén**, tack för din hjälpsamhet och generositet. **Karin Gudmundsson** och **Mikael Carlsson**, ert stöd, er omtänksamhet och er genuina värme betyder så mycket för mig. **Familjen Carlsson: Mattias, Elin, Lucas, Alva** och **Tilda**, tack för all glädje och kärlek ni sprider.

Mina fantastiska vänner, ni fyller min vardag med fina minnen, skratt och omtanke. Tack för att ni varit en så stor del av mitt välmående och min motivation de senaste åren. Särskilt tack till **Elias Olson**, **Emmelina Frick**, **Staffan Alexanderson**, **Erik Wikare**, **Filip Hedén**, **Emma Olsson**, **Emma Bengtsson**, **Emilia Jönsson**, **Sofia Anker-Kofoed** och **Linnéa Jönsson**. Jag vill också rikta ett stort tack till mina galna, roliga och fullkomligt briljanta vänner **Seamus Doyle**, **Ludvig Håkansson** och **Jonathan Envall**. Sist men störst, tack till min ”klasskompis” och bästa vän **Emma Fallenius**. Tack för alla fina minnen, för att du förstår mig så bra, för att du är min största supporter och för att du håller mig lycklig genom hembakta bröd och bullar.

Stort tack till mitt otroliga fotbollslag **Lunds BK Dam**, med **Katarina Glans** och **Patrik Carlgren** i spetsen under hela min doktorandtid. Fotbollsplanen har varit mitt ställe att andas fritt och släppa forskningen helt, oavsett hur dagen på jobbet varit, och det har varit så roligt att få dela det med alla tjejer i LBK, och ärofyllt att vara er lagkapten. Fotbollen har gett mig så mycket i livet, både egenskaper som disciplin, tidsoptimering och snabbtänkthet, liksom fantastiska vänner, lagsammanhållning och upplevelser. Jag tror aldrig jag hade lyckats lika bra akademiskt utan den. Därför vill jag också tacka alla ledare och tjejer i mina tidigare lag **Borgeby FK**, **IFK Norrköping**, **Southeastern Louisiana University** och **Eneby BK**.

Sist men viktigast av alla, tack till min fantastiska man **Andreas Carlsson**. Du är min stora kärlek och bästa vän, och vår förlovning och vårt bröllop kommer alltid vara mina största och finaste minnen när jag tänker tillbaka på min doktorandtid. Det har varit så roligt att upptäcka världen som forskare tillsammans med dig, både under intensiva diskussioner vid middagsbordet och, lyxigt nog, under konferensresor till både Portugal och Italien. Tack för att du alltid tar dig tid och lyssnar, stöttar mig när jag sätter alldeles för höga krav på mig själv, och visar lika mycket kärlek oavsett om jag når mina orimligt höga mål eller inte. Jag älskar dig.

References

[1] Bethlehem RAI, Seidlitz J, White SR, Vogel JW, Anderson KM, Adamson C, et al. Brain charts for the human lifespan. Nature 2022;604:525–33. https://doi.org/10.1038/s41586-022-04554-y.

[2] Labbadia J, Morimoto RI. The biology of proteostasis in aging and disease. Annu Rev Biochem 2015;84:435–64. https://doi.org/10.1146/annurev-biochem-060614-033955.

[3] Wyss-Coray T. Ageing, neurodegeneration and brain rejuvenation. Nature 2016;539:180–6. https://doi.org/10.1038/nature20411.

[4] Seshadri S, Wolf PA. Lifetime risk of stroke and dementia: current concepts, and estimates from the Framingham Study. Lancet Neurology 2007;6:1106–14.

[5] Fang M, Hu J, Weiss J, Knopman DS, Albert M, Windham BG, et al. Lifetime risk and projected burden of dementia. Nat Med 2025;31:772–6. https://doi.org/10.1038/s41591-024-03340-9.

[6] Nichols E, Steinmetz JD, Vollset SE, Fukutaki K, Chalek J, Abd-Allah F, et al. Estimation of the global prevalence of dementia in 2019 and forecasted prevalence in 2050: an analysis for the Global Burden of Disease Study 2019. Lancet Public Health 2022;7:e105–25. https://doi.org/10.1016/S2468-2667(21)00249-8.

[7] Jönsson L, Tate A, Frisell O, Wimo A. The Costs of Dementia in Europe: An Updated Review and Meta-analysis. Pharmacoeconomics 2023;41:59–75. https://doi.org/10.1007/s40273-022-01212-z.

[8] Nandi A, Counts N, Bröker J, Malik S, Chen S, Han R, et al. Cost of care for Alzheimer's disease and related dementias in the United States: 2016 to 2060. Npj Aging 2024;10. https://doi.org/10.1038/s41514-024-00136-6.

[9] 2025 Alzheimer's disease facts and figures. Alzheimer's & Dementia 2025;21. https://doi.org/10.1002/alz.70235.

[10] Stelzmann RA, Norman Schnitzlein H, Reed Murtagh F. An english translation of alzheimer's 1907 paper, "über eine eigenartige erkankung der hirnrinde." Clinical Anatomy 1995;8:429–31. https://doi.org/10.1002/ca.980080612.

[11] Müller UC, Deller T, Korte M. Not just amyloid: Physiological functions of the amyloid precursor protein family. Nat Rev Neurosci 2017;18:281–98. https://doi.org/10.1038/nrn.2017.29.

[12] Chen GF, Xu TH, Yan Y, Zhou YR, Jiang Y, Melcher K, et al. Amyloid beta: Structure, biology and structure-based therapeutic development. Acta Pharmacol Sin 2017;38:1205–35. https://doi.org/10.1038/aps.2017.28.

[13] Schreiner TG, Schreiner OD, Adam M, Popescu BO. The Roles of the Amyloid Beta Monomers in Physiological and Pathological Conditions. Biomedicines 2023;11. https://doi.org/10.3390/biomedicines11051411.

[14] Egan MF, Kost J, Tariot PN, Aisen PS, Cummings JL, Vellas B, et al. Randomized Trial of Verubecestat for Mild-to-Moderate Alzheimer's Disease. New England Journal of Medicine 2018;378:1691–703. https://doi.org/10.1056/nejmoa1706441.

[15] Egan MF, Mukai Y, Voss T, Kost J, Stone J, Furtek C, et al. Further analyses of the safety of verubecestat in the phase 3 EPOCH trial of mild-to-moderate Alzheimer's disease. Alzheimers Res Ther 2019;11. https://doi.org/10.1186/s13195-019-0520-1.

[16] Wessels AM, Lines C, Stern RA, Kost J, Voss T, Mozley LH, et al. Cognitive outcomes in trials of two BACE inhibitors in Alzheimer's disease. Alzheimer's and Dementia 2020;16:1483–92. https://doi.org/10.1002/alz.12164.

[17] Baranello RJ, Bharani KL, Padmaraju V, Chopra N, Lahiri DK, Greig NH, et al. Amyloid-Beta Protein Clearance and Degradation (ABCD) Pathways and their Role in Alzheimer's Disease. Curr Alzheimer Res 2015;12:32-46. doi: 10.2174/1567205012666141218140953.

[18] Thal DR, Rüb U, Orantes M, Braak H. Phases of Aβ-deposition in the human brain and its relevance for the development of AD. Neurology 2002;58:1791–800. https://doi.org/10.1212/WNL.58.12.1791.

[19] Iwatsubo T, Odaka A, Suzuki N, Mizusawa H, Nukina N, Lharall Y. Visualization of Aβ42(43) and Aβ40 in senile plaques with end-specific Aβ monoclonals: Evidence that an initially deposited species is Aβ42(43). Neuron 1994;13:45-53. doi: 10.1016/0896-6273(94)90458-8.

[20] Olsson B, Lautner R, Andreasson U, Öhrfelt A, Portelius E, Bjerke M, et al. CSF and blood biomarkers for the diagnosis of Alzheimer's disease: a systematic review and meta-analysis. Lancet Neurol 2016;15:673–84. https://doi.org/10.1016/S1474-4422(16)00070-3.

[21] Villemagne VL, Burnham S, Bourgeat P, Brown B, Ellis KA, Salvado O, et al. Amyloid β deposition, neurodegeneration, and cognitive decline in sporadic Alzheimer's disease: A prospective cohort study. Lancet Neurol 2013;12:357–67. https://doi.org/10.1016/S1474-4422(13)70044-9.

[22] Jansen WJ, Janssen O, Tijms BM, Vos SJB, Ossenkoppele R, Visser PJ, et al. Prevalence Estimates of Amyloid Abnormality Across the Alzheimer Disease Clinical Spectrum. JAMA Neurol 2022;79:228–43. https://doi.org/10.1001/jamaneurol.2021.5216.

[23] Medeiros R, Baglietto-Vargas D, Laferla FM. The Role of Tau in Alzheimer's Disease and Related Disorders. CNS Neurosci Ther 2011;17:514–24. https://doi.org/10.1111/j.1755-5949.2010.00177.x.

[24] Köpke E, Tung Y-C, Shaikh S, Alonso ADC, Iqbal K, Grundke-Iqbals I. Microtubule-associated Protein Tau: Abnormal phosphorylation of a non-paired helical filament pool in Alzheimer's disease. J Biol Chem 1993;268:24374–84.

[25] Chen Y, Yu Y. Tau and neuroinflammation in Alzheimer's disease: interplay mechanisms and clinical translation. J Neuroinflammation 2023;20. https://doi.org/10.1186/s12974-023-02853-3.

[26] Holmes BB, Furman JL, Mahan TE, Yamasaki TR, Mirbaha H, Eades WC, et al. Proteopathic tau seeding predicts tauopathy in vivo. Proc Natl Acad Sci U S A 2014;111:E4376–85. https://doi.org/10.1073/pnas.1411649111.

[27] Braak H, Braak E. Neuropathological stageing of Alzheimer-related changes. Acta Neuropathol 1991;82:239–59.

[28] Cho H, Choi JY, Hwang MS, Kim YJ, Lee HM, Lee HS, et al. In vivo cortical spreading pattern of tau and amyloid in the Alzheimer disease spectrum. Ann Neurol 2016;80:247–58. https://doi.org/10.1002/ana.24711.

[29] Hansson O. Biomarkers for neurodegenerative diseases. Nat Med 2021;27:954–63. https://doi.org/10.1038/s41591-021-01382-x.

[30] Vogel JW, Young AL, Oxtoby NP, Smith R, Ossenkoppele R, Strandberg OT, et al. Four distinct trajectories of tau deposition identified in Alzheimer's disease. Nat Med 2021;27:871–81. https://doi.org/10.1038/s41591-021-01309-6.

[31] Ferreira D, Nordberg A, Westman E. Biological subtypes of Alzheimer disease: A systematic review and meta-analysis. Neurology 2020;94:436–48. https://doi.org/10.1212/WNL.0000000000009058.

[32] Anijärv TE, Ossenkoppele R, Smith R, Pichet Binette A, Collij LE, Behjat HH, et al. Hemispheric asymmetry of tau pathology is related to asymmetric amyloid deposition in Alzheimer's Disease. Nat Commun 2025;16:8232. https://doi.org/10.1038/s41467-025-63564-2.

[33] Younes K, Smith V, Johns E, Carlson ML, Winer J, He Z, et al. Temporal tau asymmetry spectrum influences divergent behavior and language patterns in Alzheimer's disease. Brain Behav Immun 2024;119:807–17. https://doi.org/10.1016/j.bbi.2024.05.002.

[34] Murray ME, Graff-Radford NR, Ross OA, Petersen RC, Duara R, Dickson DW. Neuropathologically defined subtypes of Alzheimer's disease with distinct clinical characteristics: a retrospective study. Lancet Neurol 2011;10:785–96. https://doi.org/10.1016/S1474-4422(11)70156-9.

[35] Aarsland D, Sunde AL, Tovar-Rios DA, Leuzy A, Fladby T, Zetterberg H, et al. Prevalence of Alzheimer's disease pathology in the community. Nature 2025. https://doi.org/10.1038/s41586-025-09841-y.

[36] West MJ, Coleman PD, Flood DG, Troncoso JC. Differences in the pattern of hippocampal neuronal loss in normal ageing and Alzheimer's disease. The Lancet 1994;344:769–72. https://doi.org/10.1016/S0140-6736(94)92338-8.

[37] Jack CR, Petersen RC, Xu YC, Waring SC, O'Brien PC, Tangalos EG, et al. Medial temporal atrophy on MRI in normal aging and very mild Alzheimer's disease. Neurology 1997;49:786–94. https://doi.org/10.1212/WNL.49.3.786.

[38] Nestor SM, Rupsingh R, Borrie M, Smith M, Accomazzi V, Wells JL, et al. Ventricular enlargement as a possible measure of Alzheimer's disease progression validated using the Alzheimer's disease neuroimaging initiative database. Brain 2008;131:2443–54. https://doi.org/10.1093/brain/awn146.

[39] Desikan RS, Cabral HJ, Fischl B, Guttmann CRG, Blacker D, Hyman BT, et al. Temporoparietal MR Imaging Measures of Atrophy in Subjects with Mild Cognitive Impairment That Predict Subsequent Diagnosis of Alzheimer Disease. American Journal of Neuroradiology 2009;30:532–8. https://doi.org/10.3174/ajnr.A1397.

[40] Ferreira D, Verhagen C, Hernández-Cabrera JA, Cavallin L, Guo CJ, Ekman U, et al. Distinct subtypes of Alzheimer's disease based on patterns of brain atrophy: Longitudinal trajectories and clinical applications. Sci Rep 2017;7. https://doi.org/10.1038/srep46263.

[41] Venkatraghavan V, Archetti D, Bourgeat P, Jiang C, ten Kate M, van Loenhoud AC, et al. A large-scale multi-centre study characterising atrophy heterogeneity in Alzheimer's disease. Neuroimage 2025;318. https://doi.org/10.1016/j.neuroimage.2025.121381.

[42] Seeley WW, Crawford RK, Zhou J, Miller BL, Greicius MD. Neurodegenerative Diseases Target Large-Scale Human Brain Networks. Neuron 2009;62:42–52. https://doi.org/10.1016/j.neuron.2009.03.024.

[43] American Psychiatric Association. Diagnostic and statistical manual of mental disorders: DSM-5. American Psychiatric Association; 2013.

[44] Harvey PD. Domains of cognition and their assessment. Dialogues Clin Neurosci 2019;21:227–37. https://doi.org/10.31887/DCNS.2019.21.3/pharvey.

[45] Karantzoulis S, Galvin JE. Distinguishing Alzheimer's disease from other major forms of dementia. Expert Rev Neurother 2011;11:1579–91. https://doi.org/10.1586/ern.11.155.

[46] Atri A, Dickerson BC, Clevenger C, Karlawish J, Knopman D, Lin PJ, et al. The Alzheimer's Association clinical practice guideline for the diagnostic evaluation, testing, counseling, and disclosure of suspected Alzheimer's disease and related disorders (DETeCD-ADRD): Validated clinical assessment instruments. Alzheimer's and Dementia 2025;21. https://doi.org/10.1002/alz.14335.

[47] Jack CR, Bennett DA, Blennow K, Carrillo MC, Dunn B, Haeberlein SB, et al. NIA-AA Research Framework: Toward a biological definition of Alzheimer's disease. Alzheimer's and Dementia 2018;14:535–62. https://doi.org/10.1016/j.jalz.2018.02.018.

[48] Jack CR, Knopman DS, Jagust WJ, Petersen RC, Weiner MW, Aisen PS, et al. Personal View Tracking pathophysiological processes in Alzheimer's disease: an updated hypothetical model of dynamic biomarkers. Lancet Neurol 2013 Feb;12:207-16. doi: 10.1016/S1474-4422(12)70291-0.

[49] Drzezga A, Barthel H. Imaging and Fluid Biomarkers of Alzheimer Disease: Complementation Rather Than Competition. Journal of Nuclear Medicine 2025;66:S32–44. https://doi.org/10.2967/jnumed.125.270152.

[50] Jack CR, Andrews JS, Beach TG, Buracchio T, Dunn B, Graf A, et al. Revised criteria for diagnosis and staging of Alzheimer's disease: Alzheimer's Association Workgroup. Alzheimer's and Dementia 2024;20:5143–69. https://doi.org/10.1002/alz.13859.

[51] Hardy JA, Higgins GA. Alzheimer's Disease: The Amyloid Cascade Hypothesis. Science (1979) 1992;256:184–5. https://doi.org/10.1126/science.1566067.

[52] Wilson DM, Cookson MR, Van Den Bosch L, Zetterberg H, Holtzman DM, Dewachter I. Hallmarks of neurodegenerative diseases. Cell 2023;186:693–714. https://doi.org/10.1016/j.cell.2022.12.032.

[53] Ossenkoppele R, Coomans EM, Apostolova LG, Baker SL, Barthel H, Beach TG, et al. Tau PET positivity in individuals with and without cognitive impairment varies with age, amyloid-β status, APOE genotype and sex. Nat Neurosci 2025;28:1610–21. https://doi.org/10.1038/s41593-025-02000-6.

[54] Ossenkoppele R, Pichet Binette A, Groot C, Smith R, Strandberg O, Palmqvist S, et al. Amyloid and tau PET-positive cognitively unimpaired individuals are at high risk for future cognitive decline. Nat Med 2022;28:2381–7. https://doi.org/10.1038/s41591-022-02049-x.

[55] Ossenkoppele R, Lyoo CH, Sudre CH, van Westen D, Cho H, Ryu YH, et al. Distinct tau PET patterns in atrophy-defined subtypes of Alzheimer's disease. Alzheimer's & Dementia 2020;16:335–44. https://doi.org/10.1016/j.jalz.2019.08.201.

[56] Kiselica AM, Gaynor LS, Atkins KJ. IWG and AA Criteria - Where the Differences Matter. JAMA Neurol 2025;82:628. https://doi.org/10.1001/jamaneurol.2025.0775.

[57] Dubois B, Villain N, Schneider L, Fox N, Campbell N, Galasko D, et al. Alzheimer Disease as a Clinical-Biological Construct - An International Working Group Recommendation. JAMA Neurol 2024;81:1304–11. https://doi.org/10.1001/jamaneurol.2024.3770.

[58] Zhang Y, Chen H, Li R, Sterling K, Song W. Amyloid β-based therapy for Alzheimer's disease: challenges, successes and future. Signal Transduct Target Ther 2023;8. https://doi.org/10.1038/s41392-023-01484-7.

[59] Livingston G, Huntley J, Liu KY, Costafreda SG, Selbæk G, Alladi S, et al. Dementia prevention, intervention, and care: 2024 report of the Lancet standing Commission. The Lancet 2024;404:572–628. https://doi.org/10.1016/S0140-6736(24)01296-0.

[60] Gatz M, Reynolds CA, Fratiglioni L, Mortimer JA, Berg S, Fiske A, et al. Role of Genes and Environments for Explaining Alzheimer Disease. Arch Gen Psychiatry 2006 Feb;63:168-74. doi: 10.1001/archpsyc.63.2.168.

[61] Kanekiyo T, Xu H, Bu G. ApoE and Aβ in Alzheimer's disease: Accidental encounters or partners? Neuron 2014;81:740–54. https://doi.org/10.1016/j.neuron.2014.01.045.

[62] Liu CC, Kanekiyo T, Xu H, Bu G. Apolipoprotein e and Alzheimer disease: Risk, mechanisms and therapy. Nat Rev Neurol 2013;9:106–18. https://doi.org/10.1038/nrneurol.2012.263.

[63] Corder EH, Saunders AM, Risch N], Strittmatter WJ, Schmechep· DE, Gaskell PC, et al. Protective effect of apolipoprotein E type 2 allele for late onset Alzheimer disease. Nat Genet 1994 Jun;7:180-4. doi: 10.1038/ng0694-180.

[64] Bellenguez C, Küçükali F, Jansen IE, Kleineidam L, Moreno-Grau S, Amin N, et al. New insights into the genetic etiology of Alzheimer's disease and related dementias. Nat Genet 2022;54:412–36. https://doi.org/10.1038/s41588-022-01024-z.

[65] Wightman DP, Jansen IE, Savage JE, Shadrin AA, Bahrami S, Holland D, et al. A genome-wide association study with 1,126,563 individuals identifies new risk loci for Alzheimer's disease. Nat Genet 2021;53:1276–82. https://doi.org/10.1038/s41588-021-00921-z.

[66] Hoogmartens J, Cacace R, Van Broeckhoven C. Insight into the genetic etiology of alzheimer's disease: A comprehensive review of the role of rare variants. Alzheimer's and Dementia: Diagnosis, Assessment and Disease Monitoring 2021;13. https://doi.org/10.1002/dad2.12155.

[67] Strang KH, Golde TE, Giasson BI. MAPT mutations, tauopathy, and mechanisms of neurodegeneration. Laboratory Investigation 2019;99:912–28. https://doi.org/10.1038/s41374-019-0197-x.

[68] Robinson JL, Xie SX, Baer DR, Suh ER, Van Deerlin VM, Loh NJ, et al. Pathological combinations in neurodegenerative disease are heterogeneous and disease-associated. Brain 2023;146:2557–69. https://doi.org/10.1093/brain/awad059.

[69] Palmqvist S, Rossi M, Hall S, Quadalti C, Mattsson-Carlgren N, Dellavalle S, et al. Cognitive effects of Lewy body pathology in clinically unimpaired individuals. Nat Med 2023;29:1971–8. https://doi.org/10.1038/s41591-023-02450-0.

[70] Quadalti C, Palmqvist S, Hall S, Rossi M, Mammana A, Janelidze S, et al. Clinical effects of Lewy body pathology in cognitively impaired individuals. Nat Med 2023;29:1964–70. https://doi.org/10.1038/s41591-023-02449-7.

[71] McKhann G, Drachman D, Folstein M, Katzman R, Price D, Stadlan EM. Clinical diagnosis of Alzheimer's disease. Neurology 1984;34:939–939. https://doi.org/10.1212/WNL.34.7.939.

[72] Beach TG, Monsell SE, Phillips LE, Kukull W. Accuracy of the Clinical Diagnosis of Alzheimer Disease at National Institute on Aging Alzheimer Disease Centers, 2005-2010. J Neuropathol Exp Neurol 2012 Apr;71:266-73. doi: 10.1097/NEN.0b013e31824b211b.

[73] Palmqvist S, Tideman P, Mattsson-Carlgren N, Schindler SE, Smith R, Ossenkoppele R, et al. Blood Biomarkers to Detect Alzheimer Disease in Primary Care and Secondary Care. JAMA 2024. https://doi.org/10.1001/jama.2024.13855.

[74] Anoop A, Singh PK, Jacob RS, Maji SK. CSF Biomarkers for Alzheimer's Disease Diagnosis. Int J Alzheimers Dis 2010;2010:1–12. https://doi.org/10.4061/2010/606802.

[75] Wichmann TO, Damkier HH, Pedersen M. A Brief Overview of the Cerebrospinal Fluid System and Its Implications for Brain and Spinal Cord Diseases. Front Hum Neurosci 2022;15. https://doi.org/10.3389/fnhum.2021.737217.

[76] Margetis K, Baker S. Physiology, Cerebral Spinal Fluid. Treasure Island (FL): StatPearlsPublishing; 2025.

[77] May C, Kaye JA, Atack JR, Schapiro MB, Friedland RP, Rapoport SI. Cerebrospinal fluid production is reduced in healthy aging. Neurology 1990;40:500. https://doi.org/10.1212/WNL.40.3_Part_1.500.

[78] Fleischman D, Berdahl JP, Zaydlarova J, Stinnett S, Fautsch MP, Allingham RR. Cerebrospinal Fluid Pressure Decreases with Older Age. PLoS One 2012;7. https://doi.org/10.1371/journal.pone.0052664.

[79] Yamada S, Otani T, Ii S, Kawano H, Nozaki K, Wada S, et al. Aging-related volume changes in the brain and cerebrospinal fluid using artificial intelligence-automated segmentation. Eur Radiol 2023;33:7099–112. https://doi.org/10.1007/s00330-023-09632-x.

[80] Al-Amrani S, Al-Jabri Z, Al-Zaabi A, Alshekaili J, Al-Khabori M. Proteomics: Concepts and applications in human medicine. World J Biol Chem 2021;12:57–69. https://doi.org/10.4331/wjbc.v12.i5.57.

[81] Johnson ECB, Bian S, Haque RU, Carter EK, Watson CM, Gordon BA, et al. Cerebrospinal fluid proteomics define the natural history of autosomal dominant Alzheimer's disease. Nat Med 2023;29:1979–88. https://doi.org/10.1038/s41591-023-02476-4.

[82] Pichet Binette A, Gaiteri C, Wennström M, Kumar A, Hristovska I, Spotorno N, et al. Proteomic changes in Alzheimer's disease associated with progressive Aβ plaque and tau tangle pathologies. Nat Neurosci 2024;27:1880–91. https://doi.org/10.1038/s41593-024-01737-w.

[83] Blennow K, Zetterberg H. Biomarkers for Alzheimer's disease: current status and prospects for the future. J Intern Med 2018;284:643–63. https://doi.org/10.1111/joim.12816.

[84] Salvadó G, Horie K, Barthélemy NR, Vogel JW, Pichet Binette A, Chen CD, et al. Disease staging of Alzheimer's disease using a CSF-based biomarker model. Nat Aging 2024;4:694–708. https://doi.org/10.1038/s43587-024-00599-y.

[85] McGrowder DA, Miller F, Vaz K, Nwokocha C, Wilson-Clarke C, Anderson-Cross M, et al. Cerebrospinal fluid biomarkers of alzheimer's disease: Current evidence and future perspectives. Brain Sci 2021;11:1–56. https://doi.org/10.3390/brainsci11020215.

[86] Hansson O, Seibyl J, Stomrud E, Zetterberg H, Trojanowski JQ, Bittner T, et al. CSF biomarkers of Alzheimer's disease concord with amyloid-β PET and predict clinical progression: A study of fully automated immunoassays in BioFINDER and ADNI cohorts. Alzheimer's and Dementia 2018;14:1470–81. https://doi.org/10.1016/j.jalz.2018.01.010.

[87] Mattsson N, Zetterberg H, Hansson O, Andreasen N, Parnetti L, Jonsson M, et al. CSF Biomarkers and Incipient Alzheimer Disease in Patients With Mild Cognitive Impairment. JAMA. 2009 Jul 22;302(4):385-93. doi: 10.1001/jama.2009.1064.

[88] Janelidze S, Zetterberg H, Mattsson N, Palmqvist S, Vanderstichele H, Lindberg O, et al. CSF Aβ42/Aβ40 and Aβ42/Aβ38 ratios: Better diagnostic markers of Alzheimer disease. Ann Clin Transl Neurol 2016;3:154–65. https://doi.org/10.1002/acn3.274.

[89] Hansson O, Lehmann S, Otto M, Zetterberg H, Lewczuk P. Advantages and disadvantages of the use of the CSF Amyloid β (Aβ) 42/40 ratio in the diagnosis of Alzheimer's Disease. Alzheimers Res Ther 2019;11:1–15. https://doi.org/10.1186/s13195-019-0485-0.

[90] Palmqvist S, Janelidze S, Quiroz YT, Zetterberg H, Lopera F, Stomrud E, et al. Discriminative Accuracy of Plasma Phospho-tau217 for Alzheimer Disease vs Other Neurodegenerative Disorders. JAMA 2020;324:772–81. https://doi.org/10.1001/jama.2020.12134.

[91] Nakamura A, Kaneko N, Villemagne VL, Kato T, Doecke J, Doré V, et al. High performance plasma amyloid-β biomarkers for Alzheimer's disease. Nature 2018;554:249–54. https://doi.org/10.1038/nature25456.

[92] Mielke MM, Hagen CE, Xu J, Chai X, Vemuri P, Lowe VJ, et al. Plasma phospho-tau181 increases with Alzheimer's disease clinical severity and is associated with tau- and amyloid-positron emission tomography. Alzheimer's and Dementia 2018;14:989–97. https://doi.org/10.1016/j.jalz.2018.02.013.

[93] Janelidze S, Stomrud E, Palmqvist S, Zetterberg H, Van Westen D, Jeromin A, et al. Plasma β-amyloid in Alzheimer's disease and vascular disease. Sci Rep 2016;6. https://doi.org/10.1038/srep26801.

[94] Hansson O, Blennow K, Zetterberg H, Dage J. Blood biomarkers for Alzheimer's disease in clinical practice and trials. Nat Aging 2023;3:506–19. https://doi.org/10.1038/s43587-023-00403-3.

[95] Salvadó G, Ossenkoppele R, Ashton NJ, Beach TG, Serrano GE, Reiman EM, et al. Specific associations between plasma biomarkers and postmortem amyloid plaque and tau tangle loads. EMBO Mol Med 2023;15. https://doi.org/10.15252/emmm.202217123.

[96] Therriault J, Brum WS, Trudel L, Macedo AC, Bitencourt FV, Martins-Pfeifer CC, et al. Blood phosphorylated tau for the diagnosis of Alzheimer's disease: a systematic review and meta-analysis. Lancet Neurol 2025;24:740–52. https://doi.org/10.1016/S1474-4422(25)00227-3.

[97] Roher AE, Esh CL, Kokjohn TA, Castaño EM, Van Vickle GD, Kalback WM, et al. Amyloid beta peptides in human plasma and tissues and their significance for Alzheimer's disease. Alzheimer's and Dementia 2009;5:18–29. https://doi.org/10.1016/j.jalz.2008.10.004.

[98] Hampel H, Hu Y, Cummings J, Mattke S, Iwatsubo T, Nakamura A, et al. Blood-based biomarkers for Alzheimer's disease: Current state and future use in a transformed global healthcare landscape. Neuron 2023;111:2781–99. https://doi.org/10.1016/j.neuron.2023.05.017.

[99] Barthélemy NR, Salvadó G, Schindler S, He Y, Janelidze S, Collij LE, et al. Highly Accurate Blood Test for Alzheimer's Disease Comparable or Superior to Clinical CSF Tests. Nat Med 2024. https://doi.org/10.1038/s41591-024-02869-z.

[100] Ashton NJ, Brum WS, Molfetta G Di, Benedet AL, Arslan B, Jonaitis E, et al. Diagnostic Accuracy of a Plasma Phosphorylated Tau 217 Immunoassay for Alzheimer Disease Pathology. JAMA Neurol 2024;81:255–63. https://doi.org/10.1001/jamaneurol.2023.5319.

[101] Politis M, Piccini P. Positron emission tomography imaging in neurological disorders. J Neurol 2012;259:1769–80. https://doi.org/10.1007/s00415-012-6428-3.

[102] Clark CM, Pontecorvo MJ, Beach TG, Bedell BJ, Coleman RE, Doraiswamy PM, et al. Cerebral PET with florbetapir compared with neuropathology at autopsy for detection of neuritic amyloid-β plaques: A prospective cohort study. Lancet Neurol 2012;11:669–78. https://doi.org/10.1016/S1474-4422(12)70142-4.

[103] Curtis C, Gamez JE, Singh U, Sadowsky CH, Villena T, Sabbagh MN, et al. Phase 3 trial of flutemetamol labeled with radioactive fluorine 18 imaging and neuritic plaque density. JAMA Neurol 2015;72:287–94. https://doi.org/10.1001/jamaneurol.2014.4144.

[104] Sabri O, Sabbagh MN, Seibyl J, Barthel H, Akatsu H, Ouchi Y, et al. Florbetaben PET imaging to detect amyloid beta plaques in Alzheimer's disease: Phase 3 study. Alzheimer's and Dementia 2015;11:964–74. https://doi.org/10.1016/j.jalz.2015.02.004.

[105] Smith R, Wibom M, Pawlik D, Englund E, Hansson O. Correlation of in vivo [18 F]Flortaucipir with Postmortem Alzheimer Disease Tau Pathology. JAMA Neurol 2019;76:310–7. https://doi.org/10.1001/jamaneurol.2018.3692.

[106] Leuzy A, Smith R, Ossenkoppele R, Santillo A, Borroni E, Klein G, et al. Diagnostic performance of RO948 F 18 tau positron emission tomography in the differentiation of alzheimer disease from other neurodegenerative disorders. JAMA Neurol 2020;77:955–65. https://doi.org/10.1001/jamaneurol.2020.0989.

[107] Ossenkoppele R, Rabinovici GD, Smith R, Cho H, Scholl M, Strandberg O, et al. Discriminative accuracy of [18F]flortaucipir positron emission tomography for Alzheimer disease vs other neurodegenerative disorders. JAMA - Journal of the American Medical Association 2018;320:1151–62. https://doi.org/10.1001/jama.2018.12917.

[108] Smith R, Hägerström D, Pawlik D, Klein G, Jögi J, Ohlsson T, et al. Clinical Utility of Tau Positron Emission Tomography in the Diagnostic Workup of Patients With Cognitive Symptoms. JAMA Neurol 2023. https://doi.org/10.1001/jamaneurol.2023.1323.

[109] Altomare D, Caprioglio C, Assal F, Allali G, Mendes A, Ribaldi F, et al. Diagnostic value of amyloid-PET and tau-PET: a head-to-head comparison. Eur J Nucl Med Mol Imaging 2021;48:2200–11. https://doi.org/10.1007/s00259-021-05246-x.

[110] Chapleau M, Iaccarino L, Soleimani-Meigooni D, Rabinovici GD. The Role of Amyloid PET in Imaging Neurodegenerative Disorders: A Review. Journal of Nuclear Medicine 2022;63:13S-19S. https://doi.org/10.2967/JNUMED.121.263195.

[111] Jenkinson M, Chappell M. Introduction to Neuroimaging Analysis. Oxford University Press; 2018.

[112] Haller S, Jäger HR, Vernooij MW, Barkhof F. Neuroimaging in Dementia: More than Typical Alzheimer Disease. Radiology 2023;308. https://doi.org/10.1148/radiol.230173.

[113] Živanović M, Aracki Trenkić A, Milošević V, Stojanov D, Mišić M, Radovanović M, et al. The role of magnetic resonance imaging in the diagnosis and prognosis of dementia. Biomolecules and Biomedicine 2023;23:209–24. https://doi.org/10.17305/bjbms.2022.8085.

[114] Schindler SE, Petersen KK, Saef B, Tosun D, Shaw LM, Zetterberg H, et al. Head-to-head comparison of leading blood tests for Alzheimer's disease pathology. Alzheimer's and Dementia 2024;20:8074–96. https://doi.org/10.1002/alz.14315.

[115] Warmenhoven N, Salvadó G, Janelidze S, Mattsson-Carlgren N, Bali D, Orduña Dolado A, et al. A comprehensive head-to-head comparison of key plasma phosphorylated tau 217 biomarker tests. Brain 2025;148:416–31. https://doi.org/10.1093/brain/awae346.

[116] Horie K, Salvadó G, Koppisetti RK, Janelidze S, Barthélemy NR, He Y, et al. Plasma MTBR-tau243 biomarker identifies tau tangle pathology in Alzheimer's disease. Nat Med 2025;31:2044–53. https://doi.org/10.1038/s41591-025-03617-7.

[117] Horie K, Salvadó G, Barthélemy NR, Janelidze S, Li Y, He Y, et al. CSF MTBR-tau243 is a specific biomarker of tau tangle pathology in Alzheimer's disease. Nat Med 2023;29:1954–63. https://doi.org/10.1038/s41591-023-02443-z.

[118] Hansson O, Jack CR. A clinical perspective on the revised criteria for diagnosis and staging of Alzheimer's disease. Nat Aging 2024;4:1029–31. https://doi.org/10.1038/s43587-024-00675-3.

[119] Dubois B, Villain N, Frisoni GB, Rabinovici GD, Sabbagh M, Cappa S, et al. Clinical diagnosis of Alzheimer's disease: recommendations of the International Working Group. Lancet Neurol 2021;20:484–96. https://doi.org/10.1016/S1474-4422(21)00066-1.

[120] Therriault J, Janelidze S, Benedet AL, Ashton NJ, Arranz Martínez J, Gonzalez-Escalante A, et al. Diagnosis of Alzheimer's disease using plasma biomarkers adjusted to clinical probability. Nat Aging 2024;4:1529–37. https://doi.org/10.1038/s43587-024-00731-y.

[121] Drabo EF, Barthold D, Joyce G, Ferido P, Chang Chui H, Zissimopoulos J. Longitudinal analysis of dementia diagnosis and specialty care among racially diverse Medicare beneficiaries. Alzheimer's and Dementia 2019;15:1402–11. https://doi.org/10.1016/j.jalz.2019.07.005.

[122] Frisoni GB, Hansson O, Nichols E, Garibotto V, Schindler SE, van der Flier WM, et al. New landscape of the diagnosis of Alzheimer's disease. The Lancet 2025;406:1389–407. https://doi.org/10.1016/S0140-6736(25)01294-2.

[123] Zuliani G, Zuin M, Romagnoli T, Polastri M, Cervellati C, Brombo G. Acetyl-cholinesterase-inhibitors reconsidered. A narrative review of post-marketing studies on Alzheimer's disease. Aging Clin Exp Res 2024;36:23. https://doi.org/10.1007/s40520-023-02675-6.

[124] Xu H, Garcia-Ptacek S, Jönsson L, Wimo A, Nordström P, Eriksdotter M. Long-term Effects of Cholinesterase Inhibitors on Cognitive Decline and Mortality. Neurology 2021;96. https://doi.org/10.1212/WNL.0000000000011832.

[125] Fox NC, Belder C, Ballard C, Kales HC, Mummery C, Caramelli P, et al. Treatment for Alzheimer's disease. The Lancet 2025;406:1408–23. https://doi.org/10.1016/S0140-6736(25)01329-7.

[126] van Dyck CH, Swanson CJ, Aisen P, Bateman RJ, Chen C, Kramer LD, et al. Lecanemab in Early Alzheimer's Disease. New England Journal of Medicine 2023;388. https://doi.org/10.1056/nejmoa2212948.

[127] Mintun MA, Lo AC, Duggan Evans C, Wessels AM, Ardayfio PA, Andersen SW, et al. Donanemab in Early Alzheimer's Disease. New England Journal of Medicine 2021;384:1691–704. https://doi.org/10.1056/NEJMoa2100708.

[128] Sims JR, Zimmer JA, Evans CD, Lu M, Ardayfio P, Sparks JD, et al. Donanemab in Early Symptomatic Alzheimer Disease: The TRAILBLAZER-ALZ 2 Randomized Clinical Trial. JAMA 2023;330:512–27. https://doi.org/10.1001/jama.2023.13239.

[129] Grimm HP, Schumacher V, Schäfer M, Imhof-Jung S, Freskgård P-O, Brady K, et al. Delivery of the Brainshuttle™ amyloid-beta antibody fusion trontinemab to non-human primate brain and projected efficacious dose regimens in humans. MAbs 2023;15. https://doi.org/10.1080/19420862.2023.2261509.

[130] Cummings JL, Zhou Y, Lee G, Zhong K, Fonseca J, Leisgang-Osse AM, et al. Alzheimer's disease drug development pipeline: 2025. Alzheimer's and Dementia: Translational Research and Clinical Interventions 2025;11. https://doi.org/10.1002/trc2.70098.

[131] Blom G, Enger J, Englund G, Grandell J, Holst L. Sannolikhetsteori och statistikteori med tillämpningar. 7th ed. Lund: Studentlitteratur; 2017.

[132] Looking back on the millennium in medicine. New England Journal of Medicine 2000;342:42–9.

[133] Kaliyadan F, Kulkarni V. Types of variables, descriptive statistics, and sample size. Indian Dermatol Online J 2019;10:82–6. https://doi.org/10.4103/idoj.IDOJ_468_18.

[134] Guetterman TC. Basics of statistics for primary care research. Fam Med Community Health 2019;7. https://doi.org/10.1136/fmch-2018-000067.

[135] Bzdok D, Ioannidis JPA. Exploration, Inference, and Prediction in Neuroscience and Biomedicine. Trends Neurosci 2019;42:251–62. https://doi.org/10.1016/j.tins.2019.02.001.

[136] Hunter DJ, Holmes C. Where Medical Statistics Meets Artificial Intelligence. New England Journal of Medicine 2023;389:1211–9. https://doi.org/10.1056/nejmra2212850.

[137] Greener JG, Kandathil SM, Moffat L, Jones DT. A guide to machine learning for biologists. Nat Rev Mol Cell Biol 2022;23:40–55. https://doi.org/10.1038/s41580-021-00407-0.

[138] Bzdok D, Altman N, Krzywinski M. Statistics versus machine learning. Nat Methods 2018;15:233–4. https://doi.org/10.1038/nmeth.4642.

[139] Rosenblatt F. The perceptron: A probabilistic model for information storage and organization in the brain. Psychol Rev 1958;65:386–408. https://doi.org/10.1037/h0042519.

[140] Rajpurkar P, Chen E, Banerjee O, Topol EJ. AI in health and medicine. Nat Med 2022;28:31–8. https://doi.org/10.1038/s41591-021-01614-0.

[141] Rajkomar A, Dean J, Kohane I. Machine Learning in Medicine. New England Journal of Medicine 2019;380:1347–58. https://doi.org/10.1056/nejmra1814259.

[142] Esteva A, Robicquet A, Ramsundar B, Kuleshov V, DePristo M, Chou K, et al. A guide to deep learning in healthcare. Nat Med 2019;25:24–9. https://doi.org/10.1038/s41591-018-0316-z.

[143] Jiangtao W, Ruhaiyem NIR, Panpan F. A Comprehensive Review of U-Net and Its Variants: Advances and Applications in Medical Image Segmentation. IET Image Process 2025;19. https://doi.org/10.1049/ipr2.70019.

[144] Ali M, Ali M, Hussain M, Koundal D. Generative Adversarial Networks (GANs) for Medical Image Processing: Recent Advancements. Archives of Computational Methods in Engineering 2025;32:1185–98. https://doi.org/10.1007/s11831-024-10174-8.

[145] Jumper J, Evans R, Pritzel A, Green T, Figurnov M, Ronneberger O, et al. Highly accurate protein structure prediction with AlphaFold. Nature 2021;596:583–9. https://doi.org/10.1038/s41586-021-03819-2.

[146] Zhang K, Yang X, Wang Y, Yu Y, Huang N, Li G, et al. Artificial intelligence in drug development. Nat Med 2025;31:45–59. https://doi.org/10.1038/s41591-024-03434-4.

[147] Yang X, Huang K, Yang D, Zhao W, Zhou X. Biomedical Big Data Technologies, Applications, and Challenges for Precision Medicine: A Review. Global Challenges 2024;8. https://doi.org/10.1002/gch2.202300163.

[148] Barthélemy NR, Saef B, Li Y, Gordon BA, He Y, Horie K, et al. CSF tau phosphorylation occupancies at T217 and T205 represent improved biomarkers of amyloid and tau pathology in Alzheimer's disease. Nat Aging 2023;3:391–401. https://doi.org/10.1038/s43587-023-00380-7.

[149] Therriault J, Benedet AL, Pascoal TA, Mathotaarachchi S, Chamoun M, Savard M, et al. Association of Apolipoprotein e ϵ4 with Medial Temporal Tau Independent of Amyloid-β. JAMA Neurol 2020;77:470–9. https://doi.org/10.1001/jamaneurol.2019.4421.

[150] Gaetani L, Bellomo G, Di Sabatino E, Sperandei S, Mancini A, Blennow K, et al. The Immune Signature of CSF in Multiple Sclerosis with and without Oligoclonal Bands: A Machine Learning Approach to Proximity Extension Assay Analysis. Int J Mol Sci 2024;25. https://doi.org/10.3390/ijms25010139.

[151] Thijssen E, La Joie R, Strom AB, Fonseca CB, Iaccarino L, Wolf AB, et al. Plasma phosphorylated tau 217 and phosphorylated tau 181 as biomarkers in Alzheimer's disease and frontotemporal lobar degeneration: a retrospective diagnostic performance study. Lancet Neurol 2021;20:739–52.

[152] Retrieved 2025-12-29. https://adni.loni.usc.edu/ n.d.

[153] Sperling RA, Rentz DM, Johnson KA, Karlawish J, Donohue M, Salmon DP, et al. The A4 study: Stopping AD before symptoms begin? Sci Transl Med 2014;6. https://doi.org/10.1126/scitranslmed.3007941.

[154] Lamontagne PJ, Morris TL, Keefe JC, Sarah, Hornbeck, Russ, et al. OASIS-3: Longitudinal Neuroimaging, Clinical, and Cognitive Dataset for Normal Aging and Alzheimer Disease n.d. https://doi.org/10.1101/2019.12.13.19014902.

[155] Schwarz AJ, Yu P, Miller BB, Shcherbinin S, Dickson J, Navitsky M, et al. Regional profiles of the candidate tau PET ligand 18F-AV-1451 recapitulate key featuresof Braak histopathological stages. Brain 2016;139:1318–20. https://doi.org/10.1093/brain/aww057.

[156] Villeneuve S, Poirier J, Breitner JCS, Tremblay-Mercier J, Remz J, Raoult JM, et al. The PREVENT-AD cohort: Accelerating Alzheimer's disease research and treatment in Canada and beyond. Alzheimers Dement 2025;21:e70653. https://doi.org/10.1002/alz.70653.

[157] Ossenkoppele R, Madison C, Oh H, Wirth M, Van Berckel BNM, Jagust WJ. Is verbal episodic memory in elderly with amyloid deposits preserved through altered neuronal function? Cerebral Cortex 2014;24:2210–8. https://doi.org/10.1093/cercor/bht076.

[158] Darwish IA. Immunoassay Methods and their Applications in Pharmaceutical Analysis: Basic Methodology and Recent Advances. Int J Biomed Sci 2006;2:217–35.

[159] Simrén J, Elmgren A, Blennow K, Zetterberg H. Fluid biomarkers in Alzheimer's disease. Adv Clin Chem. 2023;112:249-281. doi: 10.1016/bs.acc.2022.09.006.

[160] Korecka M, Shaw LM. Mass spectrometry-based methods for robust measurement of Alzheimer's disease biomarkers in biological fluids. J Neurochem 2021;159:211–33. https://doi.org/10.1111/jnc.15465.

[161] Gobom J, Brinkmalm A, Brinkmalm G, Blennow K, Zetterberg H. Alzheimer's Disease Biomarker Analysis Using Targeted Mass Spectrometry. Molecular and Cellular Proteomics 2024;23. https://doi.org/10.1016/j.mcpro.2024.100721.

[162] Yarbro JM, Shrestha HK, Wang Z, Zhang X, Zaman M, Chu M, et al. Proteomic landscape of Alzheimer's disease: emerging technologies, advances and insights (2021 - 2025). Mol Neurodegener 2025;20:83. https://doi.org/10.1186/s13024-025-00874-5.

[163] Wik L, Nordberg N, Broberg J, Björkesten J, Assarsson E, Henriksson S, et al. Proximity Extension Assay in Combination with Next-Generation Sequencing for High-throughput Proteome-wide Analysis. Molecular & Cellular Proteomics 2021;20:100168. https://doi.org/10.1016/j.mcpro.2021.100168.

[164] Folstein MF, Folstein SE, McHugh PR. "Mini-mental state." J Psychiatr Res 1975;12:189–98. https://doi.org/10.1016/0022-3956(75)90026-6.

[165] Nasreddine ZS, Phillips NA, Bédirian V, Charbonneau S, Whitehead V, Collin I, et al. The Montreal Cognitive Assessment, MoCA: A Brief Screening Tool For Mild Cognitive Impairment. J Am Geriatr Soc 2005;53:695–9. https://doi.org/10.1111/j.1532-5415.2005.53221.x.

[166] Kueper JK, Speechley M, Montero-Odasso M. The Alzheimer's Disease Assessment Scale-Cognitive Subscale (ADAS-Cog): Modifications and Responsiveness in Pre-Dementia Populations. A Narrative Review. J Alzheimers Dis 2018;63:423–44. https://doi.org/10.3233/JAD-170991.

[167] Llinàs-Reglà J, Vilalta-Franch J, López-Pousa S, Calvó-Perxas L, Torrents Rodas D, Garre-Olmo J. The Trail Making Test. Assessment 2017;24:183–96. https://doi.org/10.1177/1073191115602552.

[168] Tombaugh T. Normative Data Stratified by Age and Education for Two Measures of Verbal Fluency FAS and Animal Naming. Archives of Clinical Neuropsychology 1999;14:167–77. https://doi.org/10.1016/S0887-6177(97)00095-4.

[169] Smith A. Symbol Digit Modalities Test. PsycTESTS Dataset 2016. https://doi.org/10.1037/t27513-000.

[170] Borson S, Scanlan J, Brush M, Vitaliano P, Dokmak A. The mini-cog: a cognitive "vital signs" measure for dementia screening in multi-lingual elderly. Int J Geriatr Psychiatry 2000;15:1021–7. https://doi.org/10.1002/1099-1166(200011)15:11<1021::aid-gps234>3.0.co;2-6.

[171] Randolph C, Tierney MC, Mohr E, Chase TN. The Repeatable Battery for the Assessment of Neuropsychological Status (RBANS): Preliminary Clinical Validity. J Clin Exp Neuropsychol 1998;20:310–9. https://doi.org/10.1076/jcen.20.3.310.823.

[172] Hughes CP, Berg L, Danziger W, Coben LA, Martin RL. A New Clinical Scale for the Staging of Dementia. British Journal of Psychiatry 1982;140:566–72. https://doi.org/10.1192/bjp.140.6.566.

[173] Sahakian BJ, Morris RG, Evenden JL, Heald A, Levy R, Philpot M, et al. A comparative study of visuospatial memory and learning in Alzheimer-type dementia and Parkinson's disease. Brain 1988;111:695–718. https://doi.org/10.1093/brain/111.3.695.

[174] Tideman P, Karlsson L, Strandberg O, Calling S, Smith R, Midlöv P, et al. Primary care detection of Alzheimer's disease using a self-administered digital cognitive test and blood biomarkers. Nat Med 2025. https://doi.org/10.1038/s41591-025-03965-4.

[175] Schober P, Boer C, Schwarte LA. Correlation Coefficients: Appropriate Use and Interpretation. Anesth Analg 2018;126:1763–8. https://doi.org/10.1213/ANE.0000000000002864.

[176] Bewick V, Cheek L, Ball J. Statistics review 14: Logistic regression. Crit Care 2005;9:112–8. https://doi.org/10.1186/cc3045.

[177] Peduzzi P, Concato J, Kemper E, Holford TR, Feinstein AR. A simulation study of the number of events per variable in logistic regression analysis. J Clin Epidemiol 1996;49:1373–9. https://doi.org/10.1016/S0895-4356(96)00236-3.

[178] Youden WJ. Index for rating diagnostic tests. Cancer 1950;3:32–5. https://doi.org/10.1002/1097-0142(1950)3:1<32::AID-CNCR2820030106>3.0.CO;2-3.

[179] Brum WS, Cullen NC, Janelidze S, Ashton NJ, Zimmer ER, Therriault J, et al. A two-step workflow based on plasma p-tau217 to screen for amyloid β positivity with further confirmatory testing only in uncertain cases. Nat Aging 2023;3:1079–90. https://doi.org/10.1038/s43587-023-00471-5.

[180] Thomann AE, Berres M, Goettel N, Steiner LA, Monsch AU. Enhanced diagnostic accuracy for neurocognitive disorders: a revised cut-off approach for the Montreal Cognitive Assessment. Alzheimers Res Ther 2020;12:39. https://doi.org/10.1186/s13195-020-00603-8.

[181] Pourhoseingholi MA, Baghestani AR, Vahedi M. How to control confounding effects by statistical analysis. Gastroenterol Hepatol Bed Bench 2012;5:79–83.

[182] Maassen GH, Bakker AB. Suppressor Variables in Path Models: Definitions and Interpretations. Sociological Methods & Research 2001;30:241-70. https://doi.org/10.1177/0049124101030002004

[183] Carpenter J, Bithell J. Bootstrap confidence intervals: when, which, what? A practical guide for medical statisticians. Stat Med 2000;19:1141–64. https://doi.org/10.1002/(SICI)1097-0258(20000515)19:9<1141::AID-SIM479>3.0.CO;2-F.

[184] Benjaminit Y, Hochberg Y. Controlling the False Discovery Rate: a Practical and Powerful Approach to Multiple Testing. vol. 57. 1995.

[185] Lay DC, Lay SR, McDonald JI. Linear Algebra and its applications. 5th ed. Pearson; 2016.

[186] Van Der Maaten L, Hinton G. Visualizing Data using t-SNE. vol. 9. 2008.

[187] Hartigan JA, Wong MA. Algorithm AS 136: A K-Means Clustering Algorithm. Appl Stat 1979;28:100. https://doi.org/10.2307/2346830.

[188] Sarker IH. Machine Learning: Algorithms, Real-World Applications and Research Directions. SN Comput Sci 2021;2:160. https://doi.org/10.1007/s42979-021-00592-x.

[189] Mienye ID, Sun Y. A Survey of Ensemble Learning: Concepts, Algorithms, Applications, and Prospects. IEEE Access 2022;10:99129–49. https://doi.org/10.1109/ACCESS.2022.3207287.

[190] Cortes C, Vapnik V. Support-vector networks. Mach Learn 1995;20:273–97. https://doi.org/10.1007/BF00994018.

[191] Aha DW, Kibler D, Albert MK. Instance-based learning algorithms. Mach Learn 1991;6:37–66. https://doi.org/10.1007/BF00153759.

[192] Quinlan JR. Induction of Decision Trees. Mach Learn 1986;1:81-106. https://doi.org/10.1007/BF00116251

[193] Akaike H. A new look at the statistical model identification. IEEE Trans Automat Contr 1974;19:716–23. https://doi.org/10.1109/TAC.1974.1100705.

[194] Kohavi R. A Study of Cross-Validation and Bootstrap for Accuracy Estimation and Model Selection. Proceedings of the 14th international joint conference on Artificial intelligence 1995;2:1137-43.

[195] Pelikan M, Goldberg DE, Cantú-Paz E. BOA: The Bayesian Optimization Algorithm. Proceedings of the genetic and evolutionary computation conference GECCO-99 1999;1:525-32.

[196] Snoek J, Larochelle H, Adams RP. Practical Bayesian Optimization of Machine Learning Algorithms. Advances in neural information processing systems 25 2012;2:2951-59.

[197] Lundberg SM, Allen PG, Lee S-I. A Unified Approach to Interpreting Model Predictions. 31st Conference on Neural Information Processing Systems 2017:4768-77.

[198] Mattsson-Carlgren N, Karlsson L, Tang W, Blennow K, Zetterberg H, Bateman RJ, et al. Prediction of continuous amyloid positron emission tomography with fluid measures of phosphorylated tau and β-amyloid. EMBO Mol Med 2025. https://doi.org/10.1038/s44321-025-00348-7.

[199] Karlsson L, Vogel J, Arvidsson I, Åström K, Strandberg O, Seidlitz J, et al. Machine learning prediction of tau-PET in Alzheimer's disease using plasma, MRI, and clinical data. Alzheimer's & Dementia 2025;21. https://doi.org/10.1002/alz.14600.

[200] Ronneberger O, Fischer P, Brox T. U-Net: Convolutional Networks for Biomedical Image Segmentation . Medical Image Computing and Computer-Assisted Intervention – MICCAI 2015. https://doi.org/10.1007/978-3-319-24574-4_28

[201] Kingma DP, Ba J. Adam: A Method for Stochastic Optimization. International Conference on Learning Representations (ICLR) 2017.

[202] He K, Zhang X, Ren S, Sun J. Deep Residual Learning for Image Recognition. Computer Vision and Pattern Recognition (CVPR) 2015.

[203] Vaswani A, Brain G, Shazeer N, Parmar N, Uszkoreit J, Jones L, et al. Attention Is All You Need. International Conference on Neural Information Processing Systems 2017:6000-10.

[204] Joie R La, Bejanin A, Fagan AM, Ayakta N, Baker SL, Bourakova V, et al. Associations between [18F]AV1451 tau PET and CSF measures of tau pathology in a clinical sample. Neurology 2018;90:e282–90. https://doi.org/10.1212/WNL.0000000000004860.

[205] Bucci M, Chiotis K, Nordberg A. Alzheimer's disease profiled by fluid and imaging markers: tau PET best predicts cognitive decline. Mol Psychiatry 2021;26:5888–98. https://doi.org/10.1038/s41380-021-01263-2.

[206] Shoji M, Matsubara E, Kanai M, Watanabe M, Nakamura T, Tomidokoro Y, et al. Combination assay of CSF Tau, Ab1-40 and Ab1-42(43) as a biochemical marker of Alzheimer's disease. J Neurol Sci 1998 30;158:134-40. doi: 10.1016/s0022-510x(98)00122-1.

[207] Karlsson L, Vogel J, Arvidsson I, Åström K, Janelidze S, Blennow K, et al. Cerebrospinal fluid reference proteins increase accuracy and interpretability of biomarkers for brain diseases. Nat Commun 2024;15. https://doi.org/10.1038/s41467-024-47971-5.

[208] Suárez-Calvet M, Morenas-Rodríguez E, Kleinberger G, Schlepckow K, Caballero MÁA, Franzmeier N, et al. Early increase of CSF sTREM2 in Alzheimer's disease is associated with tau related-neurodegeneration but not with amyloid-β pathology. Mol Neurodegener 2019;14. https://doi.org/10.1186/s13024-018-0301-5.

[209] Brosseron F, Maass A, Kleineidam L, Ravichandran KA, González PG, McManus RM, et al. Soluble TAM receptors sAXL and sTyro3 predict structural and functional protection in Alzheimer's disease. Neuron 2022;110:1009-1022.e4. https://doi.org/10.1016/j.neuron.2021.12.016.

[210] Nordengen K, Kirsebom BE, Henjum K, Selnes P, Gísladóttir B, Wettergreen M, et al. Glial activation and inflammation along the Alzheimer's disease continuum. J Neuroinflammation 2019;16. https://doi.org/10.1186/s12974-019-1399-2.

[211] Pichet Binette A, Franzmeier N, Spotorno N, Ewers M, Brendel M, Biel D, et al. Amyloid-associated increases in soluble tau relate to tau aggregation rates and cognitive decline in early Alzheimer's disease. Nat Commun 2022;13:6635. https://doi.org/10.1038/s41467-022-34129-4.

[212] Karlsson L, Janelidze S, Barthélemy NR, Horie K, Gaetani L, Bellomo G, et al. Reference proteins to improve Core 1 and Core 2 Alzheimer's disease CSF and plasma biomarkers. Brain 2026;5:19. https://doi.org/10.1093/brain/awaf375/8275810.

[213] World Health Organization. Preferred product characteristics of blood-based biomarker diagnostics for Alzheimer disease. 2024.

[214] Junkkila J, Oja S, Laine M, Karrasch M. Applicability of the CANTAB-PAL Computerized Memory Test in Identifying Amnestic Mild Cognitive Impairment and Alzheimer's Disease. Dement Geriatr Cogn Disord 2012;34:83–9. https://doi.org/10.1159/000342116.

[215] Riley McCarten J, Anderson P, Kuskowski MA, McPherson SE, Borson S, Dysken MW. Finding Dementia in Primary Care: The Results of a Clinical Demonstration Project. J Am Geriatr Soc 2012;60:210–7. https://doi.org/10.1111/j.1532-5415.2011.03841.x.

[216] O'Bryant SE, Humphreys JD, Smith GE, Ivnik RJ, Graff-Radford NR, Petersen RC, et al. Detecting Dementia With the Mini-Mental State Examination in Highly Educated Individuals. Arch Neurol 2008;65. https://doi.org/10.1001/archneur.65.7.963.

[217] Preston JE. Ageing choroid plexus-cerebrospinal fluid system. Microsc Res Tech 2001;52:31–7. https://doi.org/10.1002/1097-0029(20010101)52:1<31::AID-JEMT5>3.0.CO;2-T.

[218] Liu G, Mestre H, Sweeney AM, Sun Q, Weikop P, Du T, et al. Direct Measurement of Cerebrospinal Fluid Production in Mice. Cell Rep 2020;33. https://doi.org/10.1016/j.celrep.2020.108524.

[219] Chazen JL, Dyke JP, Holt RW, Horky L, Pauplis RA, Hesterman JY, et al. Automated segmentation of MR imaging to determine normative central nervous system cerebrospinal fluid volumes in healthy volunteers. Clin Imaging 2017;43:132–5. https://doi.org/10.1016/j.clinimag.2017.02.007.

[220] Hansson O, Kumar A, Janelidze S, Stomrud E, Insel PS, Blennow K, et al. The genetic regulation of protein expression in cerebrospinal fluid. EMBO Mol Med 2023;15. https://doi.org/10.15252/emmm.202216359.

[221] Mravinacová S, Bergström S, Olofsson J, de San José NG, Anderl-Straub S, Diehl-Schmid J, et al. Addressing inter individual variability in CSF levels of brain derived proteins across neurodegenerative diseases. Sci Rep 2025;15:668. https://doi.org/10.1038/s41598-024-83281-y.

[222] García-González P, Puerta R, Dehairs J, Yang C, Wang C, Timsina J, et al. CSF turnover reshapes biomarker interpretation in neurodegeneration studies. BioRxiv (Preprint) 2026. https://doi.org/10.64898/2026.02.02.26345363.

[223] Blennow K, Shaw LM, Stomrud E, Mattsson N, Toledo JB, Buck K, et al. Predicting clinical decline and conversion to Alzheimer's disease or dementia using novel Elecsys Aβ(1–42), pTau and tTau CSF immunoassays. Sci Rep 2019;9:19024. https://doi.org/10.1038/s41598-019-54204-z.

[224] Smith R, Shaw L, Palmqvist S, Mattsson-Carlgren N, Klein G, Tonietto M, et al. Clinical Performance of the Elecsys CSF pTau181/Aβ42 Ratio for Concordance with Tau-PET in Two Independent Cohorts. Neurol Ther 2025;14:2011–31. https://doi.org/10.1007/s40120-025-00798-8.

[225] Zetterberg H, Bendlin BB. Biofluid biomarkers in Alzheimer's disease and other neurodegenerative dementias. Nature 2026;650:49–59. https://doi.org/10.1038/s41586-025-10018-w.

[226] Figdore DJ, Schuder BJ, Ashrafzadeh-Kian S, Gronquist T, Bornhorst JA, Algeciras-Schimnich A. Differences in Alzheimer's disease blood biomarker stability: Implications for the use of tau/amyloid ratios. Alzheimer's & Dementia 2025;21. https://doi.org/10.1002/alz.70173.

[227] Wang J, Huang S, Lan G, Lai Y, Wang Q, Chen Y, et al. Diagnostic accuracy of plasma p-tau217/Aβ42 for Alzheimer's disease in clinical and community cohorts. Alzheimer's & Dementia 2025;21. https://doi.org/10.1002/alz.70038.

[228] Oh HS-H, Urey DY, Karlsson L, Zhu Z, Shen Y, Farinas A, et al. A cerebrospinal fluid synaptic protein biomarker for prediction of cognitive resilience versus decline in Alzheimer's disease. Nat Med 2025. https://doi.org/10.1038/s41591-025-03565-2.

[229] Nilsson J, Pichet Binette A, Palmqvist S, Brum WS, Janelidze S, Ashton NJ, et al. Cerebrospinal fluid biomarker panel for synaptic dysfunction in a broad spectrum of neurodegenerative diseases. Brain 2024:awae032. https://doi.org/10.1093/brain/awae032.

[230] Mravinacová S, Alanko V, Bergström S, Bridel C, Pijnenburg Y, Hagman G, et al. CSF protein ratios with enhanced potential to reflect Alzheimer's disease pathology and neurodegeneration. Mol Neurodegener 2024;19. https://doi.org/10.1186/s13024-024-00705-z.

[231] Hansson O, Blennow K, Zetterberg H, Dage J. Blood biomarkers for Alzheimer's disease in clinical practice and trials. Nat Aging 2023;3:506–19. https://doi.org/10.1038/s43587-023-00403-3.

[232] Pontecorvo MJ, Lu M, Burnham SC, Schade AE, Dage JL, Shcherbinin S, et al. Association of Donanemab Treatment With Exploratory Plasma Biomarkers in Early Symptomatic Alzheimer Disease. JAMA Neurol 2022;79:1250. https://doi.org/10.1001/jamaneurol.2022.3392.

[233] Tsoy E, La Joie R, VandeVrede L, Rojas JC, Yballa C, Chan B, et al. Scalable plasma and digital cognitive markers for diagnosis and prognosis of Alzheimer's disease and related dementias. Alzheimer's & Dementia 2024;20:2089–101. https://doi.org/10.1002/alz.13686.

[234] Fowler NR, Hammers DB, Perkins AJ, Summanwar D, Higbie A, Swartzell K, et al. Feasibility and Acceptability of Implementing a Digital Cognitive Assessment for Alzheimer Disease and Related Dementias in Primary Care. The Annals of Family Medicine 2025;23:191–8. https://doi.org/10.1370/afm.240293.

[235] Rabinovici GD, Knopman DS, Arbizu J, Benzinger TLS, Donohoe KJ, Hansson O, et al. Updated Appropriate Use Criteria for Amyloid and Tau PET: A Report from the Alzheimer's Association and Society for Nuclear Medicine and Molecular Imaging Workgroup. Journal of Nuclear Medicine 2025;66:S5–31. https://doi.org/10.2967/jnumed.124.268756.

[236] Iaccarino L, Burnham SC, Tunali I, Wang J, Navitsky M, Arora AK, et al. A practical overview of the use of amyloid-PET Centiloid values in clinical trials and research. Neuroimage Clin 2025;46:103765. https://doi.org/10.1016/j.nicl.2025.103765.

[237] Lee J, Burkett BJ, Min H-K, Senjem ML, Dicks E, Mester CT, et al. Synthesizing images of tau pathology from cross-modal neuroimaging using deep learning. Brain 2023. https://doi.org/10.1093/brain/awad346/7296495.

[238] Chen KT, Tesfay R, Koran MEI, Ouyang J, Shams S, Young CB, et al. Generative Adversarial Network-Enhanced Ultra-Low-Dose [18F]-PI-2620 s PET/MRI in Aging and Neurodegenerative Populations. American Journal of Neuroradiology 2023;44:1012–20. https://doi.org/10.3174/ajnr.A7961.

[239] Belder CRS, Boche D, Nicoll JAR, Jaunmuktane Z, Zetterberg H, Schott JM, et al. Brain volume change following anti-amyloid β immunotherapy for Alzheimer's disease: amyloid-removal-related pseudo-atrophy. Lancet Neurol 2024;23:1025–34. https://doi.org/10.1016/S1474-4422(24)00335-1.

[240] Gaspar-Silva F, Trigo D, Magalhaes J. Ageing in the brain: mechanisms and rejuvenating strategies. Cellular and Molecular Life Sciences 2023;80. https://doi.org/10.1007/s00018-023-04832-6.

[241] Salvadó G, Horie K, Barthélemy NR, Vogel JW, Pichet Binette A, Chen CD, et al. Disease staging of Alzheimer's disease using a CSF-based biomarker model. Nat Aging 2024;4:694–708. https://doi.org/10.1038/s43587-024-00599-y.

[242] Montoliu-Gaya L, Salvadó G, Therriault J, Nilsson J, Janelidze S, Weiner S, et al. Plasma tau biomarkers for biological staging of Alzheimer's disease. Nat Aging 2025;5:2297–308. https://doi.org/10.1038/s43587-025-00951-w.

[243] Arafah A, Khatoon S, Rasool I, Khan A, Rather MA, Abujabal KA, et al. The Future of Precision Medicine in the Cure of Alzheimer's Disease. Biomedicines 2023;11. https://doi.org/10.3390/biomedicines11020335.

[244] Eric Thomas C, Sexton W, Benson K, Sutphen R, Koomen J. Urine collection and processing for protein biomarker discovery and quantification. Cancer Epidemiology Biomarkers and Prevention 2010;19:953–9. https://doi.org/10.1158/1055-9965.EPI-10-0069.

[245] Jantos-Siwy J, Schiffer E, Brand K, Schumann G, Rossing K, Delles C, et al. Quantitative urinary proteome analysis for biomarker evaluation in chronic kidney disease. J Proteome Res 2009;8:268–81. https://doi.org/10.1021/pr800401m.

[246] Voevodskaya O, Simmons A, Nordenskjöld R, Kullberg J, Ahlström H, Lind L, et al. The effects of intracranial volume adjustment approaches on multiple regional MRI volumes in healthy aging and Alzheimer's disease. Front Aging Neurosci 2014;6:264. https://doi.org/10.3389/fnagi.2014.00264.

[247] Bleecker ML, Bolla-Wilson K, Kawas C, Agnew J. Age-specific norms for the Mini-Mental State Exam. Neurology 1988;38:1565–1565. https://doi.org/10.1212/WNL.38.10.1565.

[248] Duff K, Patton D, Schoenberg MR, Mold J, Scott JG, Adams RL. Age- and Education-Corrected Independent Normative Data for the RBANS in a Community Dwelling Elderly Sample. Clin Neuropsychol 2003;17:351–66. https://doi.org/10.1076/clin.17.3.351.18082.

[249] Borland E, Nägga K, Nilsson PM, Minthon L, Nilsson ED, Palmqvist S. The Montreal Cognitive Assessment: Normative Data from a Large Swedish Population-Based Cohort. Journal of Alzheimer's Disease 2017;59:893–901. https://doi.org/10.3233/JAD-170203.

[250] Sheller MJ, Edwards B, Reina GA, Martin J, Pati S, Kotrotsou A, et al. Federated learning in medicine: facilitating multi-institutional collaborations without sharing patient data. Sci Rep 2020;10. https://doi.org/10.1038/s41598-020-69250-1.

[251] Teo ZL, Jin L, Li S, Miao D, Zhang X, Ng WY, et al. Federated machine learning in healthcare: A systematic review on clinical applications and technical architecture. Cell Rep Med 2024;5:101419. https://doi.org/10.1016/j.xcrm.2024.101419.

[252] Kokosi T, Harron K. Synthetic data in medical research. BMJ Medicine 2022;1:e000167. https://doi.org/10.1136/bmjmed-2022-000167.

[253] Giuffrè M, Shung DL. Harnessing the power of synthetic data in healthcare: innovation, application, and privacy. NPJ Digit Med 2023;6. https://doi.org/10.1038/s41746-023-00927-3.

[254] Bocquet F, Campone M, Cuggia M. The Challenges of Implementing Comprehensive Clinical Data Warehouses in Hospitals. Int J Environ Res Public Health 2022;19. https://doi.org/10.3390/ijerph19127379.

[255] Gentner T, Neitzel T, Schulze J, Gerschner F, Theissler A. Data Lakes in Healthcare: Applications and Benefits from the Perspective of Data Sources and Players. Procedia Comput Sci 2023;225:1302–11. https://doi.org/10.1016/j.procs.2023.10.118.

[256] Lee CH, Yoon H-J. Medical big data: promise and challenges. Kidney Res Clin Pract 2017;36:3–11. https://doi.org/10.23876/j.krcp.2017.36.1.3.

[257] Bajwa J, Munir U, Nori A, Williams B. Artificial intelligence in healthcare: transforming the practice of medicine. Future Healthc J 2021;8:e188–94. https://doi.org/10.7861/fhj.2021-0095.

[258] Moor M, Banerjee O, Abad ZSH, Krumholz HM, Leskovec J, Topol EJ, et al. Foundation models for generalist medical artificial intelligence. Nature 2023;616:259–65. https://doi.org/10.1038/s41586-023-05881-4.

[259] Hollmann N, Müller S, Purucker L, Krishnakumar A, Körfer M, Hoo S Bin, et al. Accurate predictions on small data with a tabular foundation model. Nature 2025;637:319–26. https://doi.org/10.1038/s41586-024-08328-6.

[260] Tak D, Garomsa BA, Zapaishchykova A, Chaunzwa TL, Climent Pardo JC, Ye Z, et al. A generalizable foundation model for analysis of human brain MRI. Nat Neurosci 2026. https://doi.org/10.1038/s41593-026-02202-6.

[261] Jasodanand VH, Kowshik SS, Puducheri S, Romano MF, Xu L, Au R, et al. AI-driven fusion of multimodal data for Alzheimer's disease biomarker assessment. Nature Communications 2025;16. https://doi.org/10.1038/s41467-025-62590-4.

[262] Leng Y, He Y, Amini S, Magdamo C, Paschalidis I, Mukerji SS, et al. A GPT-4o-powered framework for identifying cognitive impairment stages in electronic health records. NPJ Digit Med 2025;8:401. https://doi.org/10.1038/s41746-025-01834-5.

[263] Shankar R, Bundele A, Mukhopadhyay A. Natural language processing of electronic health records for early detection of cognitive decline: a systematic review. NPJ Digit Med 2025;8:133. https://doi.org/10.1038/s41746-025-01527-z.

[264] Mormino EC, Biber SA, Rahman-Filipiak A, Arfanakis K, Clark L, Dage JL, et al. The Consortium for Clarity in ADRD Research Through Imaging (CLARiTI). Alzheimer's & Dementia 2025;21. https://doi.org/10.1002/alz.14383.

[265] Russ KA, Lacy K, Dage JL, Foroud T. The National Centralized Repository for Alzheimer's Disease and Related Dementia's Biomarker Assay Laboratory: A Resource for the Alzheimer's Disease Research Community. Alzheimer's & Dementia 2025;21. https://doi.org/10.1002/alz.70774.

[266] Sudlow C, Gallacher J, Allen N, Beral V, Burton P, Danesh J, et al. UK Biobank: An Open Access Resource for Identifying the Causes of a Wide Range of Complex Diseases of Middle and Old Age. PLoS Med 2015;12:e1001779. https://doi.org/10.1371/journal.pmed.1001779.

[267] Zhou X, Xiao Z, Wu W, Chen Y, Yuan C, Leng Y, et al. Closing the gap in dementia research by community-based cohort studies in the Chinese population. Lancet Reg Health West Pac 2025;55:101465. https://doi.org/10.1016/j.lanwpc.2025.101465.

[268] Zhi N, Ren R, Qi J, Liu X, Yun Z, Lin S, et al. The China Alzheimer Report 2025. Gen Psychiatr 2025;38:e102020. https://doi.org/10.1136/gpsych-2024-102020.

[269] Sorby-Adams AJ, Guo J, Laso P, Kirsch JE, Zabinska J, Garcia Guarniz A-L, et al. Portable, low-field magnetic resonance imaging for evaluation of Alzheimer's disease. Nat Commun 2024;15:10488. https://doi.org/10.1038/s41467-024-54972-x.

[270] Huber H, Montoliu-Gaya L, Brum WS, Vávra J, Yakoub Y, Weninger H, et al. A minimally invasive dried blood spot biomarker test for the detection of Alzheimer's disease pathology. Nat Med 2026;32:599–608. https://doi.org/10.1038/s41591-025-04080-0.

[271] Kodam P, Sai Swaroop R, Pradhan SS, Sivaramakrishnan V, Vadrevu R. Integrated multi-omics analysis of Alzheimer's disease shows molecular signatures associated with disease progression and potential therapeutic targets. Sci Rep 2023;13:3695. https://doi.org/10.1038/s41598-023-30892-6.

[272] Hristovska I, Pichet Binette A, Kumar A, Wennström M, Gaiteri C, Karlsson L, et al. Identification of distinct and shared biomarker panels in different manifestations of cerebral small-vessel disease through proteomic profiling. Nat Aging 2026. https://doi.org/10.1038/s43587-026-01081-7.

[273] Heo G, Xu Y, Wang E, Ali M, Oh HS-H, Moran-Losada P, et al. Large-scale plasma proteomic profiling unveils diagnostic biomarkers and pathways for Alzheimer's disease. Nat Aging 2025;5:1114–31. https://doi.org/10.1038/s43587-025-00872-8.

[274] Concha-Marambio L, Pritzkow S, Shahnawaz M, Farris CM, Soto C. Seed amplification assay for the detection of pathologic alpha-synuclein aggregates in cerebrospinal fluid. Nat Protoc 2023;18:1179–96. https://doi.org/10.1038/s41596-022-00787-3.

[275] Vokali E, Chevalier E, Dreyfus N, Charmey D, Melly T, Kocher J, et al. Development of [18F]ACI-19626 as a first-in-class brain PET tracer for imaging TDP-43 pathology. Nat Commun 2025;16:9358. https://doi.org/10.1038/s41467-025-64540-6.

Printed by Media-Tryck, Lund 2026 NORDIC SWAN ECOLABEL 3041 0903

About the author

Driven by a strong interest in mathematics and problem solving, **LINDA KARLSSON** completed a Master of Science in Engineering Physics at Lund University in 2022. Wanting to apply her skills to questions that could make a meaningful difference in people's lives, she turned to medicine. She joined the Clinical Memory Research Unit as a doctoral researcher, studying Alzheimer's disease biomarkers and diagnostic tools from clinical and data science perspectives. Her research represents an ideal intersection of her engineering background and strong interest in understanding the brain. Outside research, Linda has a large passion for sports, and she combined her undergraduate studies with playing football in one of Sweden's top leagues.

LUND UNIVERSITY

FACULTY OF MEDICINE

Department of Clinical Sciences, Malmö

Lund University, Faculty of Medicine
Doctoral Dissertation Series 2026:67
ISBN 978-91-8021-865-8
ISSN 1652-8220